공학석사 학위논문

Strengthening of RC beams with Ultra High Performance Concrete

초고성능 콘크리트를 이용한 보 보강 실험

2016 년 2 월

서울대학교 대학원

건축학과

최 정 택

Strengthening of RC beams with Ultra High Performance Concrete

지도 교수 홍 성 걸

이 논문을 공학석사 학위논문으로 제출함
2016 년 2 월

서울대학교 대학원
건축학과
최 정 택

최정택의 공학석사 학위논문을 인준함
2016 년 2 월

위 원 장 _____ (인)

부위원장 _____ (인)

위 원 _____ (인)

Abstract

Strengthening of RC beams with Ultra High Performance Concrete

Choi, Jung-Taek
Department of Architecture and Architectural Engineering
College of Engineering
Seoul National University

This study investigates the structural performance of retrofitted RC-UHPC (Ultra-High Performance Concrete) composite members through measuring the effectiveness of strengthened RC beams with different regions and thickness of added UHPC. Due to its high compressive and tensile strength, thin UHPC over layers are applied to increase tensile strength in flexural strength in tension region with reinforcement and the compressive resistance in flexural compression region. For adhesion between existing concrete and UHPC, sandblasting is applied to give enough roughness.

Two series of tests were performed under four-point loads. First test program consists of 12 specimens strengthened with change in thickness, regions, fiber volume and additional reinforcement except one control beam of rectangular section. For the second program, 14 ordinary reinforced concrete T-beams were prepared to develop shear failure modes. Because strengthened beams with UHPC are supposed to enhance both positive and negative moment capacity, jacketing methods applied to this experimental program have three different schemes: UHPC U shaped-jacketing, UHPC casting on the flange, and UHPC casting on the flange and Aramid FRP U shaped-wrapping.

The experimental results show that strengthening beam with UHPC is effective to enhance strength and deflection. Especially, UHPC U shaped-

jacketing method showed better performance than that of other methods by the improvement of strength, stiffness and ductility for both positive and negative moment zone. On the other hand, UHPC overlay method showed the additional treatment to improve adhesion performance between old concrete and UHPC. Strengthening effects are proportion to the strengthened thickness without shear failure. For additional reinforcement with UHPC, the increase in strength and ductility were shown. AFRP with UHPC and additional steel fiber in UHPC showed a little increase in strength. Wire mesh showed no contribution to performance.

Based on the test result of this study, theoretical analysis determined by a cross-sectional analytical model based on plane section showed 15% error range about rectangular sectional beams, 21% error range for T-shaped sectional beams.

In case of T-shaped RC beams showing debonding failure, average interfacial shear stress were calculated and compared with current design code and slant-shear test results. It showed that for positive moment, the highest shear stress occurred at overlaid UHPC panel

Keywords : UHPC, retrofit, strengthening, composite beams
Student Number : 2014-20519

Contents

List of Tables

List of Figures

List of Symbols

a = depth of equivalent rectangular stress block, mm

b = width of flange, mm

b_{ef} = effective width of a T-beam in shear. A/c. replaceable the width b_w

b_w = width of web, mm

c = distance from extreme compression fiber to neutral axis, mm

or

= cohesion factor specified in Article 5.8.4.3 of AASHTO LRFD

c_a = the coefficient for the adhesive bond; 0.4(strongly roughened surface)

d = effective depth, mm

d' = distance from extreme tension fiber to resultant tension force, mm

d'' = distance from extreme compression fiber to resultant compression force, mm

d_{fv} = effective depth of FRP shear reinforcement, mm

h = height, mm

h_f = height of flange, mm

f_c' = specified compressive strength of concrete, MPa

f_{cd} = design compressive strength of UHPC, MPa

f_{fe} = effective stress in the FRP; stress level attained at section failure, MPa

f_{tk} = characteristic tensile strength of UHPC, MPa

f_{vd} = design average tensile strength in the direction perpendicular to diagonal tensile crack of UHPC, MPa

f_{yv} = specified yield strength f_y of transverse reinforcement

s_f = span between each sheet, mm

t = UHPC jacketing thickness

t_b = base strengthened thickness, mm

t_s = side strengthened thickness, mm

t_t = top strengthened thickness, mm

y = centroid of the transformed section, mm

z = distance from the position of the resultant of the compressive stresses to the centroid of tensile steel, mm, generally $d/1.15$

A_c = area of concrete section resisting shear transfer, mm^2

A_{cv}

A_{fv} = area of FRP shear reinforcement with spacing s, mm^2

A_s = area of nonprestressed longitudinal tension reinforcement, mm^2

A_{sf} = tensile steel area having equilibrium condition with overhanging flanges, mm^2

A_{vf} = area of interface shear reinforcement, crossing the shear plane within the area A_{cv}

C = compression force, N

C_c = compressive force resisted in concrete, N

C_{cr} = crack spacing, mm

C_u = compressive force resisted in UHPC layer, N

C_{us} = compression force portion of side UHPC above neutral axis, N

E_s = modulus of elasticity of reinforcement steel, MPa

E_u = modulus of elasticity of UHPC, MPa

I = equivalent moment of inertia

I_{gt} = uncracked transformed moment of inertia, mm^4

K_1 = fraction of concrete strength available to resist interface shear, as specified in Article 5.8.4.3

K_2 = limiting interface shear resistance specified in Article 5.8.4.3

M_n = nominal flexural strength at section, N·mm

P_c = permanent net compressive force normal to the shear plane; if force is tensile, $Pc = 0$

T = tensile force, N

T_s = tensile force portion of reinforcing steel bars, N

T_{us} = tensile force portion of side UHPC below neutral axis, N

T_{ub} = tensile force portion of base UHPC below neutral axis, N

Q = equivalent section modulus, mm^3

V = shear force, N

V_{hv} = Interfacial shear force, N

V_n = nominal shear strength, N

V_{nh} = horizontal shear strength, N

V_c = nominal shear strength provided by concrete, N

V_s = nominal shear strength provided by stirrup, N

V_{rpcd} = nominal shear strength provided by matrix of UHPC, N

V_f = nominal shear strength provided by FRP stirrups, N

V_{fd} = nominal shear strength provided by fiber, N

α_t = equivalent tensile stress block coefficient

β_c = a coefficient for the strength of the compression strut

β_u = angle occurring between axial direction and diagonal tensile crack plane. This angle shall be larger than 30°

(40° is assumed in this study based on provision)

ε_{cc} = net compression strain in middle of base UHPC jacketing

ε_s' = net compression strain in longitudinal steel in compression

ε_{s1} = net strain in 1st bottom layer reinforcement

ε_{s2} = net strain in 2nd bottom layer reinforcement

μ = the friction coefficient acc. Table 7.3-2; 0.7 for rough surface

τ = vertical shear stress

τ_b = Interfacial shear stress, MPa

τ_{Rdi} = design limit value

ν = the effectiveness factor for the concrete

ν_{hv} = horizontal shear stress, MPa

ρ = ratio of reinforcement crossing the interface ($\rho = A_s/A_c$)

ρ_v = ratio of tie reinforcement area to area of contact surface

σ_n = the (lowest expected) compressive stress resulting from an eventual normal force acting on the interface.

Chapter 1. Introduction

1.1 General

According to the statistics of aging of domestic buildings, buildings built before more than 35 years charged in 29% of total building. As seen it by legal standard of 20 years, 55% of total buildings belonged to old building(**Fig 1-1**). Thereafter needs for retrofitting old building will continue to increase.

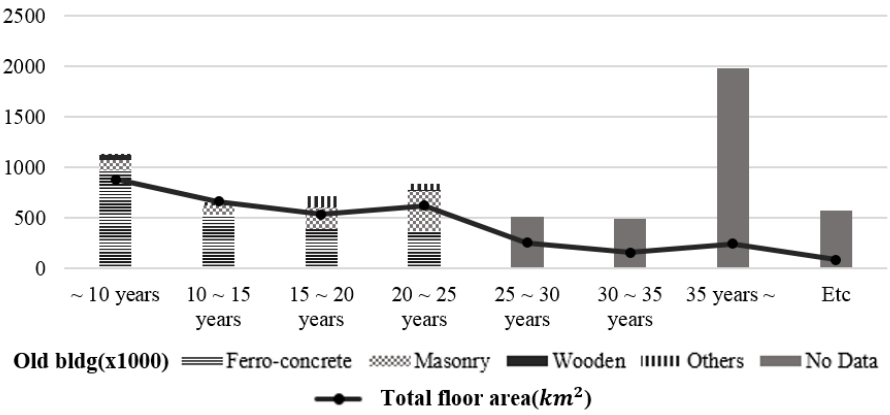

Fig 1-1 Statistics of Korea's aging building in 2014

The current techniques of rehabilitation and strengthening using externally bonded fiber-reinforced plastic(FRP) laminates and steel plates have been extensively investigated. FRP is widely used for its lightweight and excellent workability. The followings are steel plate. Unfortunately using these materials could lead to sudden undesirable failure due to material property or difference in thermal expansion coefficient between concrete and epoxy. In this condition, we are trying to use UHPC which has superior performance.

Ultra High Performance Concrete(UHPC) is a material with a cement matrix and a characteristic compressive strength of more than 150 MPa. The material is distinguished for its compact, quasi-impermeable matrix, high

strength and deformation capacity in tension. The high post-cracking tensile strength obtained by use of steel fiber in order to achieve ductile behavior under tension In **Fig 1-2**, the behavior of UHPC was compared with that of other cementitious materials.

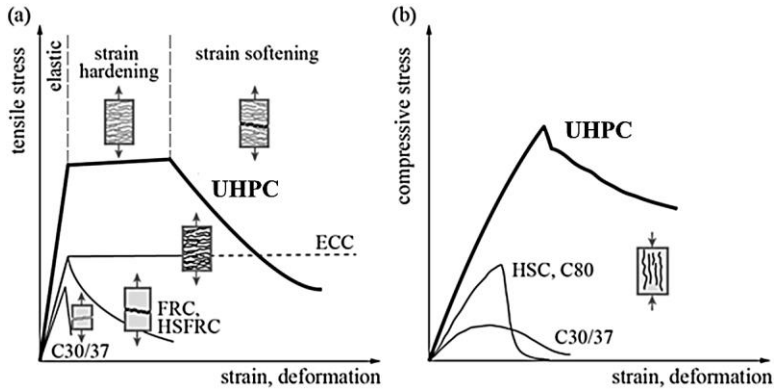

Fig 1-2 Material behavior of UHPC compared to other types of concrete :
a) response in tension; b) response in compression (Noshiravani, 2012)

Owing to its high structural performance of UHPC, it is possible to apply thin layer of UHPC over ordinary existing structural concrete to increase their insufficient capacity. There are already examples using UHPC as strengthening materials in Europe. In **Fig 1-3,** left one is overlaying UHPC on the bridge deck(HSLV pilot project, Wiesbaden) and right one is UHPC U-shaped jacking on the beam.

Fig 1-3 Examples of rehabilitation and strengthening with UHPC

1.2 Ultra-High Performance concrete

UHPC are Advanced Cementitious Materials with specifically tailored properties. They are characterized by an ultra-compact matrix with very low permeability and by tensile strain-hardening. They are part of the group of HPFRCC as described in **Fig 1-4**.

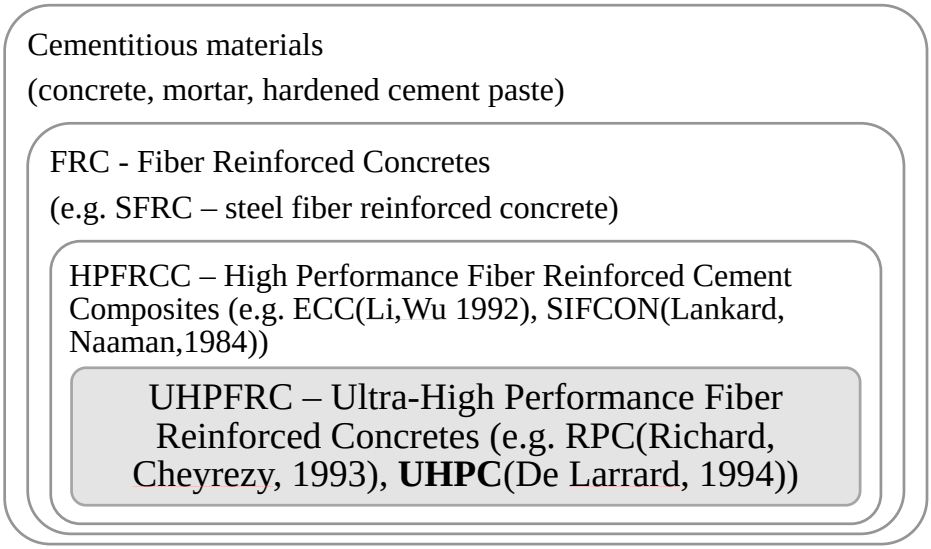

Fig 1-4 Category of UHPC(Habel 2004)

The main principles for UHPFRC design are : (Richard, Cheyrezy 1995)

- Homogeneity enhancement: The homogeneity of the material is improved by eliminating coarse aggregates,
- Compacity enhancement: The density of the matrix is increased by optimizing the packing density. The different particle size classes are silica fume (mean size: 0.1 to 0.2 mm), cement (mean size: 15 mm) and fine sand (mean size: 0.2 mm). The optimum packing density can be determined with granular packing models by calculating the optimum ratio of the different aggregate classes.
- Ductility by fibers: As the matrix of densified small particles is very brittle, steel or organic fibers have to be added to obtain strain-hardening

behavior in tension.

UHPFRC may be subjected to heat or pressure treatment. Pressure treatment of the fresh material increases the density by reducing the entrapped air, by removing excess water and by accelerating chemical shrinkage. Post-set heat-treating of 90 ℃ accelerates the pozzolanic reaction and modifies the microstructure of the hydrates. However, these two treatments are difficult to apply in case of composite "UHPFRC-concrete" elements and in-situ applications and would present major drawbacks. Though UHPFRC without heat or pressure treatment are proposed and used in the present study, in this research, 90℃ heat treatment was applied.

UHPFRC consists of cement, silica fume, sand, fibers, water and superplasticizer. Typical water/cement-ratios are 0.15 to 0.20 with 20 to 30% of silica fume. Silica fume fills voids between cement grains, enhances the rheological characteristics and forms hydration products by pozzolanic activity. To reduce water content, superplasticizer is essential for workability of UHPFRC. With low w/c ratios, UHPFRC has high strength caused by low porosity. Addition of fibers is necessary to enhance ductility. And tensile properties depend significantly on the fiber distribution and orientation. (Ekkehard Fehling, Joost Walraven, and Fröhlich 2014)

Thanks to its distinguished performance, far less material is needed to achieve the same structural requirements. This leads to much lower weight and volume of UHPC as strengthening material.

1.3 Scope and Objectives

This thesis has three principle objectives:

1. To investigate the structural response of Strengthened beam with UHPC,
2. To describe the failure modes of UHPC-RC members,
3. To compare theoretical analysis with test results.

Two kinds of tests are planned to check the efficiency of UHPC strengthening in tension side(shaded area in **Fig 1-3**) with parameters as strengthening region, thickness, and additional reinforcement in **Chapter 3**, and to check the efficiency of UHPC strengthening over shaded area, which means in negative moment zone in **Chapter 4**.

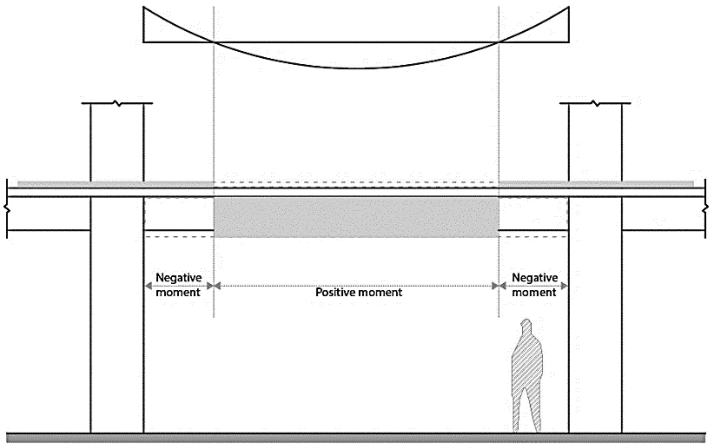

Fig 1-5 Prototype of existing concrete building frame

Chapter 2. Literature Review

This chapter introduces related design guideline(2.1) and similar research about strengthening beam(2.2, 2.3) and interfacial bond(2.4).

2.1 JSCE guideline-Recommendations for Design and Construction of HPFRCC, 2008

2.1.1 Calculation of stress and strain

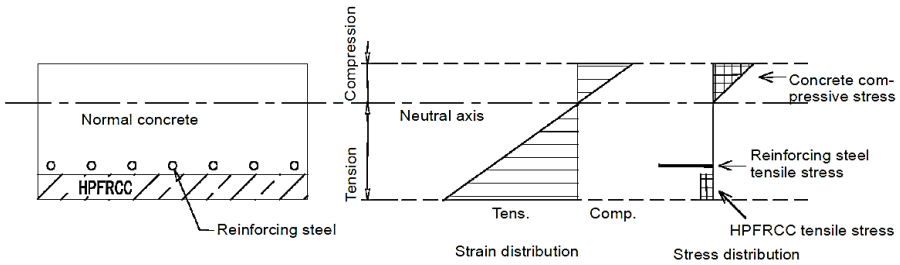

Fig 2-1 Stress and strain distributions in an HPFRCC

Calculation of stress and strain in HPFRCC and steel at a limit state of serviceability shall be based on the following assumptions.

1. Strain is proportional to the distance from the neutral axis of the cross section.

2. HPFRCC is linear elastic under compression and follows the tensile stress-strain curve as shown in section under tension.

3. Steel is linear elastic.

4. Young's modulus of HPFRCC is given

2.1.2 Design shear capacity

Design shear capacity of a steel reinforced concrete member partly reinforced by HPFRCC shall be determined with appropriate methods such as tests. However, design shear capacity of a member combined with HPFRCC and normal concrete by appropriate technology may be determined according to “Design shear capacity of linear members” as followed.

The design shear capacity of a linear member consisting solely of HPFRCC and reinforcing steels V_{yd} may be obtained by Equation below.

$$V_{yd} = V_{cd} + V_{sd} + V_{fd} + V_{ped}$$

2.2 Strengthening beam with UHPC

2.2.1 Katrin Habel(2004)

The flexural behavior of composite R-UHPFRC-RC elements may be determined by an analytical cross-sectional model and a kinematic hypothesis. The analysis is based on extension of the commonly used bending design model for RC and considers the tensile behavior of UHPFRC.

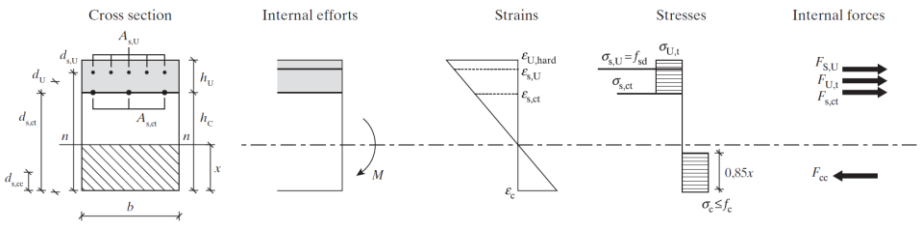

Fig 2-2 Determination of ultimate moment of R-UHPFRC-RC members

$$\Sigma F = F_{s,U} + F_{Ut} + F_{s,ct} + F_{cc} + F_{s,cc} = N$$
$$M = \Sigma M_i = M_{s,U} + M_{Ut} + M_{s,ct} + M_{ct} + M_{cc} + M_{s,cc}$$

2.2.2 Taylayeh Noshiravani(2012)

The behavior of R-UHPFRC-RC structural members subjected to combined bending and shear was investigated based on theory of plasticity. Using the principle of virtual work, it is possible to calculate the upper bound of the ultimate resistance of RU-RC composite beams. Following three kinematic models for flexural, flexure-shear and shear failure of RU-RC beams, internal works done by each constituent material can be obtained, on the assumption that by the states of cracks divide the composite member into several rigid bodies. .

2.3 Comparison UHPC strengthening method with others

There are various strengthening method for beam. Related with UHPC, namely cement based strengthening material are organized in **Table 2-1** with commonly used method, such as FRP and steel plates. Summarized data composed of reference, original beam geometry, strengthening material and method, bond method, variables, and maximum strength increase. In the respect of strength increase, these methods are compared in **Fig 2-3.**

Comparing maximum increase of strength as standard, it was ordered that R-UHPFRC(UHPFRC with rebars) > Plain UHPFRC > Concrete Jacketing > ECC, SHCC, HPFRCC > FRP > Steel plate. However, these rankings are not absolute, because it is just a standard that shows tendency. If the retrofitted layer's thickness increase or anchoring of strengthening materials is well-set, strengthening effects could be changed.

Table 2-1 Summary of strengthening beam with various method

1	**Paper(year)**	Strengthening and repair of RC beams with fiber reinforced concrete (Martinola et al. 2010)					
	Beam	geometry(mm)	fc' (Mpa)	longitudinal rebar	stirrup	a/d	# of specimen
		300x500x4550	22	2-D16	D8/150	2.42	4
	Strengthening method(C/T)	**HPFRC**(177/11.5) 40mm U-shaped jacketing					
	Bond	sandblast 1-2mm					
	Variable	ref condition(strengthened / repaired), steel reinforced o/x in ref. beam					
	Max. Increase of strength	(strengthened) 2.16 times higher than reference beam (repaired)1.92 times higher					
	Sum	Full scale beam tested for strengthening and repair by using a jacket made of HPFRC. The experimental results show the effectiveness of the proposed technique both at ultimate and serviceability limit states.					
2	**Paper(year)**	Structural Response of Reinforced UHPFRC and RC Composite Members (Oesterlee 2010)					
	Beam	geometry	fc'	longitudinal rebar	stirrup	a/d	# of specimen
		150x250x6000	30	3-D12	D8/200	6.79	14

	Strengthening method(C/T)	**UHPFRC** 50mm base strengthening with various types of rebar					
	Bond	hydro-jetting 3-5mm					
	Variable	Steel type(grade, ribs), # of rebars in UHPFRC					
	Max. Increase of strength	4-D8 ribbed steel in 50mm UHPFRC showed 2.65times higher than ref.					
	Sum	Ultimate resistance increase depending on the steel grade and reinforcement ratio Smooth rebars in UHPFRC allow for a higher rotation capacity than equivalent ribbed bars. High yield strength steel is beneficial since it allows higher deformations of composite beams with lower reinforcement ratios.					
3	**Paper (year)**	Experimental Investigation on Reinforced Ultra-High-Performance Fiber-Reinforced Concrete Composite Beams Subjected to Combined Bending and Shear (Noshiravani 2012)					
	Beam	geometry	fc'	longitudinal rebar	stirrup	a/d	# of specimen
		150x250x1600	41.6	various	various	2.3-4.2	17
	Strengthening method(C/T)	rebars within UHPFRC(160/10.2) Overlay					
	Bond	sandblast					
	Variable	a/d, the ratio & type of the steel rebars, including stirrups					
	Max. Increase of strength	(a/d=3.8, s=400mm, ρv=0.17%, ωst=8.1%, ωU=3.9%, ωsU=9.2%) showed 2.77times higher than ref					
	sum	To understand flexure-shear behavior of RU-RC beam, existing static and kinematic solutions of the theory of plasticity for RC memebers were extended by considering the additional layer of R-UHPFRC to predict the ultimate resistance and the force-displacement response of the composite beams					
4	**Paper (year)**	Shear Strengthening of Reinforced Concrete Beam with High-Performance Fiber-Reinforced Cementitious Composite Jacketing (Meda, Mostosi, and Riva 2014)					
	Beam	geometry	fc'	longitudinal rebar	stirrup	a/d	# of specimen
		200x450x2850	32.6	4-D20	-	1.9	4
	Strengthening method(C/T)	U-shaped HPFRC(self leveling(108/6.7), thixotropic(75/4.7)) combined with high performance steel mesh					
	Bond	sandblast 1mm					

	Variable	thickness, material property, epoxy o/x, height of welded wire mesh put in HPFRC jacket					
	Max. Increase of strength	50mm U-shaped HPFRC(self leveling) with wire mesh showed 1.72times higher than ref.					
	sum	2 types of HPFRC are investigated to considering the workability. All stregnthened beams reached their theoretical bending capacity.					
5	**Paper(year)**	Formwork development using UHPFRC (SG Hong, SH Kang, 2013)					
	Beam	geometry	fc'	longitudinal rebar	stirrup	a/d	# of specimen
		300x210x2300	18	4-D10	-	3.85	8
	Strengthening method(C/T)	**UHPFRC**(143/?) Permanent formwork					
	Bond	-					
	Variable	thickness, position and # of rebars					
	Max. Increase of strength	(C4U0, 4 rebars in concrete strengthened 30mm base UHPFRC) showed 1.9 times higher than C4					
	sum	As RC-UHPFRC composite beam, it showed that the number of rebar in UHPC should less than in concrete.					
6	**Paper(year)**	Retrofitting of Reinforced Concrete Beams with CARDIFRC (Karihaloo, Benson, and Alaee 2003)					
	Beam	geometry	fc'	longitudinal rebar	stirrup	a/d	# of specimen
		100x150x1200	45	D12	D6/65	2.7	32
	Strengthening method(C/T)	Precast **HPFRCC**(CARDIFRC(Mix 1 : 207/24* & Mix 2 : 185/25*)) was attached with different region(*:indirect tensile test)					
	Bond	3mm groove spacing 50mm at damaged beam + Epoxy					
	Variable	material mix, strengthened region, strip thickness(16, 20mm)					
	Max. Increase of strength	20mm U-shaped(side covered only 2/3 of beam) with Mix 1 showed 2.02times higher than ref.					
	sum	Like steel plastes stregnthening, precast HPFRCC plates attached by Epoxy. For shear strengthening, full cover of side portion is more effective than partly stregnthened beam which is covered only the predicted area where diagonal crack occurred.					
7	**Paper (year)**	Utilization of high performance fiber-reinforced micro-concrete as a repair material (Skazlić 2009)					

	Beam	geometry	fc'	longitudinal rebar	stirrup	a/d	# of specimen
		150x150x600	25	-	-		4
	Strengthening method(C/T)	**HPFRMC**(116.5/32.2*) repairing base 30,60mm and 30mm U-shaped jacketing					
	Bond	Crushing with hammer & Emulsion coat					
	Variable	thickness, scope					
	Max. Increase of strength	Base 60mm replacing with HPFRMC shows 2.32times higher than ref. 30mm U-shaped jacket shows 2.2times higher than ref.					
	sum	Keeping the same cross section size, HPFRMC replacing the original concrete portion.					
8	**Paper (year)**	Assessment of strengthening effect on RC beams with UHP-SHCC (Kamal et al. 2008)					
	Beam	geometry	fc'	longitudinal rebar	stirrup	a/d	# of specimen
		150x200x1800	24	2-D10	D6/90	2.5	7
	Strengthening method(C/T)	**UHP-SHCC**(86.7/10.5) base strengthening & RC layer base strengthening					
	Bond	using retarder to obtain a roughed surface					
	Variable	thickness(30,50,70mm), comparing UHP-SHCC with RC layer					
	Max. Increase of strength	UHP-SHCC base 70mm showed 1.87times higher than ref. 70mm base RC layer with 3-D13 showed 3.77times higher than ref.					
	Sum	Tensile strength of UHP-SHCC is larger than that of ordinary SHCC					
9	**Paper (year)**	Flexural Experiments on Reinforced Concrete Beams Strengthened with ECC and High Strength Rebar (HW CHO, 2011)					
	Beam	geometry	fc'	longitudinal rebar	stirrup	a/d	# of specimen
		300x500x4000	24	4-D19	D10/200	2.95	6
	Strengthening method(C/T)	**ECC** 60mm base strengthening with rebar o/x, CFRP, Carbon fiber mesh					
	Bond	chipping upto 60mm to replace initial concrete for ECC, Epoxy for CFRP					
	Variable	Strengthening material, # of rebar in ECC(0,3,5)					
	Max. Increase of strength	(60mm base ECC with 5 rebars) 1.3 times higher than ref					

	Sum	Embeded fiber mesh showed only 5% increase of strength. Without rebars in ECC, its strengthening effects showed only 3% strength increase.					
10	**Paper (year)**	Flexural behavior of strengthened and repaired R.C. beams by using steel fiber concrete jacket under repeated load (Yehia A. Hassanean 2013)					
	Beam	geometry	fc'	longitudinal rebar	stirrup	a/d	# of specimen
		120x300x2300	27.5	2-D16	D8/20	4	14
	Strengthening method(C/T)	**SFC**(82.5/?) U-shaped jacketing(various base thickness(3-50mm) with fixed 30mm side)					
	Bond	grind+shear connector					
	Variable	ref condition(strengthened / repaired), Vf, jacket thickness, shear connector o/x					
	Max. number of cycles	(strengthened, Vf :1.5%, tjb : 50, tjs : 30, w/ shear connector) 5.2times than ref. (repaired, Vf :1.5%, tjb : 50, tjs : 30, w/ shear connector) 4times than ref.					
	Sum	Test performed under repeated loads up to failure. Strengthened thickness's effects higher than Vf's					
11	**Paper (year)**	An Experimental Investigation on Flexural Behavior of RC Beams Strengthened with Different Techniques (Ö nal et al. 2014)					
	Beam	geometry	fc'	longitudinal rebar	stirrup	a/d	# of specimen
		100x160x2200	16	2-D12	D8/150	7.41	27
	Strengthening method(C/T)	**Full/Half Concrete jacketing**(side 30mm, up & down 50mm/difference in arrangement rebar), **steel plates**(attach beam's 3 side with 6x50x1200mm steel plates), **CFRP**(0.13mm CFRP was used with different layer, a single ply at end part, 2 ply at the center)					
	Bond	Concrete jacketing: notch & stirrup D8/150 btw old stirrups Steel plates & CFRP : Epoxy					
	Variable	Strengthening Method					
	Max. Increase of strength	Full jacketing : 2 times higher than ref Half jacketing : 1.56 times Steel plates : 1.19 times CFRP : 1.34 times					
	Sum	Concrete jacketing proven its excellence in increase of strength as well as ductility(1.51times)					

Note : (C/T) after material means its compressive / tensile strength

* means flexural tensile strength

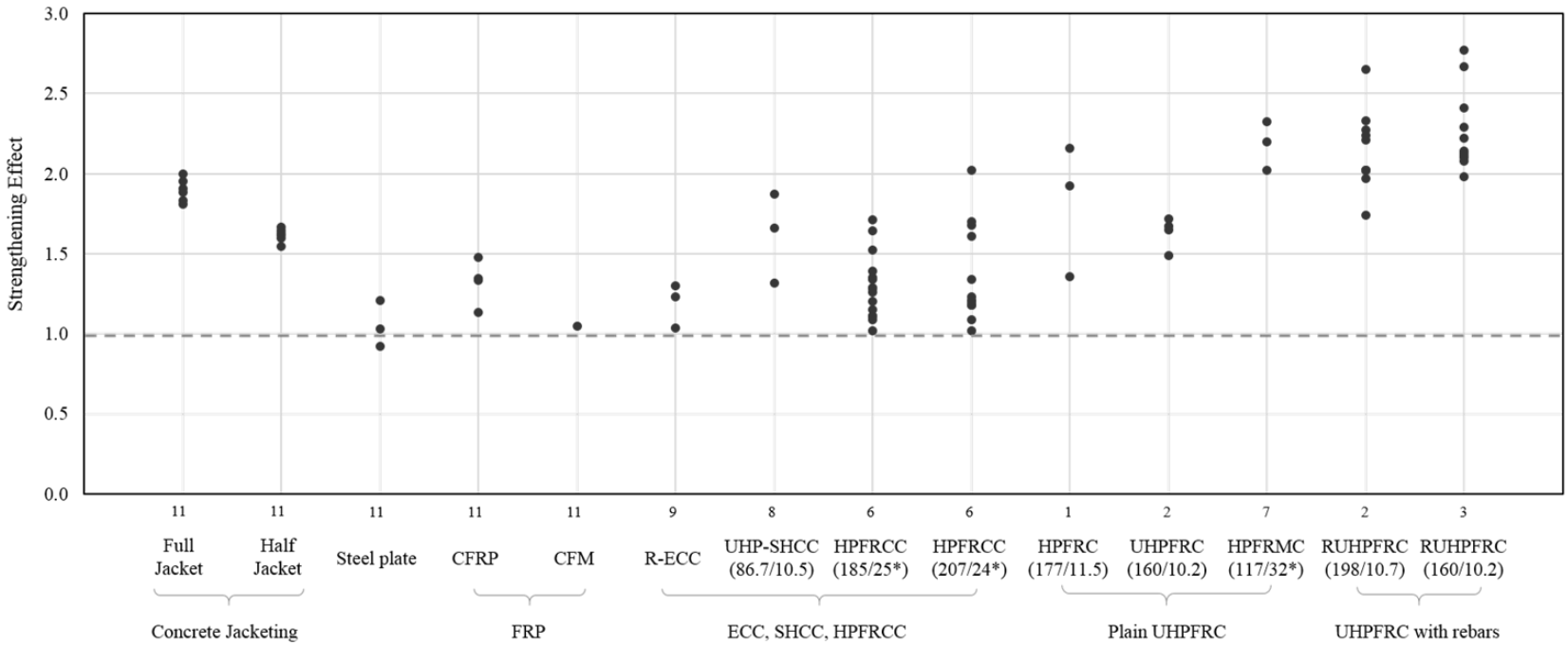

Fig 2-3 Strength increase comparison among various strengthening methods

2.4 Interfacial bond between UHPC and concrete

Because adhesion is an important factor in composite member, researchers spent particular attention to figure out the control of the adhesion between existing concrete and new material. Generally 5 kinds of tests are performed to determine the efficiency of bond performance; direct tension test, direct shear test, indirect tension test(e.g. splitting prism or cylinder test), shear and compression test(e.g. slant and shear test), and pull-off test. Most experiments were conducted by setting with surface treatment with a primary variable for their adhesion.

To sum up, sand blasting was the most excellent method as mechanical bondage. And after the surface treatment, moisture in cleaned surface is necessary to provide good bond.

Table 2-2 Preceding research about interfacial bond between UHPC and concrete

Paper (year)	Characterization of the interfacial bond between old concrete substrate and ultra high performance fiber concrete repair composite (Tayeh, Abu Bakar, and Megat Johari 2012)
Variable	Surface texture (AC - no roughness / SB - sand blast / WB - wire brush / DH - drilled holes / GR - grooves)
Sum	- 4 type of test to check bond strength btw NC(38MPa)/UHPC(170MPa) : 1. slant shear test(100*100*300-15EA), 2. splitting tensile test(10mm dia*20mm-15EA), 3.rapid chloride permeability test (RCPT), 4. scanning electron microscopy(SEM) - The surface of the roughened NC substrates was moistened for 10 min and wiped dry with a damped cloth - Test results : cast surface < DH surface < WB surface < grooved surface < SB surface Especially, the bond strength of SB surface improved upto 2 times than AC
Paper (year)	Characterization of Interface Bond of Ultra-High-Performance Concrete Bridge Deck Overlays (Harris, Sarkar, and Ahlborn 2011)
Variable	Surface texture: Smooth, Wire brush, chip(low roughness), groove(high roughness), shear key
Sum	1. slant shear cylinder test(dia.152mm × 203mm) - more sensitive to the interface roughness, test results: sm<chip<shear key≤groove - Even distribution of surface preparation show better performance 2. splitting prism test(102 mm × 76 mm × 406 mm(38 mm each)) - less sensitive, test results: sm>wire brush>groove, In the case of grooved specimens, UHPC did not completly filled in the groove.

	NC(34MPa)/UHPC(103MPa : curing under ambient conditions for 10days to mimic field conditions) 27 for sst /47 specimens for sct
Paper (year)	Bond Strength between UHPC and Normal Strength Concrete (NSC) in accordance with Split Prism and Freeze-Thaw Cycling Tests (Miguel A. Carbonell, Devin K. Harris, Sarah V. Shann, Theresa M. Ahlborn 2012)
Variable	Surface moisture, freeze thaw-cycling(300/x), surface treatment(chipped, brushed, sandblast ,grooved)
Sum	- Splitting tensile test to measure the bond strength upto the surface conditions. 60 composite specimens : NSC(45MPa)/UHPC(153MPa)-102x76x394 mm(38 mm each) - The moisture condition of the concrete substrate is saturated before placing the overlay material, regardless of the surface treatment applied. - When UHPC is used as overlay material on a saturated substrate, a simple surface treatment that removes the dust from the concrete surface is enough to achieve a good bond.
Paper (year)	Best Practices for Preparing Concrete Surfaces Prior to Repairs and Overlays - Report of U.S. Department of the interior bureau of reclamation technical service center(Bissonnette, Vaysburd, and Fay 2012)
Sum	Factors affecting bond strength 1. Interface Texture (roughness) : depending on the method of substrate surface preparation / A high interface roughness may improve shear bond strength, whereas tensile mechanical bond strength primarily depends on vertical anchorage in pores and voids. 2. Moisture condition : A dry, “thirsty” concrete surface tends to pull water from the overlay material, which may result in a weak interfacial repair layer and low bond strength. A surface that is too wet tends to dilute the repair material at the interface by increasing the water/cementitious materials ratio, which leads to lower material strength, increased shrinkage, and low bond strength. 3. Repair Material Properties: A relatively fluid mixture (made so without excess water) further enhances capillary suction in the substrate and, therefore, improves physical anchorage in substrate surface pores and cavities. Self-leveling mortar applied for overhead repair using formwork was found to have very good bond properties in terms of its ability to fill cavities at the interface. 4. Material strength and effective surface area 5. Surface cleanliness

Chapter 3. Strengthening RC beams without stirrups with Ultra High Performance Concrete

3.1 Experimental program

3.1.1 Introduction

This study investigates the structural performance of retrofitted RC-UHPC composite members through measuring the effectiveness of shear strengthened RC beams with different regions and thickness. Thanks to relatively high tensile stress of UHPC, the strengthened thickness could be thinner than conventional concrete jacketing. For adhesion between existing concrete and UHPC, sandblasting is applied to give enough roughness. 12 specimens except one control beam were strengthened with differences in thickness, regions, fiber volume and additional reinforcement. The experimental results show that jacketing beam with UHPC is effective to enhance strength and deflection.

3.1.2 Test specimens and Variables

The test specimens consists of 12 RC-UHPC composite beams and one reference RC beam. As shown in **Fig 3-1, Fig 3-6**, the shape of reference beam was 3.3m in length with a width of 200mm and a depth of 400mm. All beams were reinforced with only two bottom longitudinal rebars with 16mm diameter. The tail cover of the bottom longitudinal rebars were given enough to guarantee a good anchorage and to avoid any slip during loading. The control beam designed to be failed in flexural shear.

There are four kinds of main variables : strengthening region(soffit, side, U-shaped), thickness(20, 30, 40mm), steel fiber volume(0.5%, 1.5%, 2%) and additional reinforcement(steel rebars, wire mesh) with UHPC strengthening.

Strengthening region is divided into 3 ranges(soffit, side and U-shaped jacket). When the beams are strengthened, generally strengthening the bottom parts of beam for bending, the side parts for shear. If the both parts are retrofitted

together, the beam would be strengthened for flexure and shear.

The thickness for each ranges was set to 20mm, 40mm and in some cases set to 30mm. Habel et al(2006) recommend 10-20% thickness compared with height of original RC. Also, to reduce the jacketed thickness thinner than 50mm, chosen by pre researchers, 40mm(10% of RC height) and 20mm(5% of RC height) is chosen in this research.

Tensile stress tends to be governed by the steel fiber content of UHPC. To observe the effect of fibers, 3 types of steel fiber volume ratio were selected; 0.5%, 1.5%, 2%. The reason why these numbers are chosen is that the basic UHPC mixing has 1.5% steel fiber volume ratio and UHPC can't be mixed with more than 2% steel fiber volume ratio.

For the additional reinforcement, it is added into U-shaped 40mm jacketed UHPC. Meda et al(2014) use steel mesh fabric and Oesterlee(2010) and Noshiravani(2013) use reinforced rebars with UHPFRC. Especially Oesterlee already tested RC-UHPFRC composite beam with smooth and ribbed UHPFRC reinforcing bars and plain RC-UHPFRC. In this research, ribbed reinforcement bars(2-D10) are applied to increase ultimate strength.

The test variables for each beam are listed in **Table 3-1**. The beam names distinguish between the beams with base(b), side(s) region with strengthened thickness. In case of Specimens having different steel fiber vol. from normal portion, it was written fiber volume after Capital letter 'F'. In case of additional reinforcements, '-WM' are added for wire mesh and '-RS' are added for reinforcement bars.

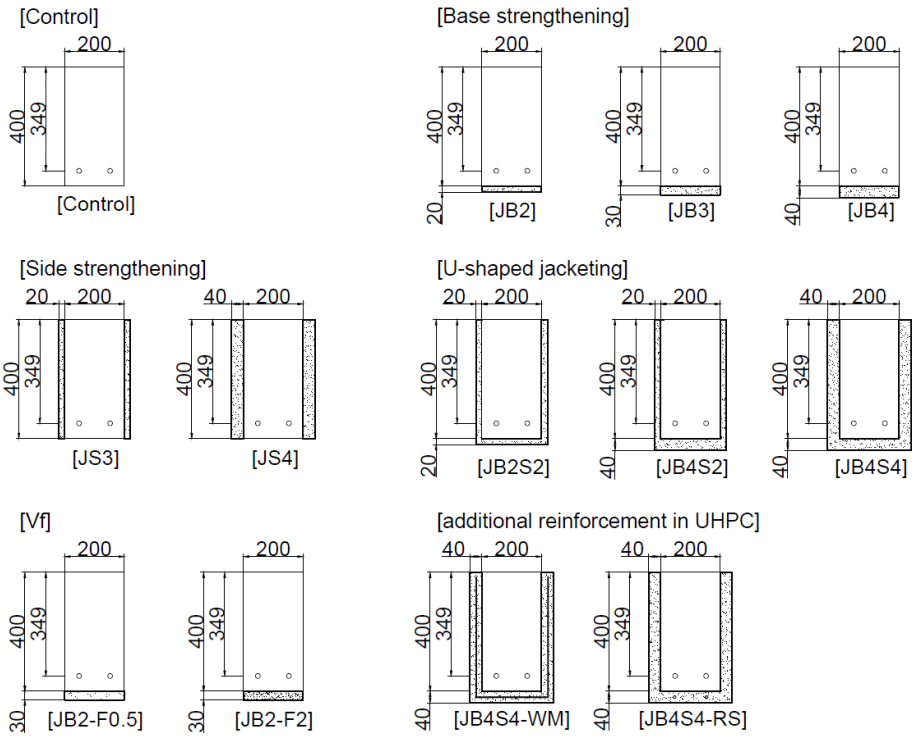

Fig 3-1 Section of Specimens

Table 3-1 Variables and Specimens

No	Name	V_f [%]	t_b [mm]	t_s [mm]	Additional reinforcement
1	CON	-	-	-	-
2	JB2	1.5	20	-	-
3	JB3	1.5	30	-	-
4	JB4	1.5	40	-	-
5	JS2	1.5	-	20	-
6	JS4	1.5	-	40	-
7	JB2S2	1.5	20	20	-
8	Jb4S2	1.5	40	20	-
9	JB4S4	1.5	40	40	-
10	JB2-F0.5	0.5	20	-	-
11	JB2-F2	2	20	-	-
12	JB4S4-WM	1.5	40	40	Wire mesh D3.2
13	JB4S4-RS	1.5	40	40	Rebar 2-D10

3.1.3 Surface preparation

The production process was shown in **Fig 3-3**. First of all, 13 existing RC members are manufactured only with longitudinal rebars.(**Fig 3-3**(a)(b)) After curing, 12 Specimens were sandblasted with 100MPa air pressure in order to reach a roughness of about 3-4mm, until the surface aggregate exposed enough.(**Fig3-3**(d), **Fig3-2**) Martinola et al(2010) already has demonstrated effectiveness of this technique. After that, molds were installed. Before applying UHPC jacketing, the surface was cleaned by air compressor and was supplied with a little humid. These methods affecting into bond strength are described in Best Practices for Preparing Concrete Surfaces Prior to Repairs and Overlays.(**Fig3-3**(e),(f)) Then the jackets were applied.(**Fig 3-3**(g)) Slump value of UHPC was 23cm and air contents of that was 2.5%. While UHPC cast, steel fibers were stick together especially in cases of 20mm side strengthened specimens and wire mesh added one, which has difficulty to distribute the fibers evenly. It is necessary to ensure the fluidity by placing UHPC more dilute. After that, All specimens were subjected to high temperature curing for 72 hours.(**Fig3-3**(h))

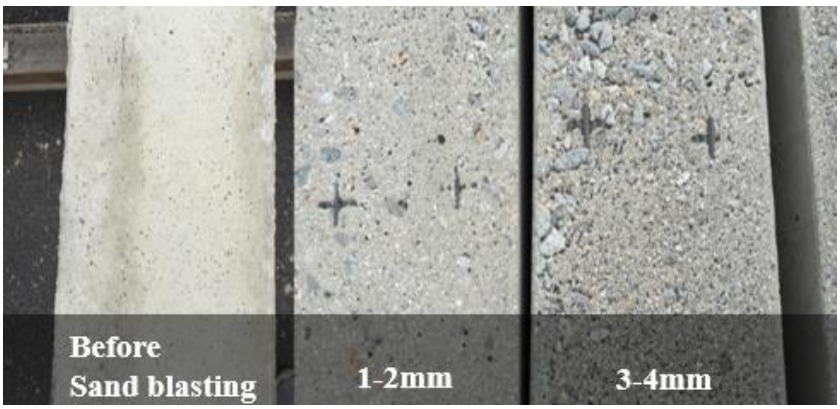

Fig 3-2 Comparison of surfaces before and after the sandblasted

(a) Arrangement re-bar

(b) Placing concrete

(c) After curing, dissolution form

(d) Sandblast

(e) Removing debris

(f) Providing humidity

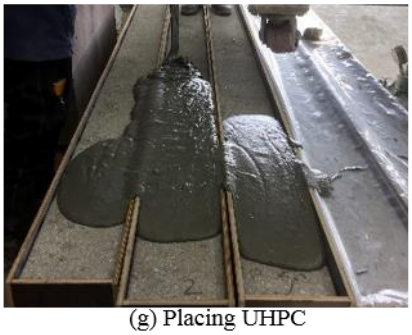

(g) Placing UHPC

(h) Steam curing

Fig 3-3 Procedure for manufacture for strengthening beam

3.1.4 Material properties

The mixture portions of concrete with nominal compressive strength of 35MPa are shown in **Table 3-2.** Concrete standard specimens of 10cm x 20cm size were casted according to KS F 2403 and 3 specimens were tested following with KS F 2405. The test results are shown in **Fig 3-4**(a)**.** Actual compressive strength of concrete was 38MPa.

In the case of reinforcement used in this research, direct tension test results and material properties are listed in **Table 3-3.** D16 acting as main longitudinal reinforcement in RC beams showed 540MPa yield strength. The yielding strength of D10 and wire mesh used as additional reinforcement with UHPC showed 521MPa and 462MPa, respectively.

Table 3-2 Mixture portions of concrete

Nominal Strength (Mpa)	W/C (%)	S/a (%)	Unit weight(kgf/m³)				
			Cement	Water	Sand	Gravel	Admixture
35	37.5	40.5	440	165	701	1049	3.08

Table 3-3 Material properties of reinforcement

Type	Steel grade	Dia.	spacing(cm*cm)	f_{sy} (Mpa)	f_{su} (Mpa)	Surface
Rebar	SD400	D16	-	540	628	Ribbed
Rebar	SD400	D10	-	521	628	Ribbed
Wire Mesh		D3.2	10*10	462	578	Smooth

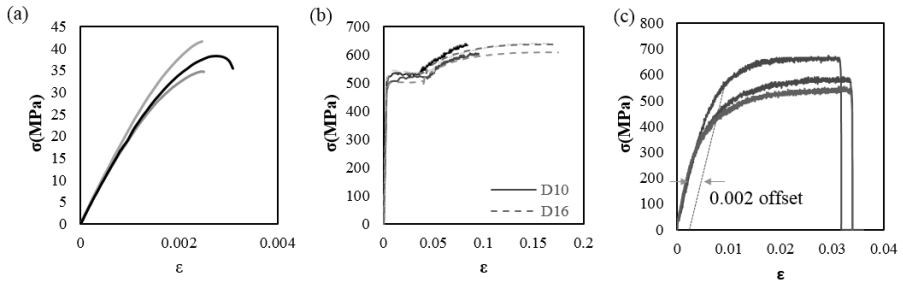

Fig 3-4 Material properties of existing RC beams and additional reinforcements : a) Compressive stress-strain curve of 35MPa concrete, b) Tensile stress-strain curve of SD400 D10, D16 and c) Tensile stress-strain curve of wire mesh D3.2

UHPC mixing proportion is like as **Table 3-4.** The steel fiber consisted of 19.5mm and 16.3mm fibers mixed in the ratio of 2:1. According to the characteristic values provided by manufacturer, the fibers tensile strength is 2500MPa.

Compression test for UHPC was carried out in the same way for normal concrete. Its compressive strength was 177MPa and maximum strain is about 0.004.(**Fig 3-5**(a)) **Fig 3-6**(b),(c) showed the results of direct tensile test of notched dog-bone specimens and flexural tensile test of notched prisms.

Table 3-4 UHPC mixing composition

Nominal Strength	W/B	Cement	Silica fume	Sand	Filing powder	Superplasticizer	Steel fiber vol.
(Mpa)	(%)	(kg/m³)	(kg/m³)	(kg/m³)	(kg/m³)	(kg/m³)	(%)
180	23	783.2	195.8	861.52	234.96	15.66	1.5

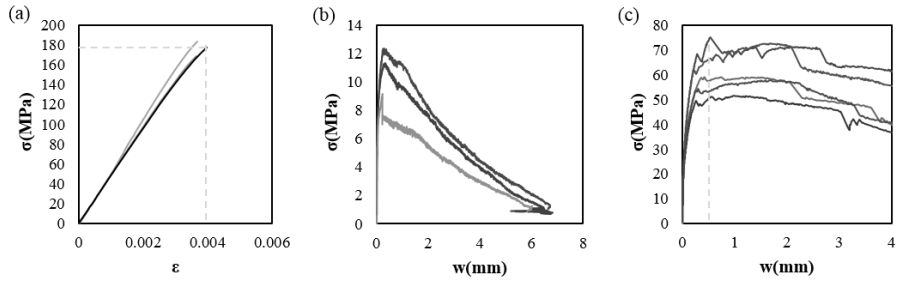

Fig 3-5 UHPC properties: a) Compressive stress-strain curve, b)Tensile stress-crack width curve, c)Flexural tensile stress-crack width curve

3.1.5 Test setup and procedure

Four point bending tests were performed under displacement control at a rate of 2 mm/min. (**Fig.3-7**) To measure the displacements, linear variable displacement transducers were installed at 3 points under the beam. Steel gauges were attached on the center of 2 longitudinal reinforcing bars. Concrete gauges were attached along the sections at different heights in the middle of beams. Shear-span/effective depth ratio (a/d) = 3 for beams was selected. (**Fig.3-6**)

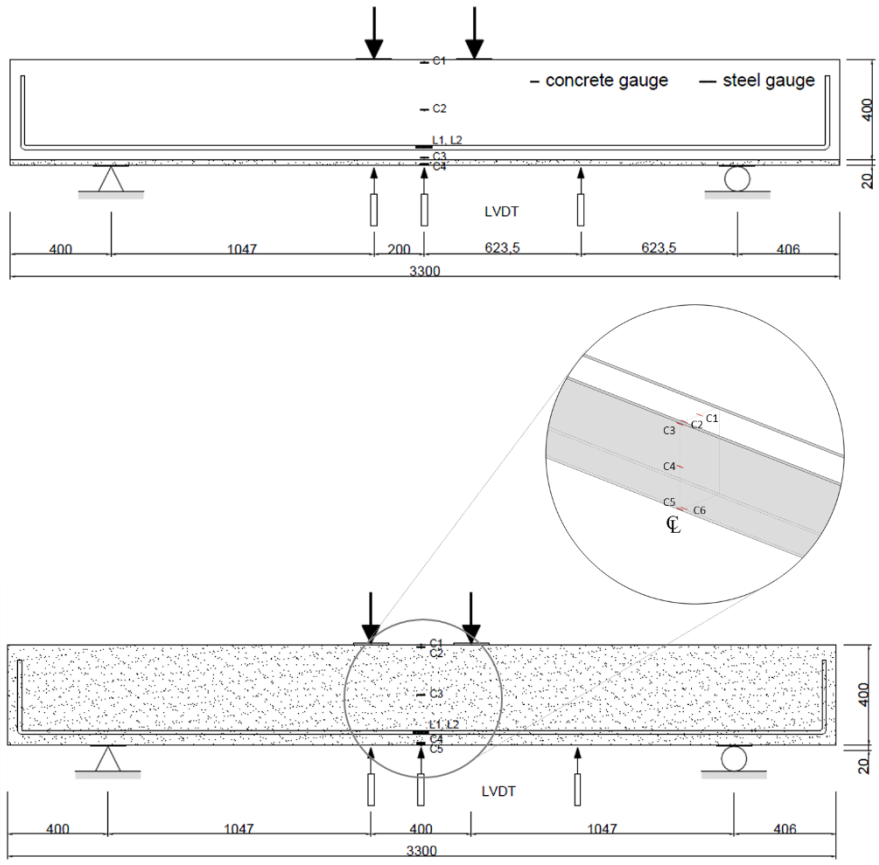

Fig 3-6 Beam geometry and instrument devices

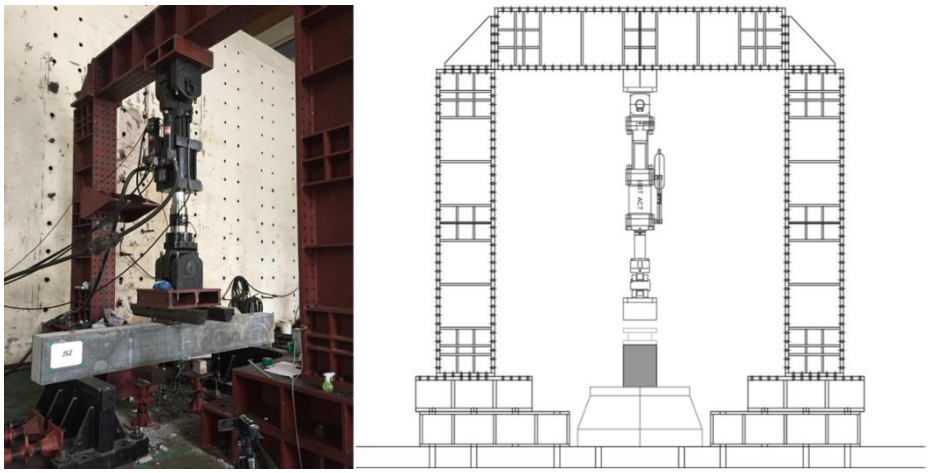

Fig 3-7 Test set-up

3.2 Test results

The beams are divided into three groups according to their failure along a flexural, a flexure-shear or shear collapse crack which is used to define the failure mode. The plots show the beam response either up to the first rupture of the tensile rebars.

3.2.1 Reference beam

Reference beam exhibits a linear elastic behavior up to 42 kN when initial crack occurred at mid-point of span. At the load value of 64.8 kN, reinforcement bars yields. Then diagonal crack developed suddenly at 70kN with an angle close to 21 degrees to the axis in the shear span. Soon the beam reached its ultimate strength at 71.3 kN. To compare the result of reference beam with strengthened beam, its load-deflection response is attached in other specimens' responses.

3.2.2 UHPC Side strengthened beam

Side strengthened beams showed a behavior controlled by flexural. They behaved according to the same failure pattern. Under increasing load, initial flexural crack appeared from the mid-point, however, the number of crack is less than reference beam. The yielding of reinforcements was observed at both beams. All monitored points are demonstrated in **Table 3-5**.

On the extreme compression layer RC beam, concrete crushing occurred only at RC parts. UHPC parts divided by macro crack at center behaves as rigid body hanging on to RC. At the bottom part of mid-span, RC behaved separately with UHPC by deflected more. The reason might be poor attachment of UHPC due to its shrinkage, so interface slip about 8mm occurred in the course of the experiment.

To compare the compressive strain value, the additional gauges are installed on these two specimens, because the maximum extreme compressive strain is different between concrete (ε_{cu}=0.003) and UHPC($\varepsilon_{cu,uphc}$=0.0035-0.004). The results showed that the difference is less than 10%.

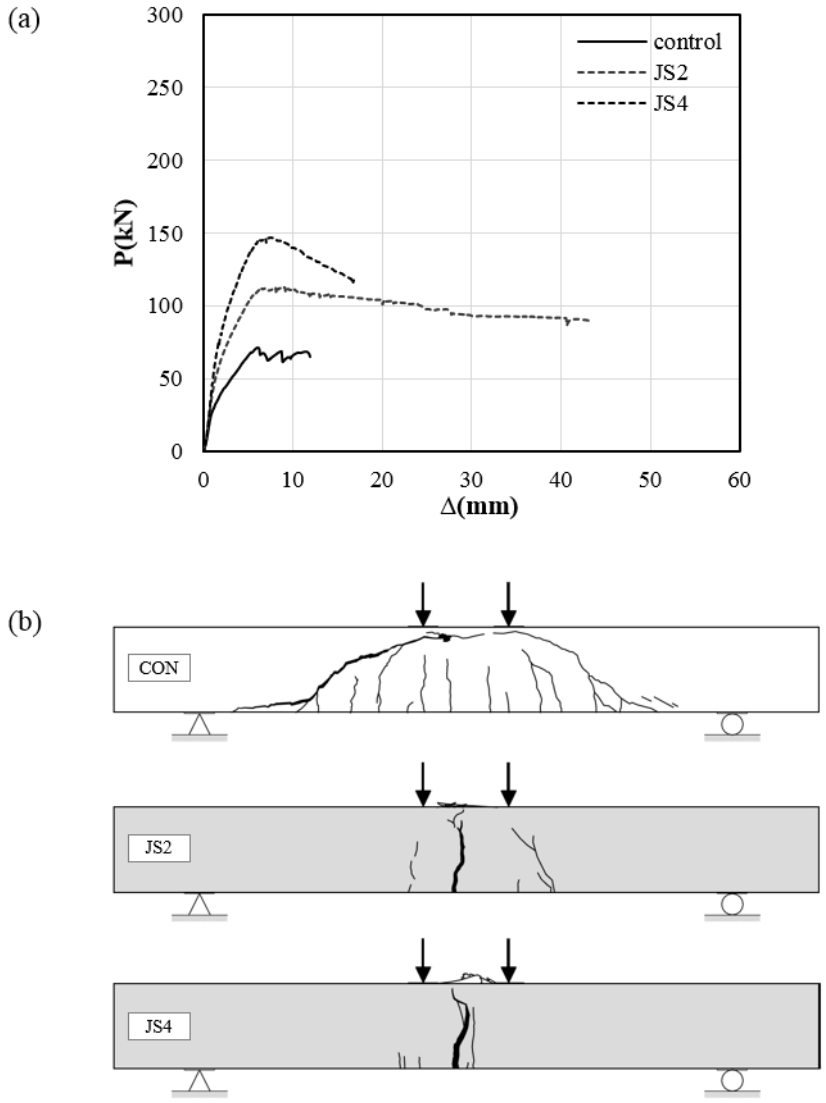

Fig 3-8 Test results of reference beam and UHPC side strengthened beams : a)Load-center deflection responses, b) Fully developed crack patterns at the end of the test

Table 3-5 Test results of reference beam and UHPC side strengthened beams

Beam	Failure	$\mathbf{P}_{cr}$[kN]	$\mathbf{P}_{y}$[kN]	$\mathbf{P}_{u}$[kN]	$\mathbf{P}_{failure}$[kN]	$\mathbf{K}_{e}$[kN/mm]	$\boldsymbol{\theta}_{c}$(ICD)[°]
CON	**FS**	**42.0**	**64.8**	**71.3**	**57.1**	**19.5**	**21**
JS2	F	87.5	110.7	112.2	89.7	25.7	86
JS4	F	80.0	146.0	147.2	117.8	16.8	83

3.2.3 UHPC Base strengthened beam

Base strengthened beams showed change of failure mode flexure-shear(JB2, JB3) to shear(JB4) as increasing UHPC thickness. The strengthened UHPC panel played a role as additional tension member like longitudinal rebar. Up to 30 mm strengthening, even though beams failed in flexure-shear, their ultimate strength increased in proportion to the UHPC thickness. Strength increase of JB2 is 1.32 times the ultimate resistance of the reference beam and that of JB3 is 1.49 times. However, JB4 showed 1.45 times the ultimate strength of the reference beam, which is less than the JB3. This is because JB4's tension side is heavily strengthened by 40 mm UHPC panel. So it caused the collapse of compression side of concrete and thereby rebars in existing beam did not yield. Also, by excessively strengthening on tension side, concrete crushing on compressive side was monitored at JB3 and JB4, which did not appear at JB2.

Concrete and UHPC have different extreme tensile strain value in the cracking point. In case of normal concrete, crack occurred in 300 μm and for UHPC in 2000 μm. But initial crack occurred from the bottom part of UHPC panel which positioned bottom part of the beams. Some kinds of cracks showed starting from lower part of the existing RC without link with UHPC.

As (Noshiravani 2012) mentioned, the diagonal crack starting from the web and as the crack developed to the tension side, especially close to the UHPC panel, its crack angle went lower. This Intermediated-Crack induced Debonding(ICD) lead hard to evaluate the behavior of UHPC strengthened beam based on the analysis of the monolithic composite section.

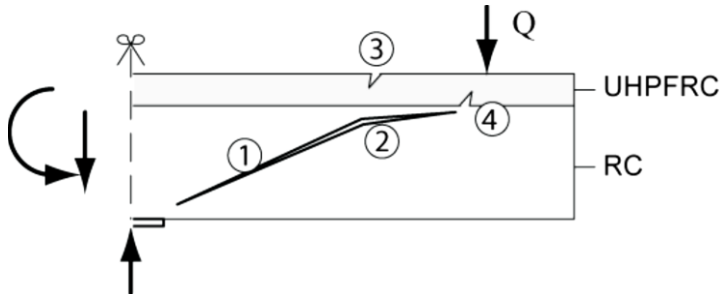

Fig 3-9 Flexural-shear collapse mechanism: typical crack pattern and formation of hinges(Talayeh Noshiravani 2010)

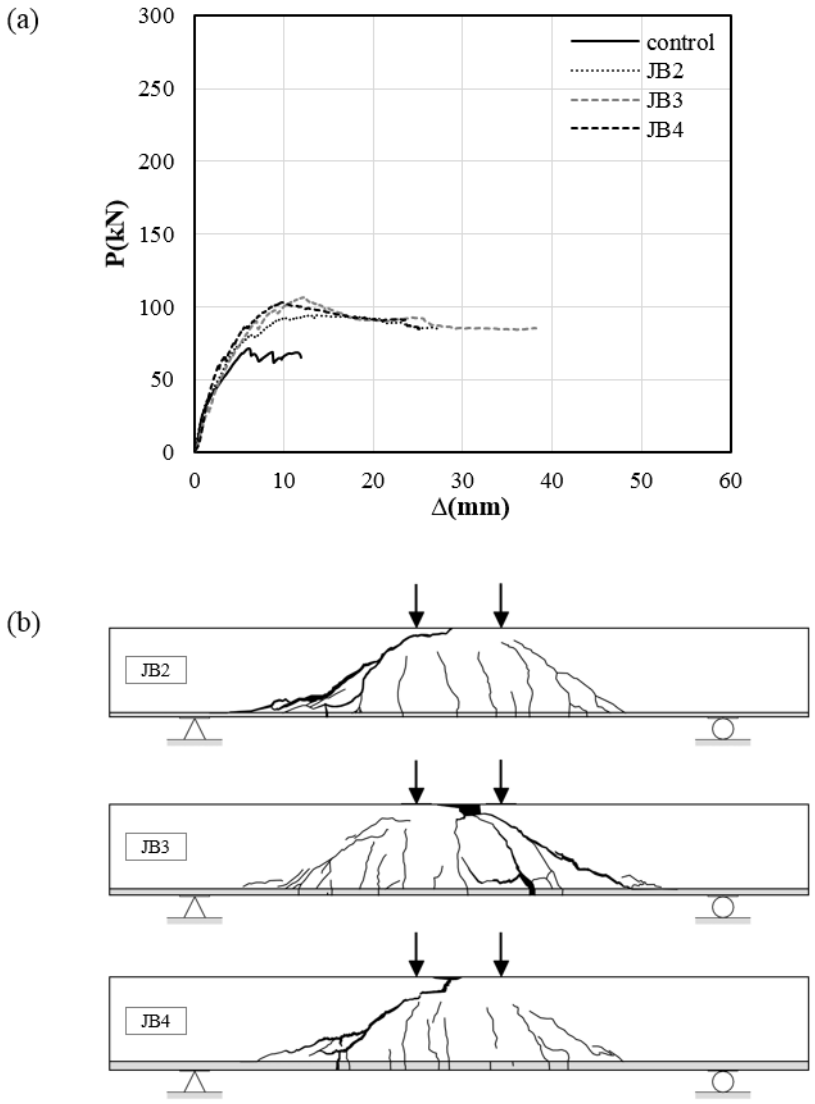

Fig 3-10 Test results of UHPC base strengthened beams : a)Load-center deflection responses, b) Fully developed crack patterns at the end of the test

Table 3-6 Test results of UHPC base strengthened beams

Beam	Failure	$\mathbf{P}_{cr}$[kN]	$\mathbf{P}_{y}$[kN]	$\mathbf{P}_{u}$[kN]	$\mathbf{P}_{failure}$[kN]	$\mathbf{K}_{e}$[kN/mm]	$\boldsymbol{\theta}_{c}$(ICD)[°]
CON	**FS**	**42.0**	**64.8**	**71.3**	**57.1**	**19.5**	**21**
JB2	FS	35.0	83.5	94.0	75.2	20.1	36(9)
JB3	FS	55.0	82.6	106.2	85.0	23.5	28(7)
JB4	S	65.0	-	103.3	82.7	42.1	40(15)

3.2.4 UHPC U-shaped jacketing

The three U-shaped jacketed beams exhibited mainly flexural failure. Ductile behavior with limited softening after maximum load, and a final collapse with bending. The collapse was triggered by the development of a macro vertical crack, located at mid-span. Their collapse were similar to those of the side strengthened beam which increase shear resistance. So, U-shaped jacketing also changed the flexure-shear failure of RC beam to flexural failure mode. Especially, with 20 mm side strengthening enough to switch failure mode. And the test results showed that it seemed more efficient to strength the soffit of the beam by sufficient shear resistance. Between JB2S2 and JB4S2, increase of the load is 17.2 kN which is higher than 9.9 kN that is the increase of the load between JB4S2 and JB4S4. Unlike JS2 and JS4, the debonding failure didn't occurred in U-shaped jacketing due to three-sided jacket. However, from the upper part of UHPC jacket where compressive stress work, the jacket become widen from the RC beam.

After the peak load, the flexural response started softening until the UHPC contribution was fully exhausted at some point where load reduced minutely(JB2S2 : Δ=19 mm, JB4S2 : Δ=32 mm, JB4S4 : Δ=31 mm) and that point, the steel gauge values soared up. Because the tensile strain of UHPC is smaller than that of rebars, UHPC in tension side reached its ultimate stated at first. According to previous research(Oesterlee 2010), in this phase the deformation of the beam was concentrated in one macro crack. Since in the mid-span the moment was constant, UHPC macro-crack occurred at the weakest section.

By the investigation of the extreme compressive strain, it increased linearly up to the maximum load, then the gauge values are as follows: 2273 μm in JB2S2, 1457 μm in JB4S2, 3381 μm in JB4S4. Except JB4S2, the extreme compressive values are maximum value. In case of JB4S2 reached its maximum value after the maximum load and then the value is 2910 μm.

All observed points are demonstrated in **Table 3-7**.

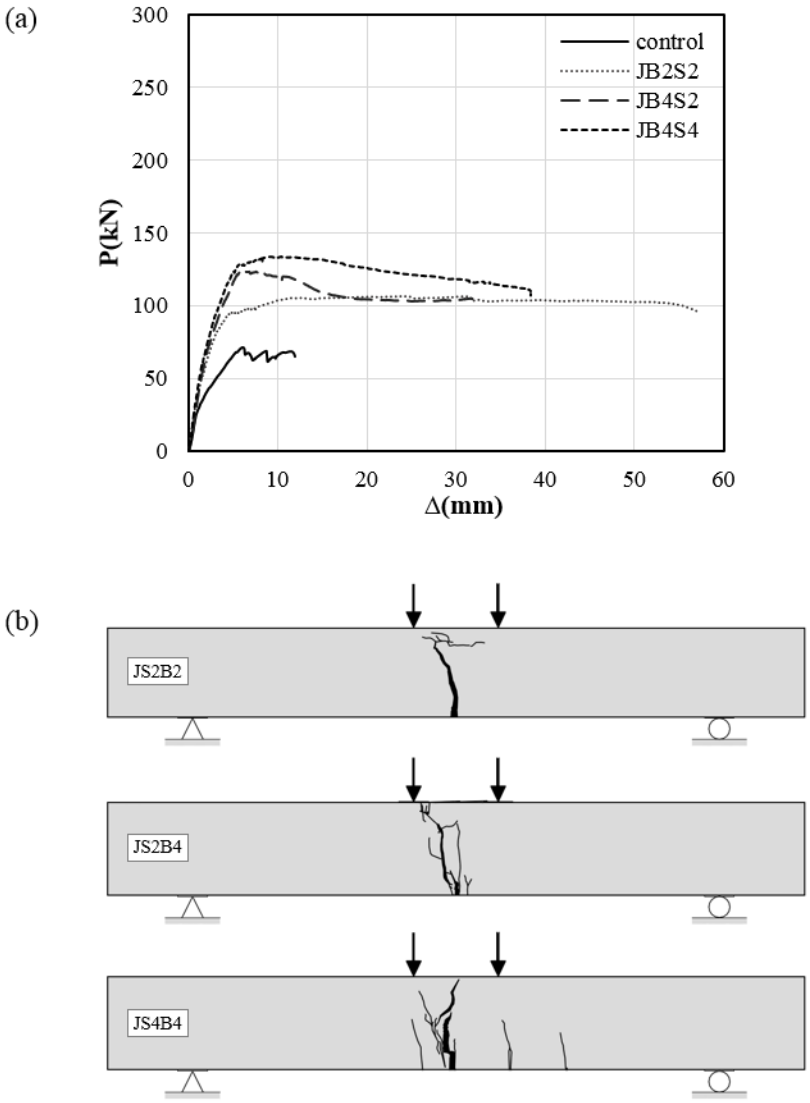

Fig 3-11 Test results of UHPC U-shaped jacketed beams : a)Load-center deflection responses, b) Fully developed crack patterns at the end of the test

Table 3-7 Test results of UHPC U-shaped jacketing beams

Beam	Failure	$\mathbf{P}_{cr}$[kN]	$\mathbf{P}_{y}$[kN]	$\mathbf{P}_{u}$[kN]	$\mathbf{P}_{failure}$[kN]	$\mathbf{K}_{e}$[kN/mm]	$\boldsymbol{\theta}_{c}$(ICD)[°]
CON	**FS**	**42.0**	**64.8**	**71.3**	**57.1**	**19.5**	**21**
JB2S2	F	25.1	106.4	106.6	94.7	44.0	77
Jb4S2	F	55.1	104.2	123.8	104.3	35.3	79
jB4S4	F	40.1	116.2	133.7	106.9	42.6	88

3.2.5 UHPC Base strengthened beam with different fiber volume

Theoretically ultimate tensile strength of steel fiber reinforced concrete is affected by fiber's orientation, distribution, aspect ratio, and volume. Especially, in this research, due to strengthened UHPC acting mainly as tensile member, steel fiber is supposed to be most significant parameter. However, the results show that its effects are very small.

Due to the strengthening region restricted to base, their failure modes are similar to those of the base strengthened beams in **3.2.3**. The strengthened thickness restricted in 20mm. At first, flexural crack occurred like other specimens. Then rebars yielding was observed after diagonal cracking. After reaching ultimate strength, the beam failed in flexure-shear.

The increase of ultimate load for specimens is proportional to fiber contents : JB2-F2(+31.7 kN) > JB2-F1.5(22.7 kN) > JB2-F0.5(+20.5 kN). However, it was difficult to conclude that the fiber volume affect to increase of strength proportionally. JB2-F1.5 containing steel fiber three times more than JB2-F0.5 showed little increase of strength. Compared with steel fiber contents, the ultimate strength difference between JB2-F2 and JB2-F1.5 is smaller than that between JB2-1.5 and JB2-0.5, on the other hand, strength increase is bigger. It showed that the steel fiber volume is less important in strengthening.

1.5% of steel fiber volume showed less effective compared with 0.5%. However, 1.5% of steel fiber volume was default value, all specimens except JB2-F0.5 and JB2-F2 strengthened with it. Moreover it seems that 0.5% steel fiber volume UHPC could be possible to use as strengthening material.

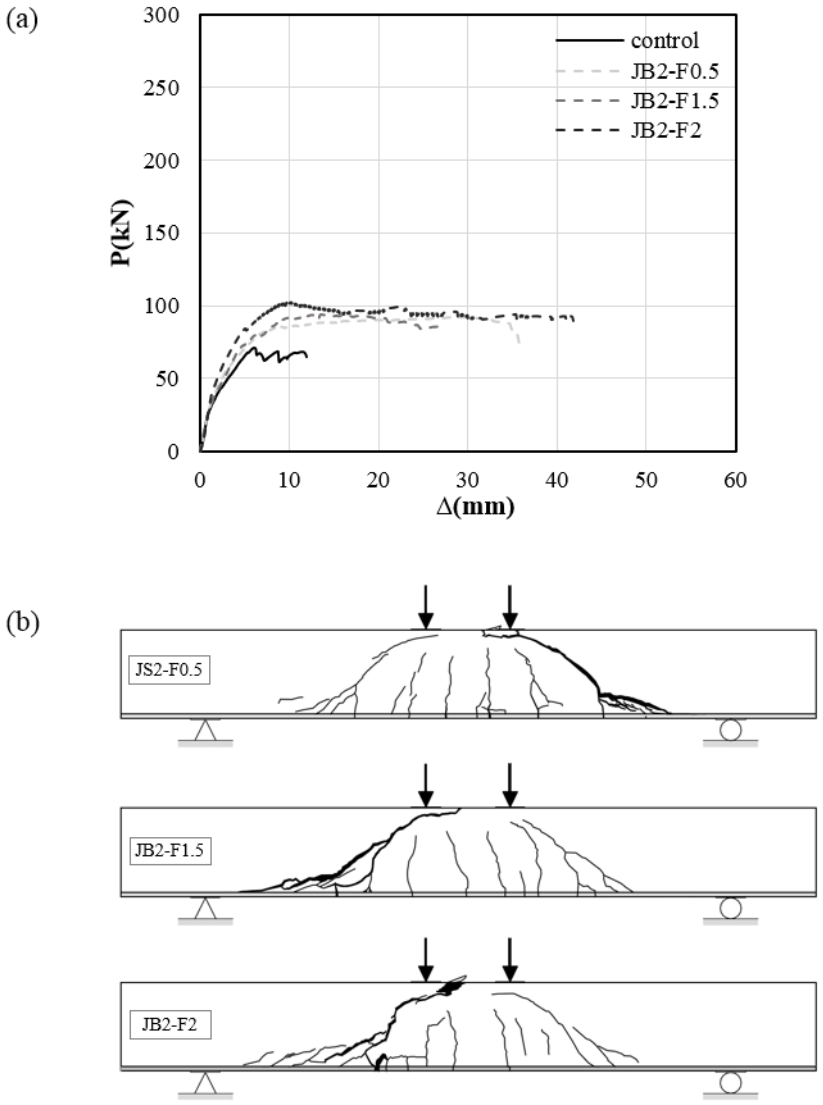

Fig 3-12 Test results of UHPC base strengthened beams with different fiber volume : a)Load-center deflection responses, b) Fully developed crack patterns at the end of the test

Table 3-8 Test results of UHPC base strengthened beams with different fiber volume

Beam	Failure	$\mathbf{P}_{cr}$[kN]	$\mathbf{P}_{y}$[kN]	$\mathbf{P}_{u}$[kN]	$\mathbf{P}_{failure}$[kN]	$\mathbf{K}_{e}$[kN/mm]	$\boldsymbol{\theta}_{c}$(ICD)[°]
CON	**FS**	**42.0**	**64.8**	**71.3**	**57.1**	**19.5**	**21**
JB2-F0.5	FS	45.0	84.4	91.8	72.5	22.4	35(14)
JB2-F1.5	FS	35.0	83.5	94.0	75.2	20.1	36(9)
JB2-F2	FS	60.0	102.6	103.0	89.9	23.2	30(11)

3.2.6 UHPC U-shaped jacketing with additional reinforcement

With additional reinforcement bars in UHPC, JB4S4-RS showed the most effective strengthening method. Strength increase of JB4S4-RS is 2.42 times the ultimate resistance of the reference beam. Stiffness increase also 2.42 times the initial stiffness of reference beam. On the other hand, JB4S4-WM showed less effective than JB4S4 which is strengthened only UHPC. This is because when UHPC was placing, the fiber caught by wire mesh which is installed before placing.

The failure mode of JB4S4-RS was governed by bending. After initial flexural crack at 55kN, the load reached its peak at 172.9 kN without existing rebar yielding. At points(Δ=22, 36 mm) where the load deflection curve showed sudden drop, the reinforcing bars in UHPC were ruptured two time(2 rebars were placed in UHPC as additional reinforcement). After that, likewise U-shaped jacketing, as UHPC's contribution in tension was fully exhausted where the deflection is 42.8 mm, the steel gauge value soared up. About the crack pattern, JB4S4-RS showed multiple micro-cracking with macro-crack.

The failure mode of JB4S4-WM was also governed by bending. This specimen reached its ultimate limit strength 119.2 mm at Δ=26 mm. When deflection is 28 mm, the rebars seemed to be under sudden load as extreme tensile part of UHPC didn't resist.

In the view of the extreme compressive strain, the maximum gauge values are as follows: 2750 μm in JB4S4-RS after maximum load, 3589 μm in JB4S4-WM at maximum load.

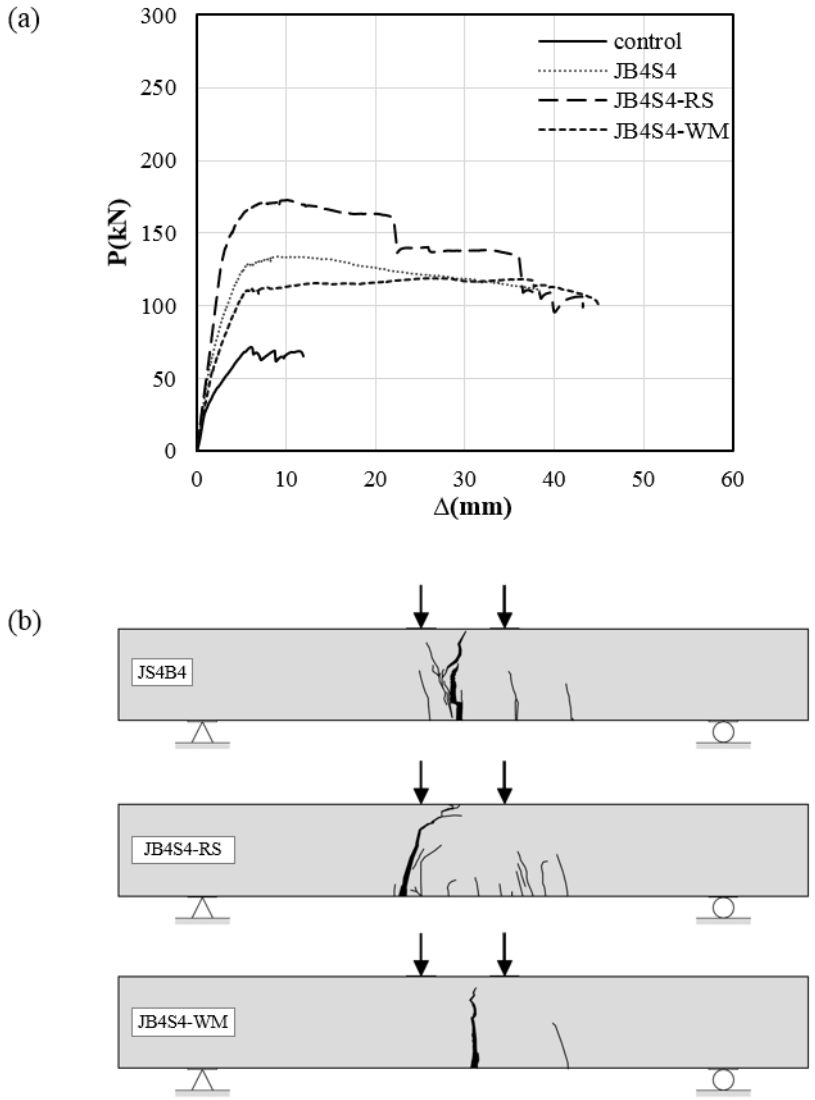

Fig 3-13 Test results of UHPC U-shaped jacketing with additional reinforcements : a)Load-center deflection responses, b) Fully developed crack patterns at the end of the test

Table 3-9 Test results of UHPC U-shaped jacketing with additional reinforcement

Beam	Failure	$\mathbf{P}_{cr}$[kN]	$\mathbf{P}_{y}$[kN]	$\mathbf{P}_{u}$[kN]	$\mathbf{P}_{failure}$[kN]	$\mathbf{K}_{e}$[kN/mm]	$\boldsymbol{\theta}_{c}$(ICD)[°]
CON	**FS**	**42.0**	**64.8**	**71.3**	**57.1**	**19.5**	**21**
JB4S4	F	40.1	116.2	133.7	106.9	42.6	88
JB4S4-RS	F	55.2	106.4	172.9	138.4	47.2	78
JB4S4-WM	F	60.0	118.4	119.2	100.5	29.9	87

Table 3-10 Summary of test results

Name	Failure	Load [KN]			Δ_u[mm]	Ductility Index			θ_c(ICD) [°]	ψ_u[rad]		Initial stiffness	Strengthened Effect		
		Initial vertical crack	Initial diagonal crack	P_u		Δ_u/Δ_{cr}	Δ_u/Δ_y	Δ_{max}/Δ_u		ψ_L	ψ_R		Strength Increase	Stiffness Increase	Ductility Increase
CON	FS	42	70	71.32	6.1	2.83	1.24	1.97	21	0.012	0.014	19.5	1.00	1.00	1.00
JB2	FS	35	75	94	13.5	9.96	1.77	2.00	36(9)	0.029	0.021	25.7	1.32	1.32	1.02
JB3	FS	55	90	106.2	12.2	3.74	2.04	3.13	28(7)	0.032	0.041	16.8	1.49	0.86	1.59
JB4	S	65	90	103.3	9.7	3.00	-	2.59	40(15)	0.026	0.024	20.1	1.45	1.03	1.32
JS2	F	87.5	107.5	112.2	9.0	2.42	1.43	4.79	86	0.039	0.035	23.5	1.57	1.20	2.43
JS4	F	80	-	147.2	7.5	3.92	1.10	2.26	83	0.014	0.012	42.1	2.06	2.15	1.15
JS2B2	F	25	-	106.6	23.7	41.58	0.76	2.42	77	0.049	0.044	44.0	1.50	2.25	1.23
JS2B4	F	55	-	123.8	6.0	3.83	0.31	5.46	79	0.029	0.025	35.3	1.74	1.81	2.78
JS4B4	F	40	-	133.7	8.8	9.40	0.27	4.34	88	0.034	0.037	42.6	1.88	2.18	2.20
JB2-F0.5	FS	45	70	91.8	29.0	14.41	3.42	1.23	35(14)	0.030	0.040	22.4	1.29	1.15	0.63
JB2-F2	FS	60	70	103	9.9	3.83	1.01	4.21	30(11)	0.049	0.040	23.2	1.44	1.19	2.14
JB4S4-RS	F	55	-	172.9	10.1	8.60	0.23	4.30	78	0.044	0.036	47.2	2.42	2.42	2.19
JB4S4-WM	F	60	-	119.2	26.0	12.96	0.91	1.73	87	0.037	0.038	29.9	1.67	1.53	0.88

3.3 Collapse mechanisms

The failure depends on its geometry, material properties, reinforcement detailing and loading configuration. Each failure mode can be described at **Table 3-11** and all specimens distinguished based on this table. This criterion is also applied in T-beams in **Chapter 4**.

Table 3-11 Collapse mechanisms

Failure	Property	Crack angle	Yielding	
			longitudinal	Stirrup
Flexural (F) failure	• Pure rotational mechanism • Rupture of rebar or crush of concrete at compression zone is observed	60° - 90°	o	x
Shear (S) failure	• Due to crushing of concrete weakened by the web-shear crack or the yielding of any vertical reinforcement crossing the crack • Occur in the presence of large concentrated forces close to supports	20° - 60°	x	o
Flexure-shear (FS) failure	• Begining as a rotational mechanism, nevertheless, the collapse of the member is a translational movement due to the crushing of concrete downstream from the crack tip	20° - 60°	o	o

3.4 Strengthening Effect

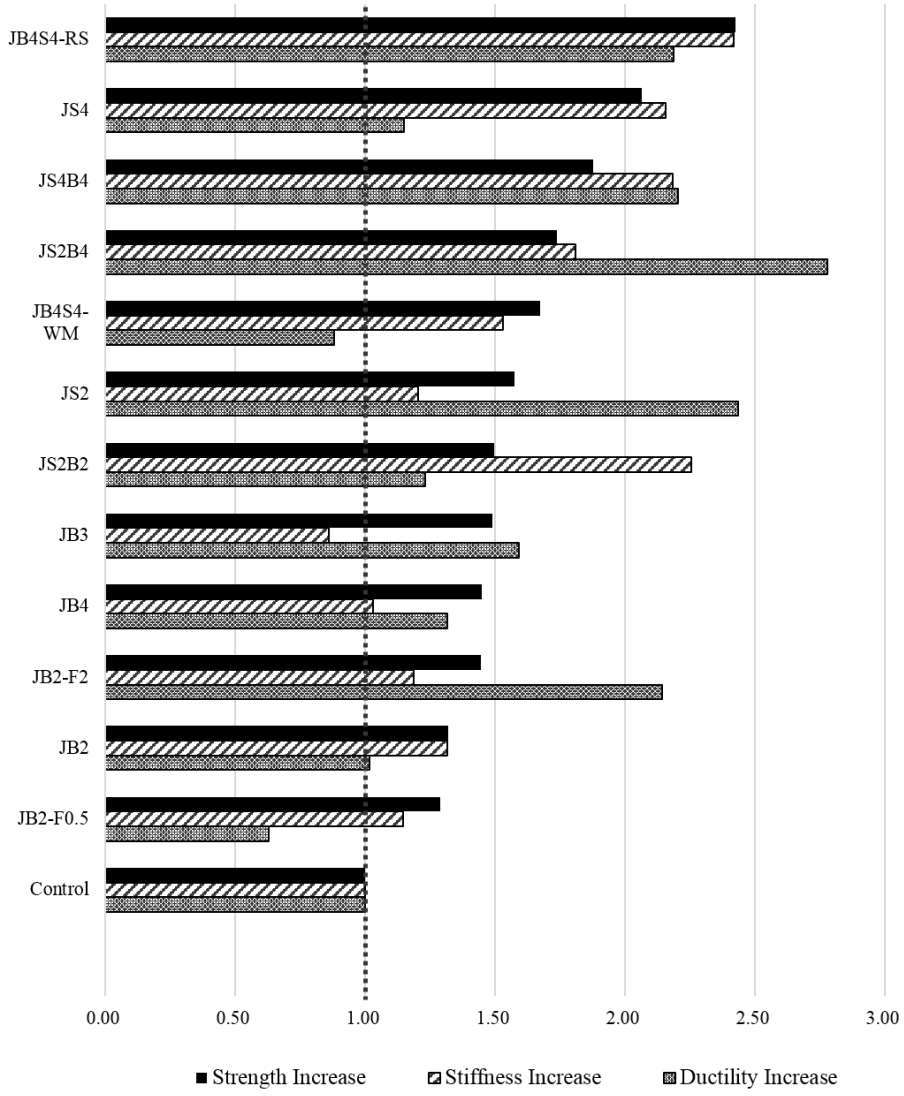

Fig 3-14 Strengthening effect compared with reference beam

To recognize strengthening effect, the entire beams were compared to the reference beam with ultimate strength, initial stiffness and ductility. The ductility index was obtained from the ratio between the displacements at failure which is defined as 80% of the maximum load and the displacements at maximum load. Strengthened effect are shown in **Table 3-10** and **Fig 3-14**. In **Fig 3-14**, the order of the chart was listed in descending order of strength increase.

From a strengthening viewpoint with improvement of strength, stiffness and ductility based on reference beam, JB4S4-RS showed the highest increase of capacity. Next, JS4 seemed like having good strengthening performance. However, it has low ductility level and UHPC panel fell off when the beam failed. Followed by JB4S4 has a good strengthening performance. Overall U-shaped jacketing was proved its efficiency as strengthening method. Especially, with additional rebars in UHPC, strength increase of JB4S4-RS is 1.29 times higher than that of JB4S4.

Fig 3-15 showed the increase of strength according to the test parameters. Except base strengthened member, all strengthened members are in proportion to the thickness of UHPC. In case of base strengthened with 40mm, excessive tensile reinforcement cause sudden shear failure before yielding of rebars. With regard to steel fiber volume, the strength increased slightly. The width of the difference between 5% and 15% is about 15%. For additional reinforcement in UHPC U-shaped jacketing, inserting rebar verified its excellent performance,

while wire mesh didn’t.

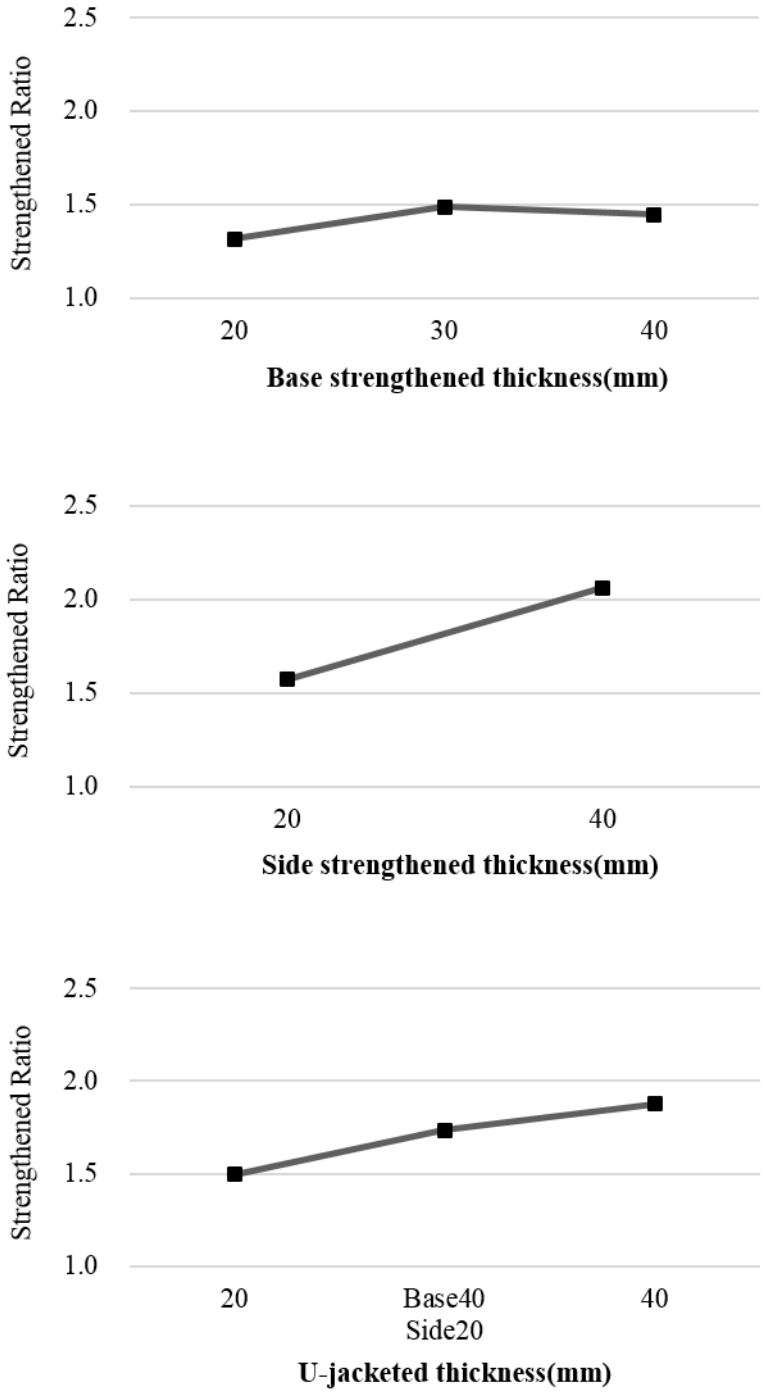

Fig 3-15 Increase of strength for strengthening region

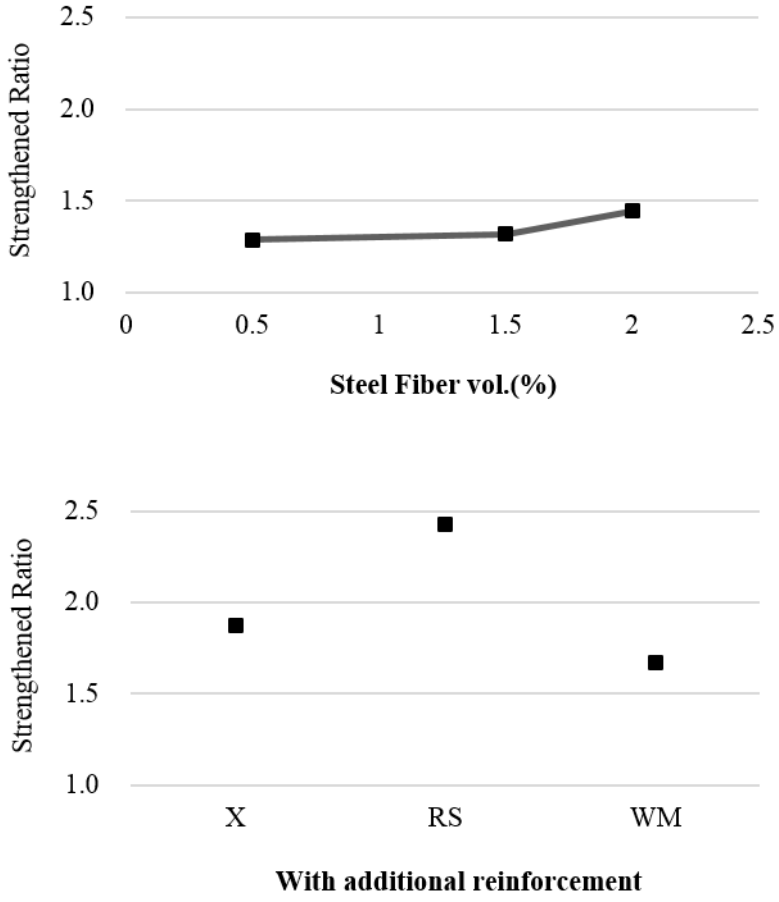

Fig 3-16 Increase of strength for additional reinforcement

3.5 Theoretical analysis

3.5.1 Flexural strength

1) Hypotheses

The strength model for flexural capacity is based on the following hypothesis :

1. Plane sections remain plane after bending. This means perfect adhesion between RC and UHPC, i.e. no debonding occurs at the interface and the structural element shows monolithic behavior. Also difference between ε_c and ε_{cu} are neglected.

2. The behavior of steel and cementitious materials follow linear elastic and plastic.

3. The equilibrium condition is satisfied.

2) Material laws

The stress-strain relationship of UHPC is modelled like **Fig 3-16**. The compressive behavior is modelled with a linear diagram based on the results of compressive test.(**Fig 3-6**(a)) It represents a nearly straight line up to maximum stress. So compressive stress can be estimated using the block of triangular shaped zone

The tensile behavior of the UHPC is modelled in constant value $\alpha_t f_{tk}$. Actual tensile stress-strain curve consists of multi-linear shape like **Fig 3-6**(b). However, for practical purpose many researchers simplified fiber effect in tension. In ACI544.4R-10, Henager and Doherty(1976) developed a method to predict the strength of beams with both bars and fibers by simplifying fibers effect as rectangular stress block. About UHPC, according to FHWA-HIF-13-032 report(Aaleti, Petersen, and Sritharan 2013), there is a proposal of rectangular tensile stress block in flexural behavior of UHPC members. Also, Yang who studied with same material suggested simplified representation of tensile block based on calculating from inverse analysis of the load-CMOD curves, as derived from the 3-points bending tests with notched specimens. (Yang, In Hwan·Joh 2010) Especially he suggested that $\alpha_t = 0.8$ showed

appropriate prediction of flexural capacity.

Elastoplastic behavior is assumed for the streel reinforcement. It is symmetric in tension and compression.

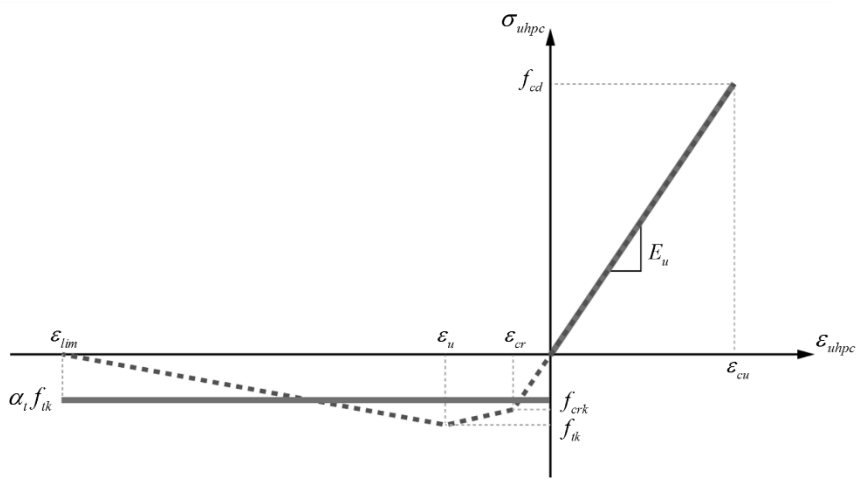

Fig 3-17 Stress-strain relationship modelling of UHPC

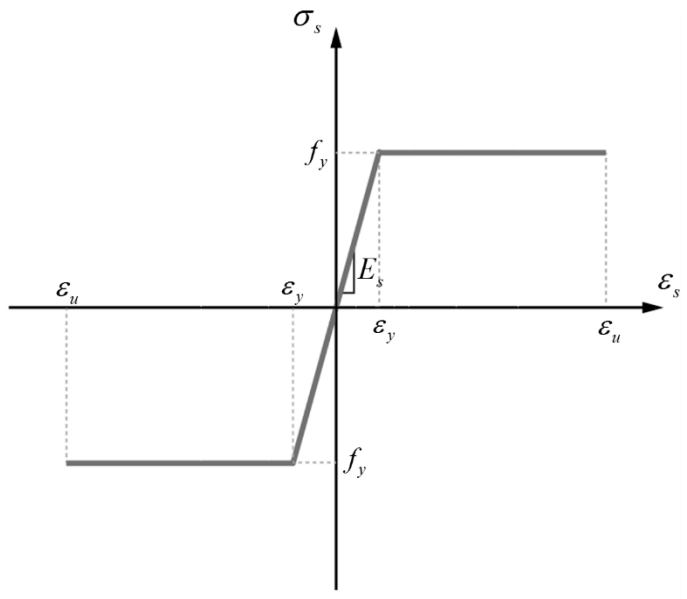

Fig 3-18 Stress-strain relationship of reinforcement rebar

3) Cracking moment

The limit of elastic state can be expressed from the conventional flexure formula, **Equation 1.** Rupture of concrete (f_r) came from KCI 2012.(**Equation 2**) Characteristic crack strength of UHPC is derived from direct tensile test. (From **Fig 3-5**(b), $f_{crk} = 4.3MPa$)

$$M_{cr} = \frac{f_r I_{gt}}{y} \tag{1}$$

$$f_r = 0.7\sqrt{f_c'} \tag{2}$$

where,

I_{gt} = uncracked transformed moment of inertia

y = centroid of the transformed section

4) Nominal flexural strength

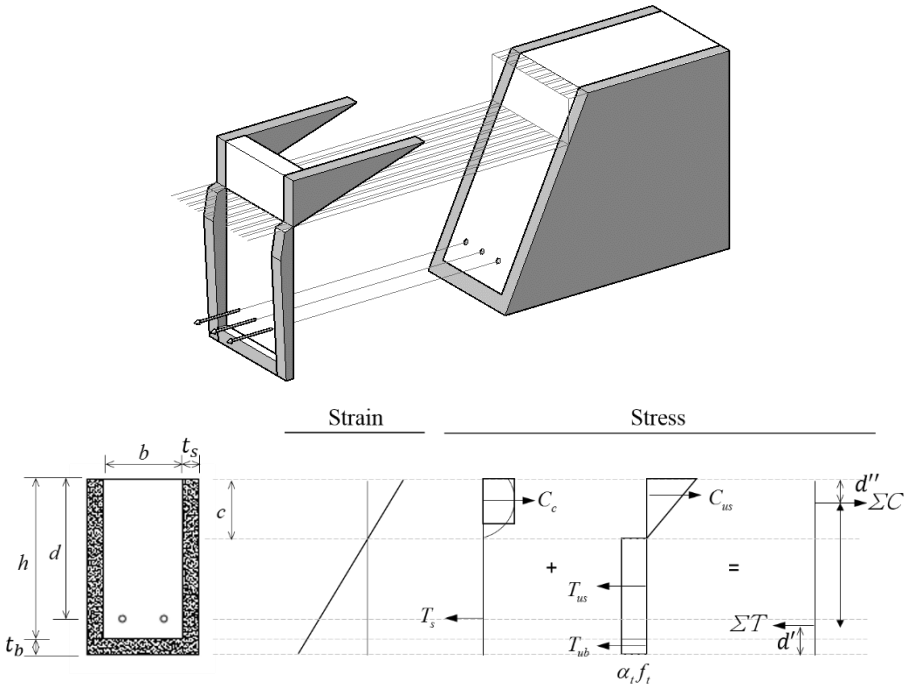

Fig 3-19 Strain and stress distribution for cross section of strengthened beam with UHPC

The equilibrium of the normal forces is established in **Equation (3)**. From force equilibrium condition, neutral axis c is calculated.

$$0.85 f_c' b_w a + \frac{1}{2} f_{cd} 2t_s c = A_s f_y + \alpha_t f_{tk}(h-c)2t_s + \alpha_t f_{tk} t_b (b_w + 2t_s) \quad (3)$$

where

a = depth of equivalent rectangular stress block, mm

b_w = width of web, mm

c = distance from extreme compression fiber to neutral axis, mm

h = height, mm

f_c' = specified compressive strength of concrete, MPa

f_{cd} = design compressive strength of UHPC, MPa

f_{tk} = characteristic tensile strength of UHPC, MPa

t_b = base strengthened thickness, mm

t_s = side strengthened thickness, mm

f_y = specified yield strength of reinforcement, MPa

A_s = area of nonprestressed longitudinal tension reinforcement,mm^2

α_t = equivalent tensile stress block coefficient

Considering extreme compressive strain as 0.003(ε_c=0.003), it is necessary to check whether reinforcement bars are yielded.

To compute M_n, arm length calculated from the positions of resultant forces of the compression(**Equation(4)**) and tension(**Equation(5)**). Finally the

moment is calculated from **Equation (6)**

$$C_c \frac{a}{2} + C_s \frac{c}{3} = \Sigma C \cdot d'' \tag{4}$$

$$T_s(h + t_b - d) + T_s \frac{(h + t_b - c)}{2} + T_b \frac{t_b}{2} = \Sigma T \cdot d' \tag{5}$$

$$M_n = \Sigma C \cdot (h + t_b - d' - d'') \tag{6}$$

where

a = depth of equivalent rectangular stress block, mm

c = distance from extreme compression fiber to neutral axis, mm

d = effective depth, mm

d' = distance from extreme tension fiber to resultant tension force, mm

d'' = distance from extreme compression fiber to resultant compression force, mm

h = height, mm

f_c' = specified compressive strength of concrete, MPa

f_{cd} = design compressive strength of UHPC, MPa

f_{tk} = characteristic tensile strength of UHPC, MPa

t_b = base strengthened thickness, mm

t_s = side strengthened thickness, mm

C = compression force, N

C_c = compression force portion of concrete, N

C_{us} = compression force portion of side UHPC above neutral axis, N

T = tensile force, N

T_s = tensile force portion of reinforcing steel bars, N

T_{us} = tensile force portion of side UHPC below neutral axis, N

T_{ub} = tensile force portion of base UHPC below neutral axis, N

M_n = nominal flexural strength at section, N·mm

3.5.2 Shear strength

In K-UHPC provision proposed by KCI, shear strength formula of beam member was proposed based on the same concept of JSCE recommendations. This proposed equations expressed as the sum of matrix, fiber, shear reinforcement, and prestressing contributions. To get nominal shear strength of strengthened beam, except shear reinforcement and prestressing portions, shear strength of UHPC portion is added to original member's shear strength which consists of concrete.

$$V_n = V_c + V_{rpcd} + V_{fd} \tag{7}$$

$$V_c = \frac{1}{6}\sqrt{f_c'}\, b_w d \tag{8}$$

$$V_{rpcd} = \phi_b (0.18\sqrt{f_{cd}}\, b_w d) \tag{9}$$

$$V_{fd} = \phi_b \frac{f_{vd}}{\tan \beta_u} b_w z \tag{10}$$

where

V_n = nominal shear strength, N

V_c = nominal shear strength provided by concrete, N

V_{rpcd} = nominal shear strength provided by matrix of UHPC, N

V_{fd} = nominal shear strength provided by fiber, N

f_{vd} = design average tensile strength in the direction perpendicular to diagonal tensile crack of UHPC, MPa

z = distance from the position of the resultant of the compressive stresses to the centroid of tensile steel, mm, generally $d/1.15$

β_u = angle occurring between axial direction and diagonal tensile crack plane. This angle shall be larger than 30° (40° is assumed in this study based on provision)

3.5.3 Validation

Fig 3-20, 21 and **Table 3-12, 13, 14** showed the comparison between experimental results and theoretical results predicted by the simplified analysis model. Except a few cases, reasonably good agreements are evident.

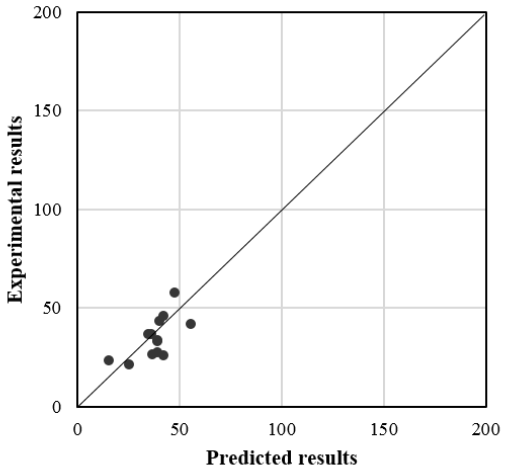

Fig 3-20 Comparison of experimental results with theoretical predictions about cracking moment

Table 3-12 Comparison of experimental results with theoretical predictions about cracking moment

Name	I_{gt}	y_{top}	f_r	$M_{cr,\exp}$	$M_{cr,\mathrm{cal}}$	cal/exp
CON	1.1E+09	203.9	4.6	21.3	25.1	1.18
JB2	1.4E+09	218.7	5.6	36.6	34.7	0.95
JB3	1.5E+09	225.8	5.6	26.6	36.8	1.38
JB4	1.6E+09	232.8	5.6	33.1	38.9	1.17
JS2	1.3E+09	203.0	5.6	36.9	36.3	0.99
JS4	1.5E+09	202.4	5.6	46.2	42.3	0.92
JS2B2	1.6E+09	216.7	5.6	26.3	41.9	1.59
JS2B4	2.0E+09	229.9	5.6	57.7	47.3	0.82
JS4B4	2.3E+09	228.1	5.6	42.0	55.6	1.33
JB2-F0.5	1.4E+09	218.7	6.4	23.6	15.2	0.64
JB2-F2	1.4E+09	218.7	2.4	43.3	40.0	0.92
JB4S4-RS	1.6E+09	233.1	5.6	33.8	38.9	1.15
JB4S4-WM	1.6E+09	232.9	5.6	27.8	38.9	1.40

Except JB4S4, predicted value are within 15% error range. When ultimate strength are compared, more tests are required to verify shear strength prediction, since only one specimen destroyed by pure shear. Beams failed in flexural shear included in both comparison charts.

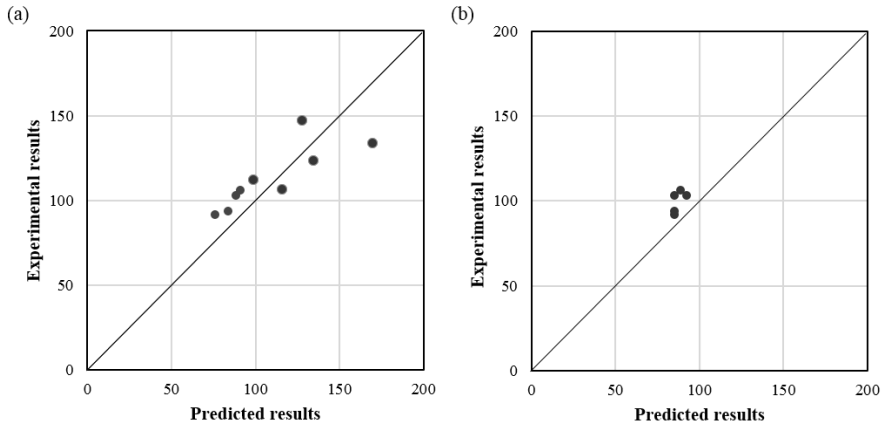

Fig 3-21 Comparison of experimental results with theoretical predictions: a) about flexural strength b) about shear strength

Table 3-13 Comparison of experimental results with theoretical predictions about flexural strength

Name	Failure	Theoretical results		Experimental results (2)	(1)/(2)
		M_n/a (1)	V_n		
JS2	F	98.45	205.63	112.20	0.88
JS4	F	127.50	333.79	147.20	0.87
JB2S2	F	115.60	213.00	106.60	1.08
JB4S2	F	134.26	220.38	123.80	1.08
jB4S4	F	169.60	348.54	133.70	1.27

Table 3-14 Comparison of experimental results with theoretical predictions about shear strength

Name	Failure	Theoretical results		Experimental results (2)	(1)/(2)
		M_n/a	V_n (1)		
JB2	FS	83.43	84.84	94.00	0.89
JB3	FS	91.08	88.53	106.20	0.83
JB4	S	98.88	92.22	103.30	0.89
JB3-F0.5	FS	76.01	84.84	91.80	0.83
JB3-F2	FS	88.34	84.84	103.00	0.82

3.6 Discussion

Total 12 specimens except the one reference beam were tested to investigate strengthening effect of UHPC in rectangular sectional beam without stirrup. Based on the preceding research, test variables were strengthening region, thickness, and additional reinforcement with UHPC. On basis of the test results, behavior of UHPC-RC composite beams were analyzed and conclusion of this study is as follows:

1. All strengthened beams shows strength increase from 29%(JB2-F0.5) to 142%(JB4S4-RS). Except one specimen(JB3(-14%))'s stiffness decrease, every specimens shows stiffness increase from 3%(JB4) to 142%(JB4S4-RS). In the point of ductility improvement, all beams shows ductility increase from 2%(JB2) to 178%(JS2B4), except 2 specimen; JB4S4-WM(-12%) due to construction defect, and JB2-F0.5(-37%) for less steel fibers.

2. Based on observation of the strengthening methods in this study, it is shown that the increase in structural performance of retrofitted members are in proportion to the thickness of UHPC.

3. About additional reinforcement, rebars showed the best combination with UHPC(2.42 times, which is the most highly increased case). Additional steel fiber in UHPC showed a little increase in strength, but showed increase of ductility(2%vol.(the most amount of fiber)(+114%). Wire mesh didn't help to increase performance.

4. Based on sectional level analysis, theoretical values showed 21% tolerance with experimental values.

Chapter 4. Strengthening T-shaped RC beams with Ultra High Performance Concrete

4.1 Experimental program

4.1.1 Summary

This study investigates the structural performance of reinforced concrete T beams retrofitted by ultra-high performance concrete (UHPC) to compare the effectiveness of strengthened T-beams with different regions and thickness of layers. Due to its high compressive and tensile strength, thin UHPC over layers are applied to increase tensile strength in flexural tension region with reinforcement and the compressive resistance in flexural compression region. Therefore, strengthened beams with UHPC enhance both positive and negative moment capacity. Fourteen ordinary reinforced concrete T-beams were prepared to intend shear failure modes. Jacketing methods applied to this experimental program has three different schemes: UHPC U shaped-jacketing, UHPC casting on the flange, and UHPC casting on the flange and Aramid FRP U shaped-wrapping. The results clearly show that the effectiveness of UHPC U shaped-jacketing method is better than that of other methods.

4.1.2 Introduction

Owing to its high structural performance of UHPC (Ultra High Performance Concrete), it is possible to apply thin layer of UHPC over ordinary existing structural concrete to increase their insufficient capacity. Many of researchers from literature have demonstrated the applicability of UHPC as one of efficient strengthening methods for retrofit; (Martinola et al. 2010) 5mm U-shaped jacket for flexural strengthening, (Meda et al. 2014) shear strengthening for beams with 3 or 5mm U-jacketing with wire mesh. (Noshiravani 2012) the overlay of UHPC with small diameter reinforcing bars and the thickness with 10-20% of depth of RC based on (Habel et al. 2006)'s numerical analysis. Most of these strengthening methods have focused on

tensile strengthening. Using both the high compressive and high tensile strength of UHPC, the overlay method can be applied not only to tension regions, but also to compression regions. Similarly, UHPC can be applied to the increase of flexural strength of the positive and negative moment (Fig. 1). Therefore, this research examines the effectiveness of one singly reinforced beams by retrofitting positive/negative moment zone. Also, AFRP strengthening methods were compared with UHPC methods with combination of two methods.

4.1.3 Test specimens and Variables

In order to demonstrate the efficient retrofit of concrete frames the experiment program in this study prepared 14 full-scale reinforced concrete (RC) beams of T-shaped cross-section. The beam specimen details and dimensions are shown in **Fig. 4-1**. All RC T-beams were cast with concrete of nominal cylindrical strength of 24 MPa and reinforced with five bottom longitudinal reinforcing bars (D22), four top longitudinal reinforcing bars (D10) and stirrups (D10) with a spacing of 150mm. After 28 days curing, the surface of beams were sandblasted to make roughness of about 2-3mm to give enough bond strength along the interfaces between concrete and UHPC layers. After cleaning the surface with air compressor and moisturizing the surface, UHPC was placed on the concrete beams. All of strengthened beams were intended to fail in flexure failure modes by theoretical calculation. Four beams were strengthened for shear strength enhancement using continuous surface bonded U-shaped wraps with AFRP throughout the beam span without end anchorage.

Table 4-1 Variables and Specimens

Specimen	UHPC			AFRP
	t_b	t_s	t_t	
CON				
U2	20	20		
U4	40	40		
T2			20	
T4			40	
F2				0.22
T2F2			20	0.22
T4F2			40	0.22

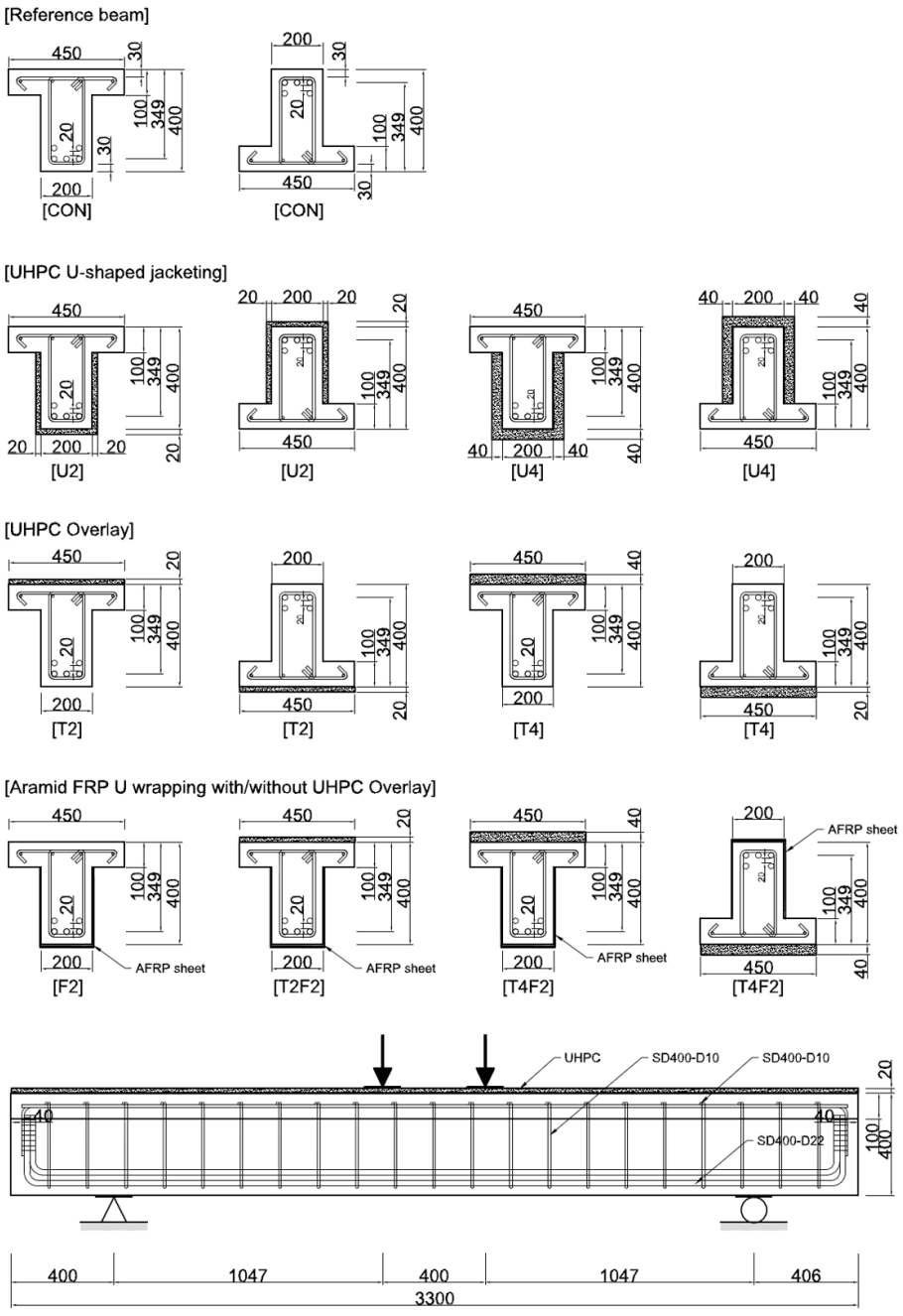

Fig 4-1 Section of Specimens

The test main variables are listed in **Table 4-1**. The beam denotations represent the strengthened region (U: UHPC U-shaped jacketing, T: UHPC overlay, F: AFRP U-wrapping) and thickness of overlay (2: 20mm, 4: 40mm). Except F2, T2F2, other beams are made for the test of enhancement of capacity of beams in positive and negative moment regions. F2 and T2F2 of beam behaviors in negative moment were excluded by (Sinaph M. Namboorimadathil).

4.1.4 Material properties

Ready mixed concrete with an aggregate maximum size of 25mm was provided to prepare the RC beams. The average values of mechanical characteristics of material and UHPC mixing compositions are listed in **Table 4-2, 4-3**. **Fig 4-2** (a), (b), and (c) showed the relationship between stress and strain of normal strength concrete, steel and AFRP, respectively. **Fig 4-3** (a), (b) and (c) showed the results of compressive test, flexural tensile test with notched prisms and direct tensile test of notched dog-bone specimens.

Table. 4-2 Material properties

Concrete		**UHPC**		
f_c' [MPa]	E_c [MPa]	f_{Uc} [MPa]	f_{tk} [MPa]	E_U [MPa]
24.7	24374	164	9.5	46821

Steel				**AFRP**		
ϕ [mm]	f_{sy} [MPa]	f_{su} [MPa]	E_s [GPa]	t [mm]	f_{fu} [MPa]	E_f [GPa]
10	521	628	200	0.22	2063.9	133.1
22	551	677	200			

Table 4-3 UHPC mixing composition

Nominal Strength	W/B	Cement	Silica fume	Sand	Filing powder	Superplasticizer	Steel fiber vol.
(MPa)	(%)	(kg/m³)	(kg/m³)	(kg/m³)	(kg/m³)	(kg/m³)	(%)
180	23	783.2	195.8	861.52	234.96	15.66	1.5

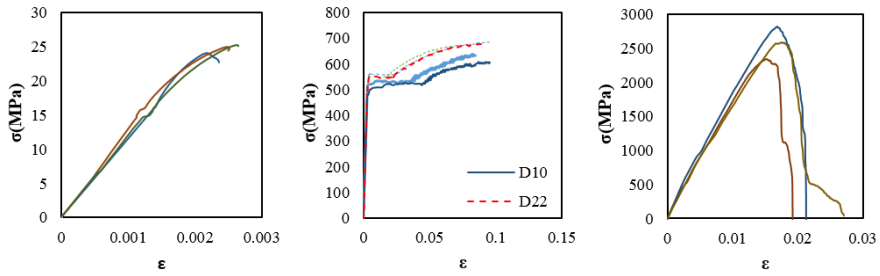

Fig 4-2 Material properties of existing RC beams and AFRP : a) Compressive stress-strain curve of 21MPa concrete, b) Tensile stress-strain curve of SD400 D10, D22 and c) Tensile stress-strain curve of AFRP 0.228mm

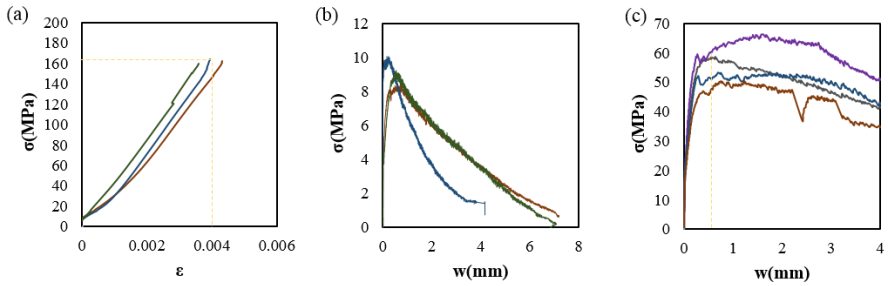

Fig 4-3 UHPC properties: a) Compressive stress-strain curve, b)Tensile stress-crack width curve, c)Flexural tensile stress-crack width curve

UHPC mixing proportion is like as **Table 4-3.** The steel fiber consisted of 19.5mm and 16.3mm fibers mixed in the ratio of 2:1. According to the characteristic values provided by manufacturer, the fibers tensile strength is 2500MPa.

Compression test for UHPC was carried out in the same way for normal concrete. Its compressive strength was 177MPa and maximum strain is about 0.004.(**Fig 3-6**(a)) Fig 3-6(b),(c) showed the results of direct tensile test of notched dog-bone specimens and flexural tensile test of notched prisms.

4.1.5 Specimen preparation

In case of UHPC strengthening, giving enough roughness by sandblasting until the aggregate are exposed. After installing framework, UHPC was placed to spread out. After curing, mold was get rid of. In AFRP strengthening, likewise UHPC, the surface was grinded at first, and then primer and epoxy and resin were applied orderly. Then, Aramid sheet was attached. After hardening, additional resin was coated on the FRP sheet.

(a) Arrangement re-bar

(b) Placing concrete

(c) After curing, dissolution form

(d) Sandblast

(e) Removing debris

(f) Providing humidity

(g) Placing UHPC

(h) Steam curing

Fig 4-4 Procedure of manufacturing specimen for strengthening with UHPC

(a) Grinding the surface

(b) Primer coating

(c) Applying epoxy putty

(d) Resin under coat

(e) AFRP sheet Impregnation

(f) Attaching AFRP sheet

(g) After hardening, resin top coat

(h) Curing

Fig 4-5 Procedure of shear strengthening beam with AFRP sheet

4.1.6 Test setup and procedure

Four point bending tests were performed under displacement control at a rate of 2 mm/min. The six beam specimens were placed upside down to examine the flexural behavior of retrofitted beams in negative moments. To measure the deformations, linear variable displacement transducers were installed at 3 points under the beam. Steel gauges were attached on the center of 3 longitudinal reinforcing bars and 4 stirrups. Concrete gauges were attached along the sections at different heights in the middle of beams. Strain gauges for FRP were mounted at the expected location of shear cracks. Shear-span/effective depth ratio (a/d) = 3 for beams was selected. (**Fig.4-6**)

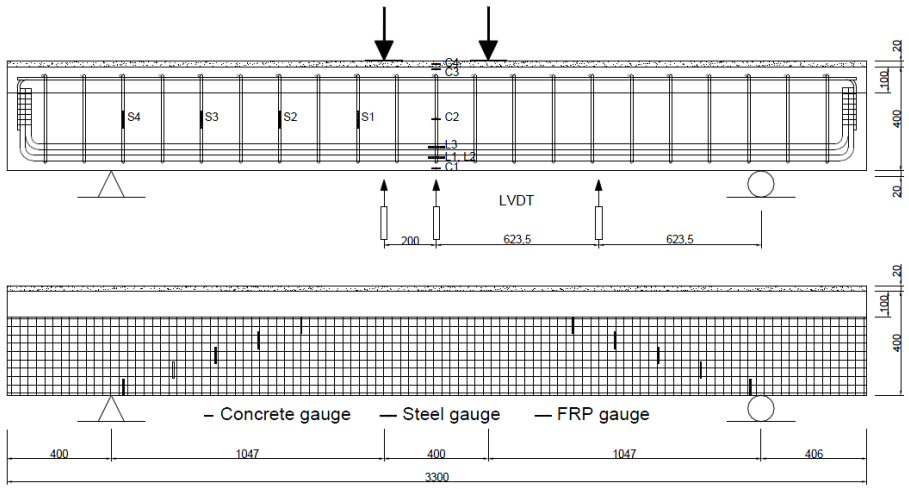

Fig 4-6 Beam geometry and instrument devices

4.2 Test results

For the investigation of behaviors of beams in positive moment, only U4 was intended to fail in flexure. Other specimens were prepared to fail in shear, especially by delamination of overlaid UHPC thin layer. For the investigation of behavior of beams in negative moment, all specimens were prepared to fail in flexure. In case of specimens strengthened with aramid FRP, the load at initial cracking was not measured. Specific test results up to ultimate states are listed in **Table 2**.

4.2.1 Reference beam

For investigation of the behavior of beams in positive moment, the reference beam showed elastic behavior up to 66 kN. After the vertical crack developed, initial shear crack occurred at 77 kN. Without yielding of longitudinal reinforcement, the beam failed in shear. For investigation the behavior of beams in negative moment, the reference beam behavior were controlled by bending due to relatively low reinforcement ratio about top longitudinal reinforcing bars (0.4%).

4.2.2 UHPC U-shaped jacketing

As a reliable method, U-shaped jacketing showed the high effectiveness of the increase of capacity both in positive and negative moment. In case of U2 in positive moment, even though the beam's crack pattern showed the shear controlled failure modes, the longitudinal rebar yielded at 169.2 kN. The behavior of U4 was controlled obviously by flexure and locally macro crack developed at the mid-span. This was the only case of non-yielding of the stirrups. For the behavior of beams in negative moment, UHPC layers contributed increase in compressive resistance. Both U2 and U4 showed the same behavior. The initial vertical crack occurred in the flange of T-beam where the maximum tensile stress were developed. Thereafter, the crack developed on the layer of UHPC jacketing. The crushing of UHPC on the compression zone resulted in the first sudden drop of resistance as the applied load after the maximum load. (At that point, U2 : ε_{cu} =3000 μm, U4 : ε_{cu} =3000 μm) With the sufficient bondage with substrate beams along three sides, the spalling failure was observed at the upper faces of the mid-span of beams.

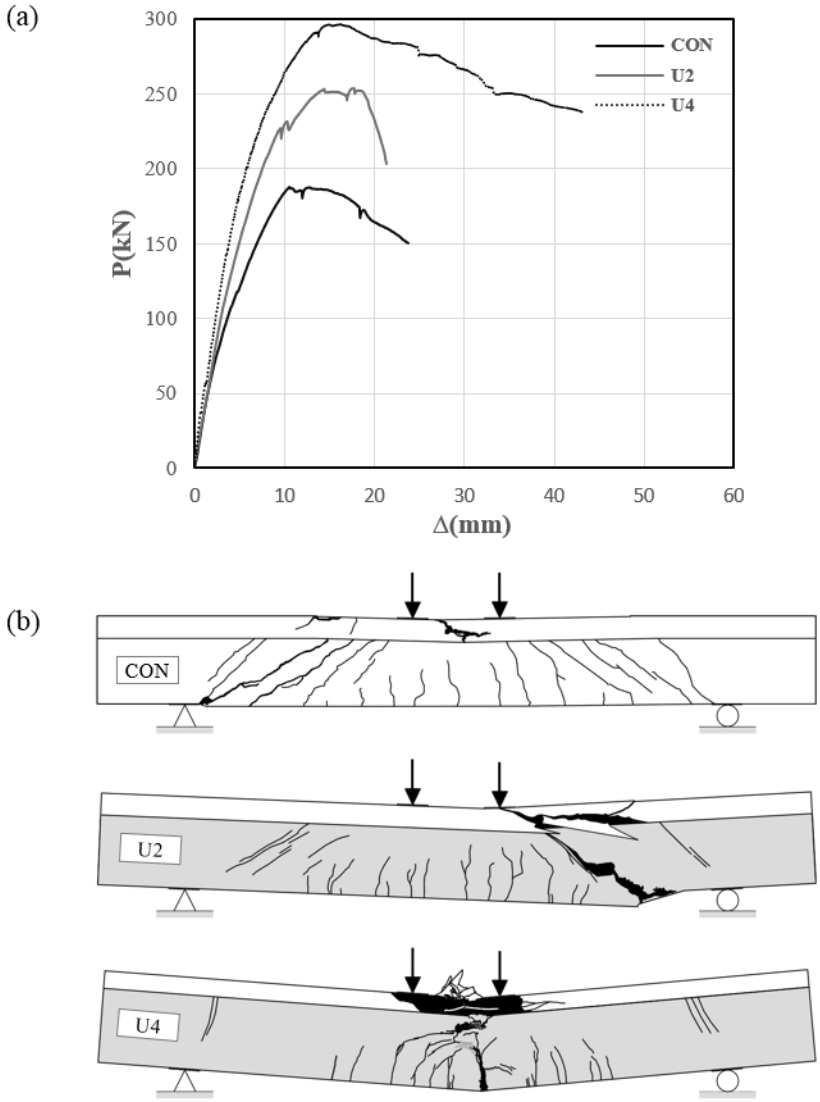

Fig 4-7 Test results of reference beam and UHPC U-shaped jacketing in positive moment : a)Load-center deflection responses, b) Fully developed crack patterns at the end of the test

Table 4-4 Test results of reference beam and UHPC U-shaped jacketing in positive moment

Beam	Failure	$\mathbf{P}_{cr}$[kN]	$\mathbf{P}_{y}$[kN]	$\mathbf{P}_{u}$[kN]	$\mathbf{P}_{failure}$[kN]	$\mathbf{K}_{e}$[kN/mm]	$\boldsymbol{\theta}_{c}$[°]
CON	**S**	**66.0**	**-**	**187.7**	**150.1**	**31.9**	**27**
U2	FS	57.5	169.2	235.9	203.3	34.0	32
U4	F	100.0	267.4	297.1	297.1	42.6	90

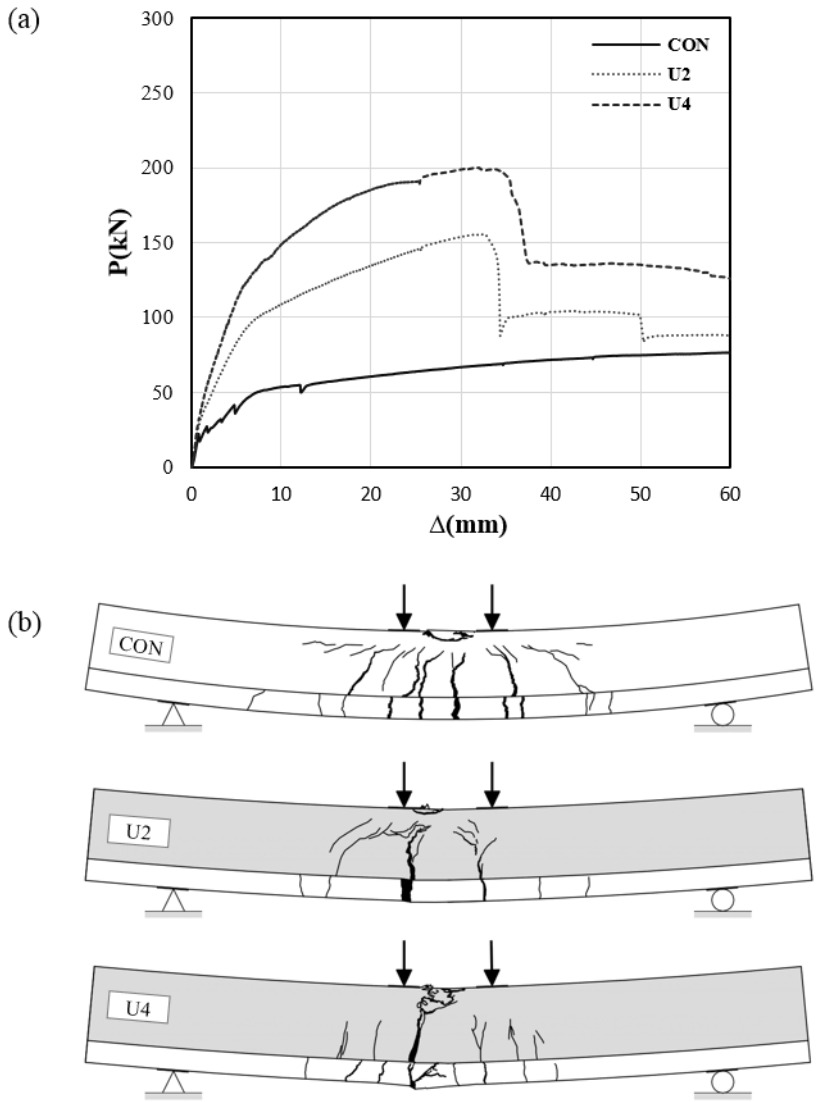

Fig 4-8 Test results of reference beam and UHPC U-shaped jacketing in negative moment : a)Load-center deflection responses, b) Fully developed crack patterns at the end of the test

Table 4-5 Test results of reference beam and UHPC U-shaped jacketing in negative moment

Beam	Failure	$\mathbf{P}_{cr}$[kN]	$\mathbf{P}_{y}$[kN]	$\mathbf{P}_{u}$[kN]	$\mathbf{P}_{failure}$[kN]	$\mathbf{K}_{e}$[kN/mm]	$\boldsymbol{\theta}_{c}$[°]
CON	**F**	**22.5**	**51.7**	**77.5**	**73.7**	**17.6**	**90**
U2	F	50.0	155.0	155.5	138.0	21.9	86
U4	F	57.5	133.1	199.7	172.0	31.1	85

4.2.3 UHPC Overlay

The overlay method of UHPC on the top of flange was preferred because its easy construction for existing members. For investigation of behavior of beams in positive moment, the vertical flexural and shear crack occurred at beams as the applied load increased. After cracking, thin UHPC layers were interpreted to contribute the reduction in further deflection. When the specimens reached its maximum load, After the ultimate state, the interface failure was developed between UHPC layer and the beam. Despite of the low contribution of strength, the proposed technique remarkably contributed the increase in the initial stiffness.

In the view of concrete gauge, upto 151 kN the extreme compressive strain value(ε_{cu}) of T2 had increased linearly. When the load showed a little sudden drop before reaching maximum load, the gauge also showed a sudden drop and the strain curve showed non linear behavior with the reduce of increase rate. Its maximum value was ε_{cu}= 629 μm. About T4, the compressive strain was 652 μm.

For investigation the behavior of beams in negative moment, the strengthened thin layer behaved as additional tensile reinforcement. Both of beams developed the initial crack at 60 kN. As the beam collapsed in a bent shape with multiple cracks, the UHPC layer's one macro crack mouth opened gradually resisting with fiber's bridge effects. After this phenomenon, the divided layers kept rigid.

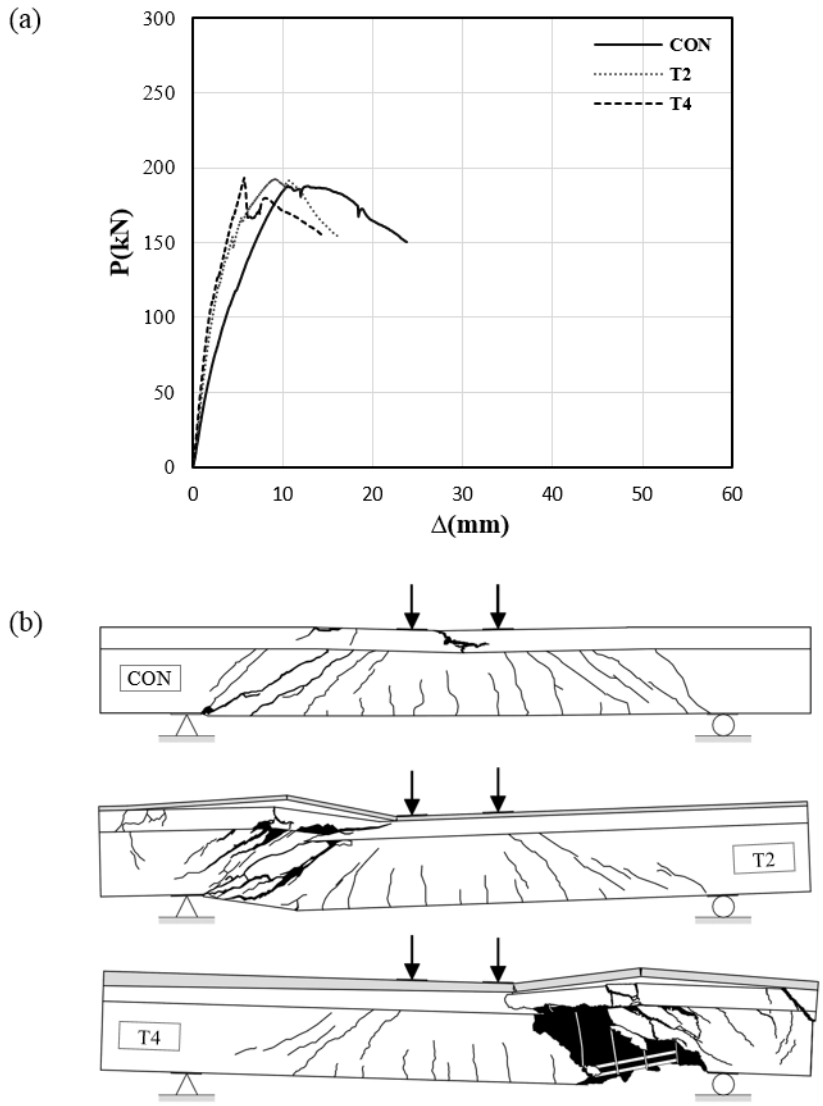

Fig 4-9 Test results of UHPC Overlay in positive moment : a)Load-center deflection responses, b) Fully developed crack patterns at the end of the test

Table 4-6 Test results of UHPC Overlay in positive moment

Beam	Failure	$\mathbf{P}_{cr}$[kN]	$\mathbf{P}_{y}$[kN]	$\mathbf{P}_{u}$[kN]	$\mathbf{P}_{failure}$[kN]	$\mathbf{K}_{e}$[kN/mm]	$\boldsymbol{\theta}_{c}$[°]
CON	**F**	**22.5**	**51.7**	**77.5**	**73.7**	**17.6**	**90**
T2	F	60.0	57.9	86.9	78.0	28.2	87
T4	F	60.0	67.9	96.3	77.1	16.8	59

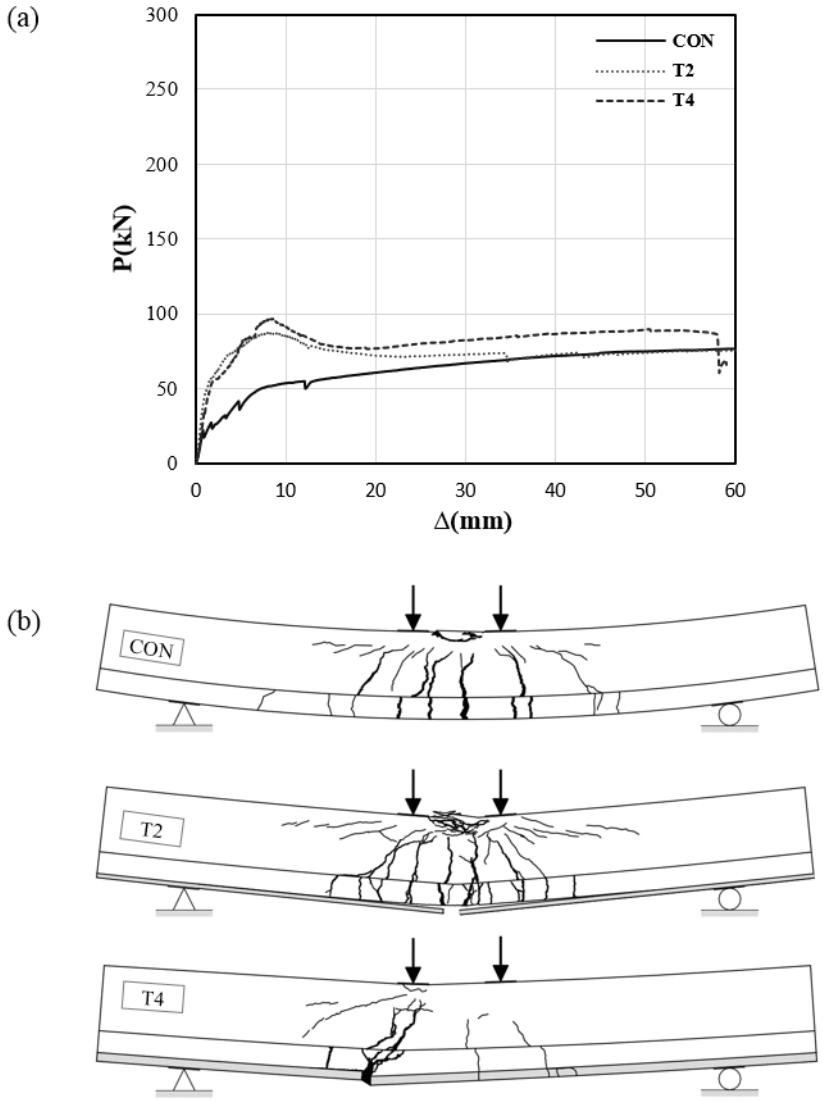

Fig 4-10 Test results of UHPC Overlay in negative moment : a)Load-center deflection responses, b) Fully developed crack patterns at the end of the test

Table 4-7 Test results of UHPC Overlay in negative moment

Beam	Failure	$\mathbf{P}_{cr}$[kN]	$\mathbf{P}_{y}$[kN]	$\mathbf{P}_{u}$[kN]	$\mathbf{P}_{failure}$[kN]	$\mathbf{K}_{e}$[kN/mm]	$\boldsymbol{\theta}_{c}$[°]
CON	**F**	**22.5**	**51.7**	**77.5**	**73.7**	**17.6**	**90**
T2	F	60.0	57.9	86.9	78.0	28.2	87
T4	F	60.0	67.9	96.3	77.1	16.8	59

4.2.4 Aramid FRP U wrapping with/without UHPC Overlay

With AFRP shear strengthening, 3 specimens tested in positive moment. The initial behavior of T2F2, T4F2 followed the similar load-deflection patterns of T2, T4 before they reached their ultimate states, respectively. With the effects of AFRP, the strengthened ratio of T2F2 and T4F2 were 1.1 and 1.27, compared with T2, T4. In case of F2, strengthened with only AFRP, there is no stiffness improvement, but only the strength increase. All three FRP strengthened beams showed brittle failure of AFRP near the support region.

For hybrid strengthened beams failed in positive moment, it reached its maximum load while the interfacial failure was happened. Then the extreme compressive strain didn't reached its ultimate value as following : ε_{cu} = 866 μm for T2F2, ε_{cu} = 995 μm for T4F2. After that, AFRP was ripped off near the support.(**Fig 4-10**)

T4F2 was the only specimen with AFRP performed the test under negative moment. Its behavior is similar to T2 or T4 under negative moment. However, the influence of AFRP U wrapping, the stiffness increased. And the strength increased 40% than control beam.

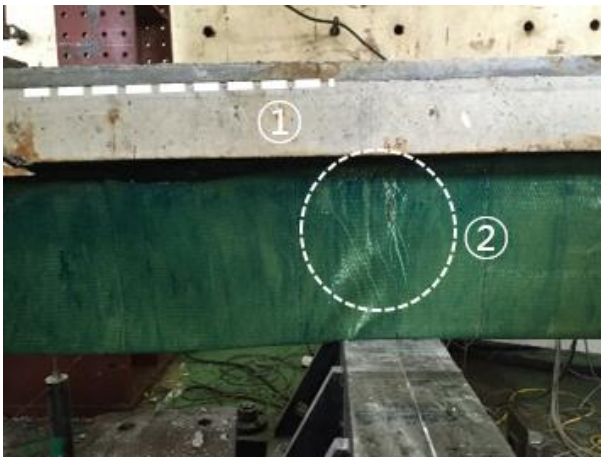

Fig 4-11 Collapse mechanism of Aramid FRP U wrapping with UHPC Overlay

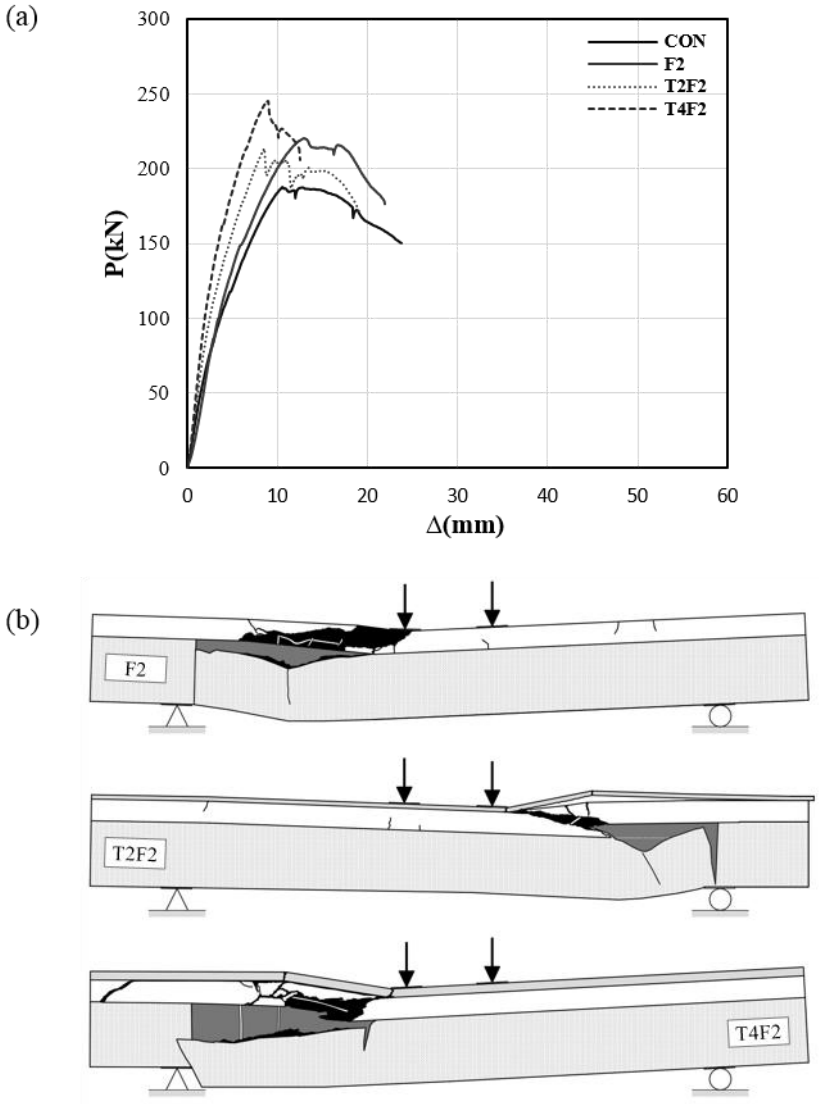

Fig 4-12 Test results of AFRP U wrapping with/without UHPC Overlay in positive moment : a)Load-center deflection responses, b) Fully developed crack patterns at the end of the test

Table 4-8 Test results of AFRP U wrapping with/without UHPC Overlay in positive moment

Beam	Failure	$\mathbf{P_{cr}}$[kN]	$\mathbf{P_y}$[kN]	$\mathbf{P_u}$[kN]	$\mathbf{P_{failure}}$[kN]	$\mathbf{K_e}$[kN/mm]	$\boldsymbol{\theta_c}$[°]
CON	**S**	**66.0**	**-**	**187.7**	**150.1**	**31.9**	**27**
F2	S	?	-	213.4	170.7	27.7	25
T2F2	S	?	-	220.1	176.1	43.2	31
T4F2	S	?	-	244.8	205.5	48.4	32

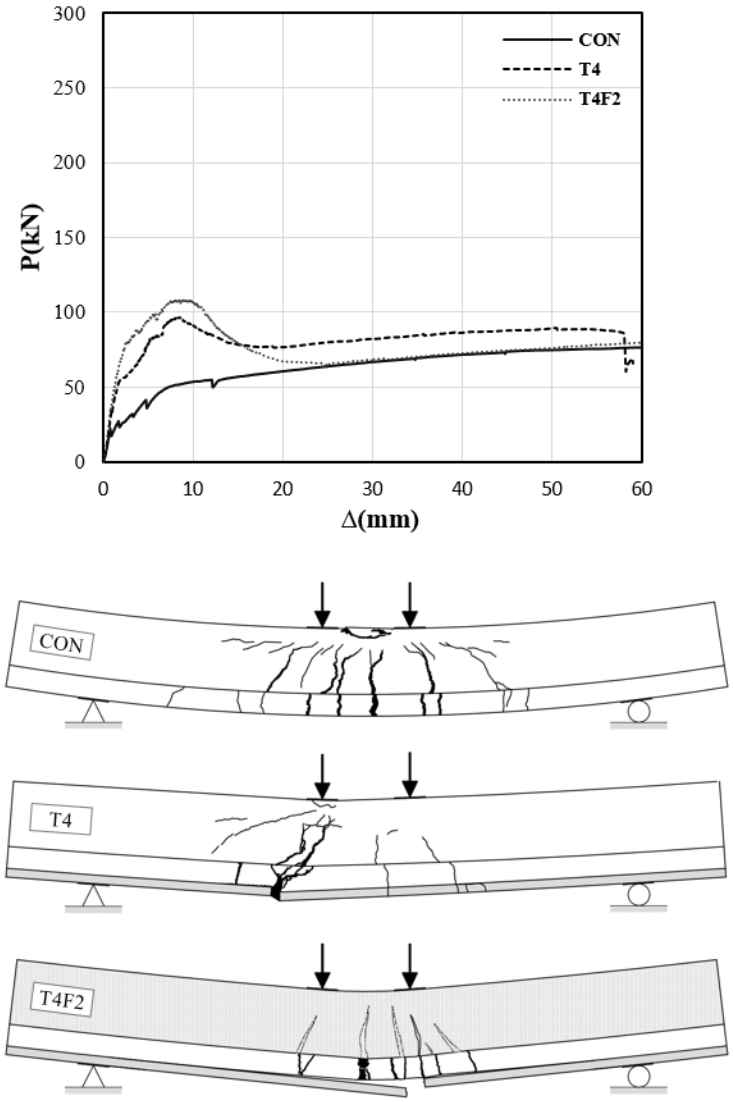

Fig 4-13 Test results of AFRP U wrapping with UHPC Overlay in negative moment : a)Load-center deflection responses, b) Fully developed crack patterns at the end of the test

Table 4-9 Test results of AFRP U wrapping with UHPC Overlay in negative moment

Beam	Failure	$\mathbf{P}_{cr}$[kN]	$\mathbf{P}_{y}$[kN]	$\mathbf{P}_{u}$[kN]	$\mathbf{P}_{failure}$[kN]	$\mathbf{K}_{e}$[kN/mm]	$\boldsymbol{\theta}_{c}$[°]
CON	**F**	**22.5**	**51.7**	**77.5**	**73.7**	**17.6**	**90**
T4	F	60.0	67.9	96.3	77.1	16.8	59
T4F2	F	60.2	71.1	108.3	86.7	36.9	80

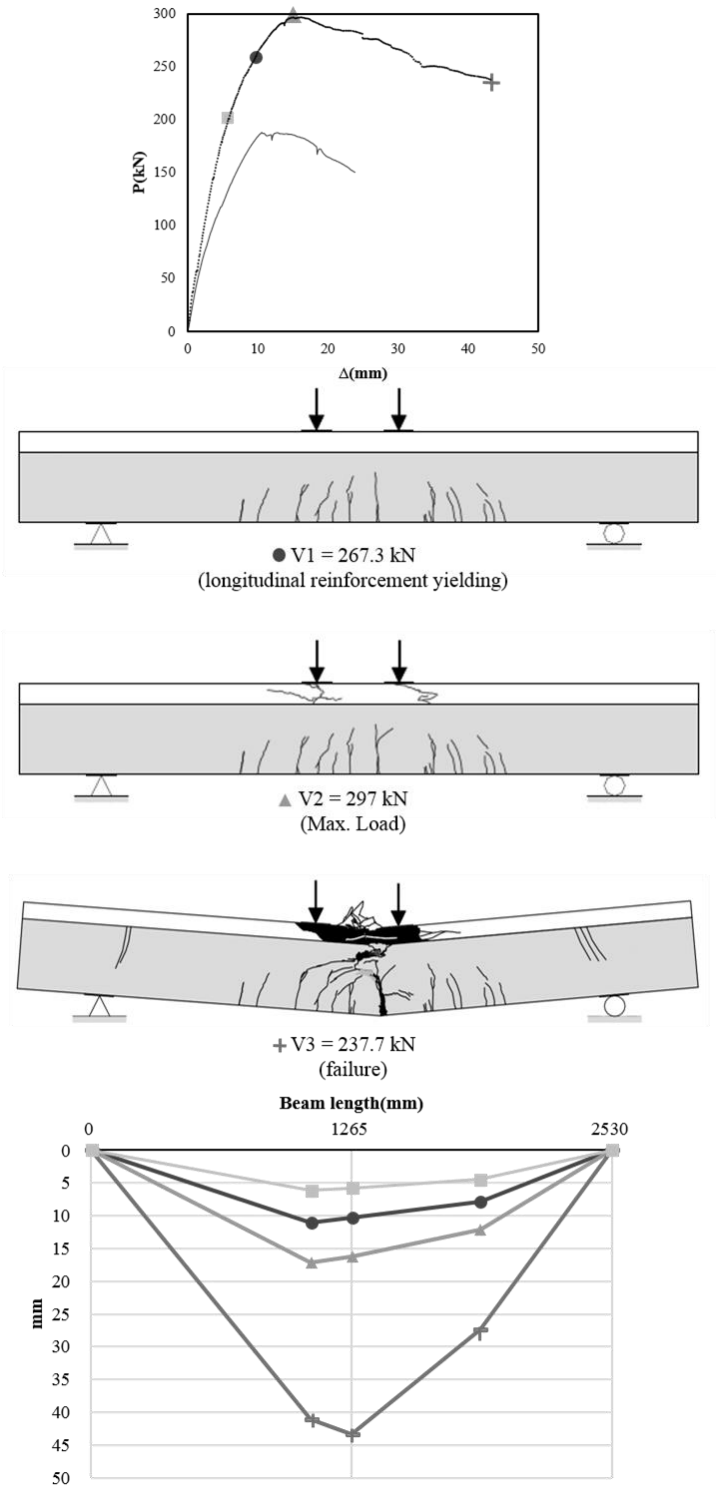

Fig 4-14 Failure mode development – U4(flexural failure)

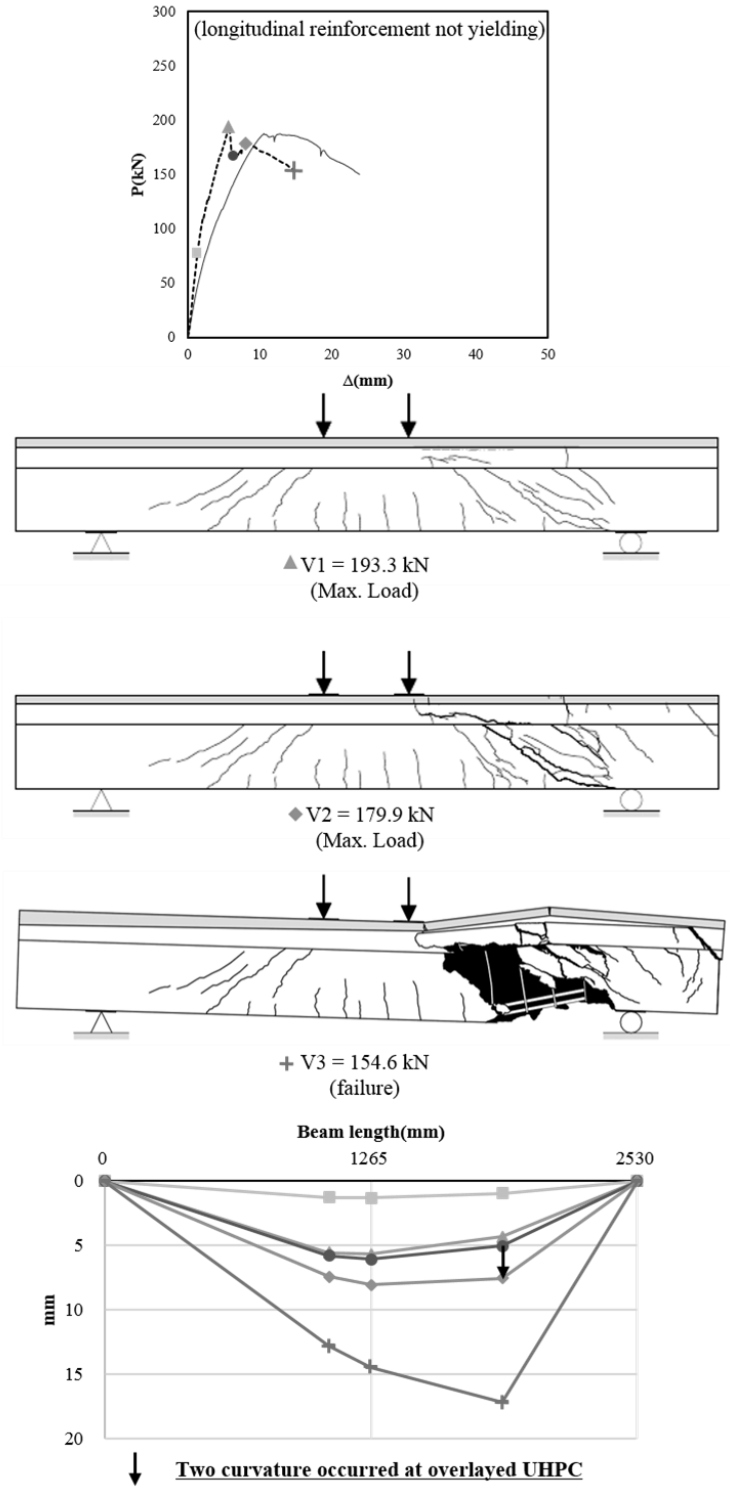

Fig 4-15 Failure mode development –T4(shear failure)

Fig 4-16 Collapse mechanism of T4

4.2.5 Flexural failure vs. shear failure

Two specimens, U4 and T4, showed different failure modes (**Fig 6**). Due to sufficient bond strength along the interface between UHPC and concrete beams, the controlling failure mode of retrofitted U4 changed from shear to flexural failure. As the applied load increased, micro flexural cracks developed in the mid-span and the compressive zone crushed at the maximum load at the ultimate state. After that, the deformation energy was accumulated along macro crack in the middle of the beam and the major crack was developed instead of micro crack closing.

On the other hand, T4 for specimen by the overlay of UHPC demonstrated the typical shear failure modes. As the applied load increased, the vertical crack and the diagonal crack occurred at the substrate beam, however, the upper thin layer experienced the rigid body deformation in a bent shape. When the load arrived at ultimate point, the interface crack was observed. After the sudden drop of resistance due to the interface failure, the load increased as UHPC thin layer bent developed in two curvature pattern along the thin layer. Right after the load again dropped because of the formation of plastic hinges at UHPC layer.

Table 4-10 Summary of test results``

	Name	Failure	Load [KN]			Δ_u [mm]	Ductility Index			θ_c[°]	ψ_u[rad]		Initial stiffness	Strengthened Effect		
			Initial vertical crack	Initial diagonal crack	P_u		Δ_u/Δ_{cr}	Δ_u/Δ_y	Δ_{max}/Δ_u		ψ_L	ψ_R		Strength Increase	Stiffness Increase	Ductility Increase
For Positive Moment	CON	S	66.0	79.0	187.7	23.8	5.1	-	2.2	27	0.024	0.024	31.9	1.00	1.00	1.00
	U2	SF	57.5	170.0	235.9	86.6	10.5	3.0	1.2	32	0.019	0.033	34.0	1.26	1.07	0.54
	U4	F	100.0	-	205.5	21.4	6.9	1.6	2.7	90	0.039	0.044	42.6	1.58	1.33	1.19
	T2	S	60.0	115.0	192.6	43.4	7.5	-	1.8	30	0.017	0.015	49.6	1.03	1.55	0.80
	T4	S	77.5	110.0	193.3	34.0	4.3	-	2.5	26	0.012	0.028	58.7	1.03	1.84	1.13
	F2	S	?	?	205.5	36.4	-	-	1.7	25	0.021	0.024	27.7	1.14	0.87	0.63
	T2F2	S	?	?	213.4	16.3	-	-	2.2	31	0.017	0.029	43.2	1.17	1.35	0.99
	T4F2	S	?	?	244.8	14.5	-	-	1.4	32	0.012	0.013	48.4	1.30	1.52	0.75
For Negative Moment	CON	F	22.5	-	77.5	146.3	67.1	10.2	1.0	90	0.076	0.078	17.6	1.00	1.00	1.00
	U2	F	50.0	132.5	155.5	22.8	14.2	1.0	1.1	86	0.065	0.057	21.9	2.01	1.25	1.04
	U4	F	57.5	-	199.7	19.1	17.2	4.3	1.1	85	0.034	0.029	31.1	2.58	1.77	1.13
	T2	F	60.0	-	86.9	21.9	3.8	4.1	18.3	87	0.044	0.041	28.2	1.12	1.60	18.13
	T4	F	60.0	71.5	96.3	12.5	3.5	3.1	1.8	59	0.017	0.015	16.8	1.24	0.95	1.83
	T4F2	F	60.0	-	108.3	87.9	5.8	0.3	9.3	80	0.069	0.066	36.9	1.40	2.10	9.23

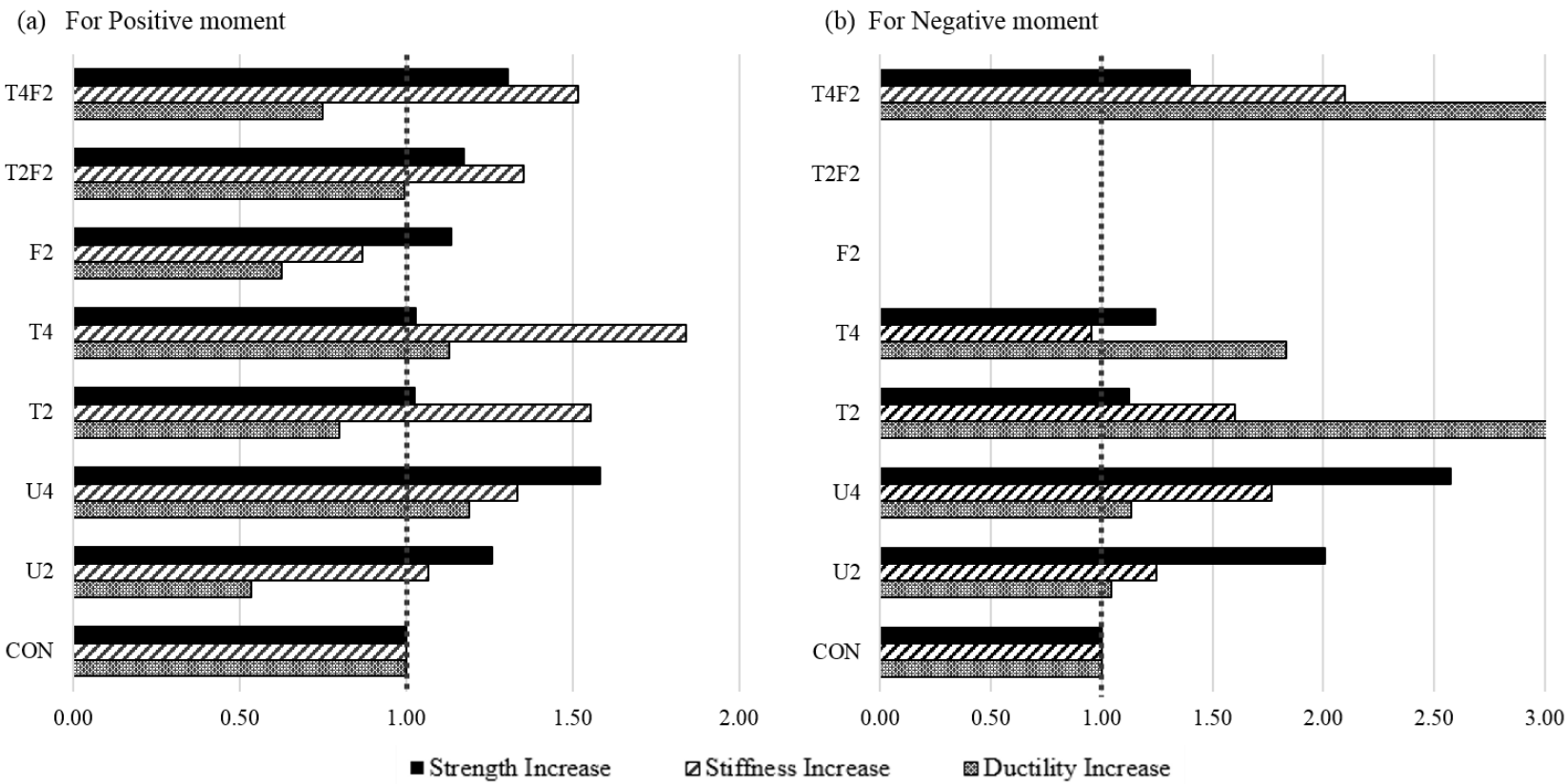

Fig 4-17 Strengthening Effect compared with reference beam for positive and negative moment

4.3 Strengthening Effect

Fig 4-15 and **Table 4-10** showed the strengthening effects compared with reference beams for positive and negative moment. Increase of strength, stiffness and ductility are illustrated in previous chart. Each specimens in both charts positioned in same horizontal line.

From a strengthening viewpoint with improvement of strength, stiffness and ductility based on reference beam, 40 mm UHPC U-shaped jacketing beam showed the highest increase of capacity both in positive and negative moment. U4 demonstrated the increases in strength (1.58 / 2.58 times), stiffness (1.33 / 1.77 times), ductility (1.19 / 1.13 times) improvement compared with the reference beam (increased ratio in positive / in negative moment).

According to the thickness from **Fig 4-16**, except the overlay method for positive moment which failed in delamination, every strengthened beams were proportional to the thickness.

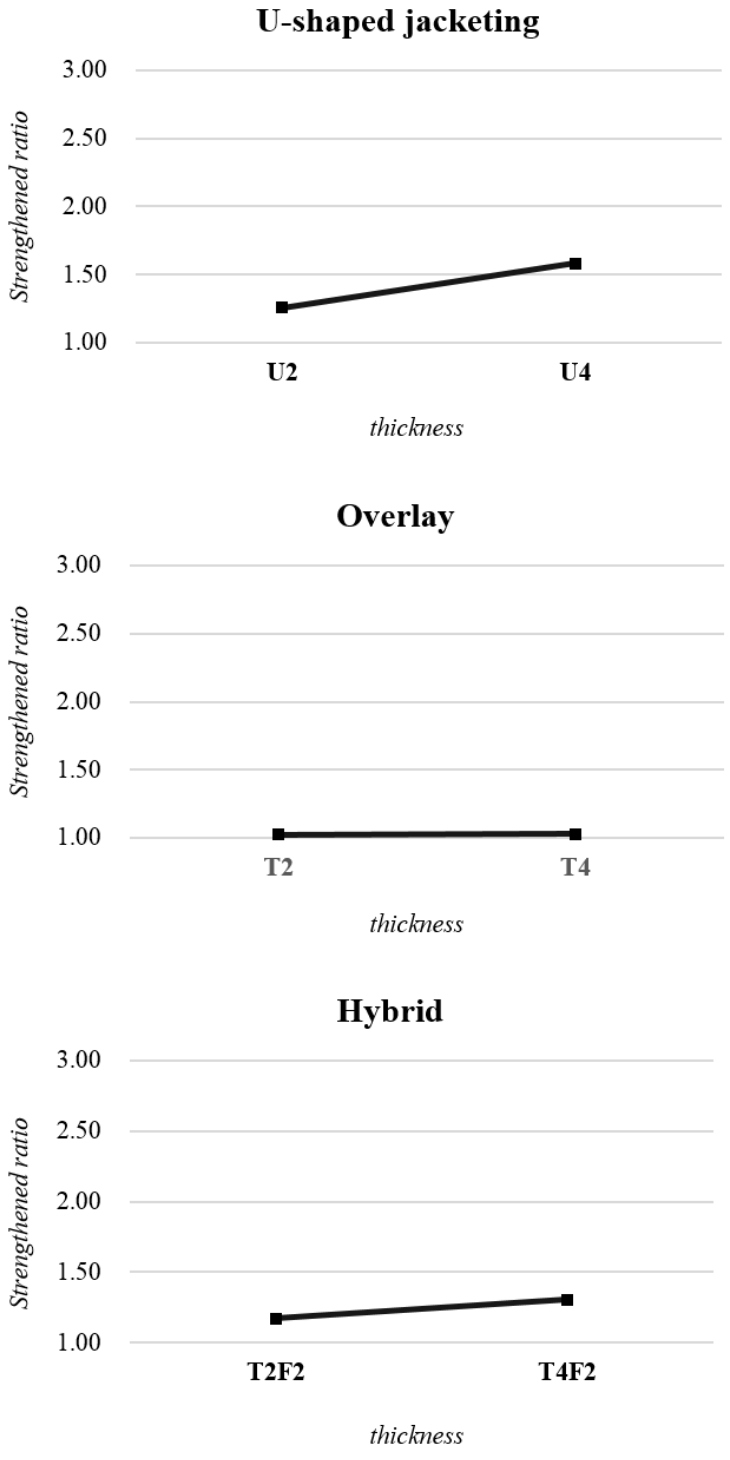

Fig 4-18 Increase of strength for UHPC thickness in positive moment

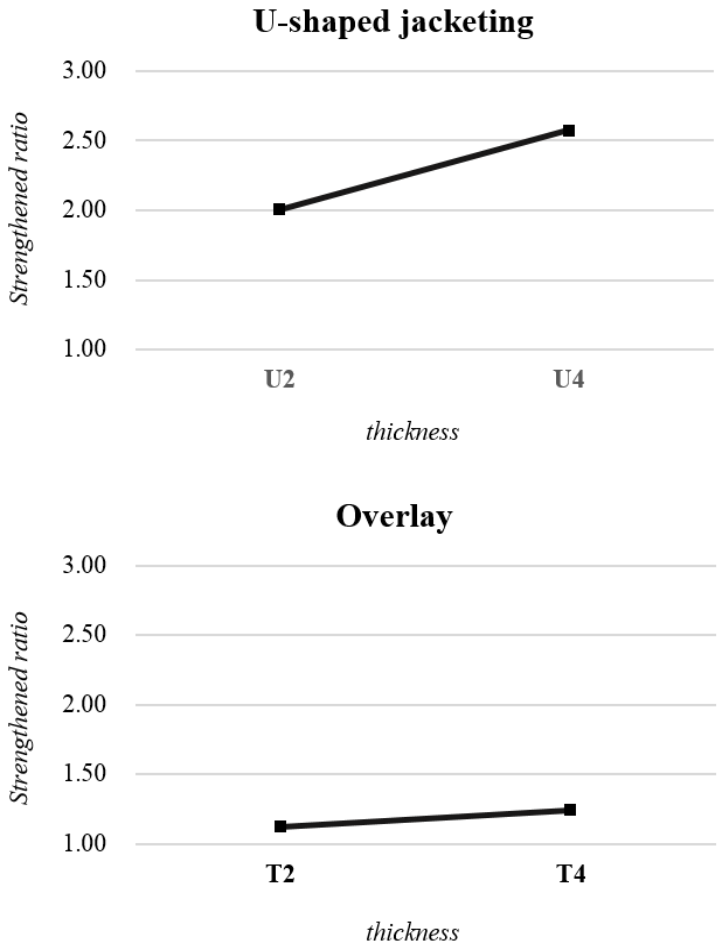

Fig 4-19 Increase of strength for UHPC thickness in negative moment

4.4 Theoretical analysis

4.4.1 Flexural strength

In the same way in **Chapter 3.5**, Euler-Bernoulli beam theory and simplified material behaviors are adapted. Cracking moment is also calculated by flexure formula, **Equation 1** in **Chapter 3.5.1.3.** In this experiment, cracking strength of UHPC was 4.258 MPa.($f_{crk} = 4.258 MPa$)

1) Nominal flexural strength of UHPC U-shaped jacketing for positive moment

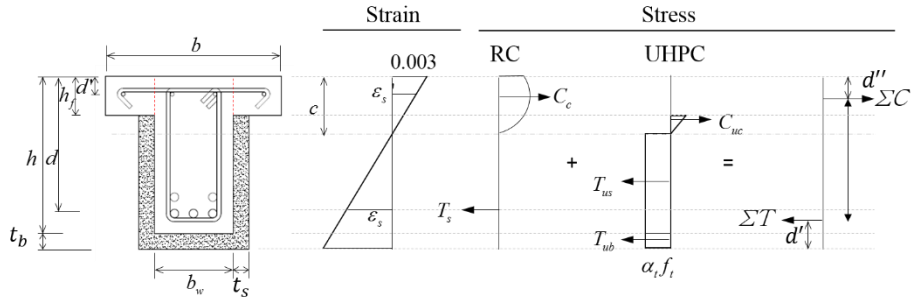

Fig 4-20 Strain and stress distribution for cross section of UHPC U-shaped jacketing for positive moment

The equilibrium of the normal forces is established in **Equation (11)** when $c > h_f$. In this case, as UHPC strengthened in tension side, the neutral axis became larger. From force equilibrium condition, neutral axis c is calculated. The overhanging flanges considered separately by A_{sf} (**Equation (12)**). Compressive rebar's strain was calculate by compatibility based on extreme compressive strain (0.003). (**Equation (13)**)

$$0.85 f_c' b_w a + E_u \varepsilon_s' A_s + \frac{1}{2} E_u \varepsilon_u 2t_s (c - h_f) = f_y (A_s - A_{sf}) + f_{tk} (2t_s (h - c) + (b_w + 2t_s) t_b) \quad (11)$$

$$A_{sf} = \frac{0.85 f_c' (b - b_w) h_f}{f_y} \quad (12)$$

$$\varepsilon_s' = \frac{c - d'}{c} 0.003 \quad (13)$$

where

a = depth of equivalent rectangular stress block, mm

b_w = width of web, mm

c = distance from extreme compression fiber to neutral axis, mm

h = height, mm

h_f = flange thickness, mm

f_c' = specified compressive strength of concrete, MPa

f_{tk} = characteristic tensile strength of UHPC, MPa

t_b = base strengthened thickness, mm

t_s = side strengthened thickness, mm

f_y = specified yield strength of reinforcement, MPa

A_s = area of nonprestressed longitudinal tension reinforcement, mm^2

A_s' = area of nonprestressed longitudinal compression reinforcement, mm^2

A_{sf} = tensile steel area having equilibrium condition with overhanging flanges, mm^2

E_s = modulus of elasticity of reinforcement steel, MPa

E_u = modulus of elasticity of UHPC, MPa

α_t = equivalent tensile stress block coefficient

ε_s' = net compression strain in longitudinal steel in compression

Considering extreme compressive strain as 0.003(ε_c=0.003), it is necessary to check whether reinforcement bars are yielded.

To compute M_n, arm length calculated from the positions of resultant forces of the compression(**Equation(14)**) and tension(**Equation(15)**). Finally the moment is calculated from **Equation (16)**

$$0.85 f_c' b_w a \cdot \frac{a}{2} + E_s \varepsilon_s' A_s' \cdot d' + \frac{1}{2} E_u \varepsilon_u 2t_s (c - h_f) \cdot (\frac{1}{3}(c - h_f) + h_f) = \Sigma C \cdot d'' \quad (14)$$

$$f_y A_s \cdot (h + t_b - d) + f_{tk} 2t_s (h - c) \cdot (\frac{h - h_f}{2} + t_b) + f_{tk} (b_w + 2t_s) t_b \cdot \frac{t_b}{2} = \Sigma T \cdot d' \quad (15)$$

$$M_n = \sum C \cdot (h + t_b - d' - d'') + f_y A_{sf} \cdot (d - \frac{h_f}{2}) \quad (16)$$

2) Nominal flexural strength of UHPC U-shaped jacketing for negative moment

In the same way, neutral axis can be obtained from equilibrium. And each strain value of rebar layer can be calculated based on extreme compressive strain(0.0035).

$$0.85 f_c' b_w (c - t_b) + \frac{1}{2} f_{cu} 2 t_s c + E_u \varepsilon_{cc} (t_b b_w) + E_s \varepsilon_{s1} \frac{3}{5} A_s + E_s \varepsilon_{s2} \frac{2}{5} A_s = A_s' f_y + 2 t_s (h - h_f + t_b - c) f_{tk} \quad (17)$$

$$\varepsilon_{cc} = \frac{c - \frac{t_b}{2}}{c} 0.0035 \quad (18)$$

$$\varepsilon_{s1} = \frac{c - d_1 - t_b}{c} 0.0035 \quad (19)$$

$$\varepsilon_{s2} = \frac{c - d_2 - t_b}{c} 0.0035 \quad (20)$$

where

ε_{cc} = net compression strain in middle of base UHPC jacketing

ε_{s1} = net strain in 1st bottom layer reinforcement

ε_{s2} = net strain in 2nd bottom layer reinforcement

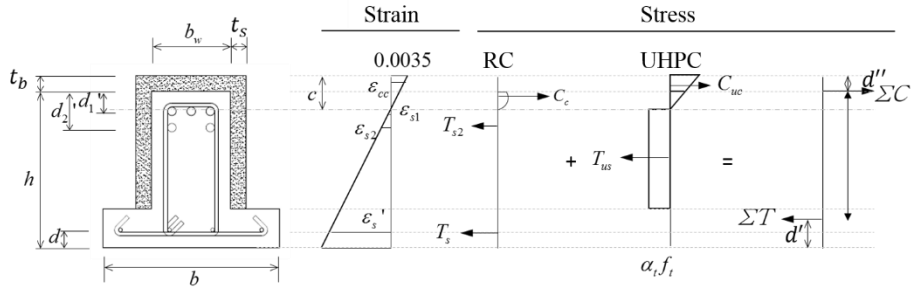

Fig 4-21 Strain and stress distribution for cross section of UHPC U-shaped jacketing for negative moment

To compute M_n, arm length calculated from the positions of resultant forces of the compression(**Equation(21)**) and tension(**Equation(22)**). Finally the moment is calculated from **Equation (23)**

$$0.85 f_c' b_w (c - t_b) \cdot (\frac{a}{2} + t_b) + \frac{1}{2} f_{cu} 2 t_s c \cdot \frac{c}{3} + E_u \varepsilon_{cc} (t_b b_w) \cdot \frac{t_t}{2} = \Sigma C \cdot d'' \quad (21)$$

$$T_s d + T_{us}((h + t_b - c - h_f)/2 + h_f) + T_{s2}(h - d_2') = \Sigma T \cdot d' \quad (22)$$

$$M_n = \Sigma C \cdot (h + t_b - d' - d'') \quad (23)$$

3) Nominal flexural strength of UHPC Overlay for positive moment

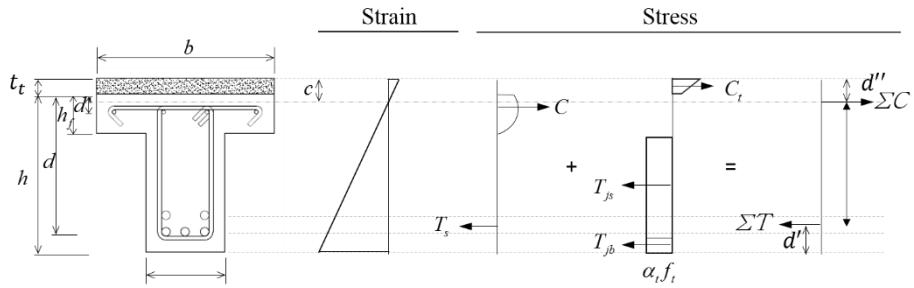

Fig 4-22 Strain and stress distribution for cross section of UHPC Overlay for positive moment

In the same way, neutral axis can be obtained from equilibrium. And each strain value of rebar layer can be calculated based on extreme compressive strain(0.0035). However, this calculation is wrong due to the imperfect bond between UHPC and concrete.

4) Nominal flexural strength of UHPC Overlay for negative moment

In the same way, neutral axis can be obtained from equilibrium. And each strain value of rebar layer can be calculated based on extreme compressive strain(0.003).

$$0.85 f_c' b_w a + E_s \varepsilon_{s1} \frac{3}{5} A_s + E_s \varepsilon_{s2} \frac{2}{5} A_s = A_s' f_y + t_t b f_{tk} \tag{24}$$

$$\varepsilon_{s1} = \frac{c - d_1}{c} 0.003 \tag{25}$$

$$\varepsilon_{s2} = \frac{c - d_2}{c} 0.003 \tag{26}$$

where

t_t = Overlayed thickness, mm

To compute M_n, arm length calculated from the positions of resultant forces of the compression(**Equation(27)**) and tension(**Equation(28)**). Finally the moment is calculated from **Equation (29)**

$$0.85 f_c' b_w a \cdot \frac{a}{2} + E_s \varepsilon_s' A_s' \cdot d' = \Sigma C \cdot d'' \tag{27}$$

$$f_y A_s' \cdot (t_t + d') + f_{tk} t_t b \cdot \frac{t_t}{2} = \Sigma T \cdot d' \tag{28}$$

$$M_n = \Sigma C \cdot (h + t_t - d' - d'') \tag{29}$$

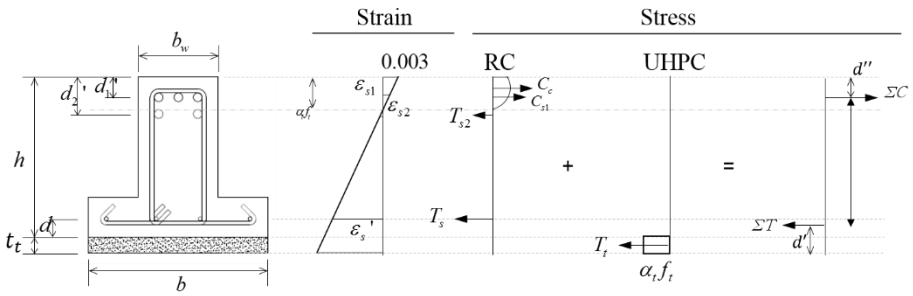

Fig 4-23 Strain and stress distribution for cross section of UHPC Overlay for negative moment

To compute M_n, arm length calculated from the positions of resultant forces of the compression(**Equation(27)**) and tension(**Equation(28)**). Finally the moment is calculated from **Equation (29)**

$$0.85 f_c' b_w a \cdot \frac{a}{2} + E_s \varepsilon_s' A_s' \cdot d' = \Sigma C \cdot d'' \tag{27}$$

$$f_y A_s' \cdot (t_t + d') + f_{tk} t_t b \cdot \frac{t_t}{2} = \Sigma T \cdot d' \tag{28}$$

$$M_n = \sum C \cdot (h + t_t - d' - d'') \tag{29}$$

4.4.2 Shear strength

Shear strength of existing RC T-beam can be obtained from (Ioannis P. Zararis, Maria K. Karaveziroglou 2006)'s theory. It consists of concrete shear force V_{cr} and dowel shear force of longitudinal reinforcement ΔV_d and contribution of the force of stirrups V_s.(**Equation (30)**) Effective width of a T-beam in shear is $b_{ef} = A/c$ (A is area of upper part of neutral axis of T-beam) in **Equation (31)**

$$V_u = V_{cr} + \Delta V_d + V_s$$

$$V_u = [(1.2 - 0.2\frac{a}{d}d)\frac{b_{ef}}{b_w} \times \frac{c}{d} f_{ct} + (0.5 + 0.25\frac{a}{d})\rho_v f_{yv}]b_w d \quad (30)$$

$$b_{ef} = b_w[1 + 0.5 \times \frac{h_f}{d}(\frac{b}{b_w} - 1) / \frac{c}{d}] \quad (31)$$

where

b_{ef} = effective width of a T-beam in shear, A/c, replaceable b_w

ρ_v = ratio of tie reinforcement area to area of contact surface

f_{yv} = specified yield strength f_y of transverse reinforcement

To calculate strengthened shear strength by UHPC, only the side portion of the UHPC from U shaped jacketing superposed into ultimate shear strength of reference beam. Shear strength of UHPC portion is expressed as the sum of the contributions of UHPC matrix, steel fiber as mentioned in **3.5.2**.

$$V_{uhpc} = V_{rpcd} + V_{fd} \quad (32)$$

FRP contribution to shear strength V_f is calculated according to ACI 440.2R-08(ACI committee 440 2004).

$$V_f = \frac{A_{fv} f_{fe} (\sin\alpha + \cos\alpha) d_{fv}}{s_f} \quad (33)$$

4.4.3 Validation

Fig 4-21, 22, 23 and **Table 4-11, 12** showed the comparison between experimental results and theoretical results predicted by the simplified analysis model. Except 3 specimens, reasonably good agreements are evident.

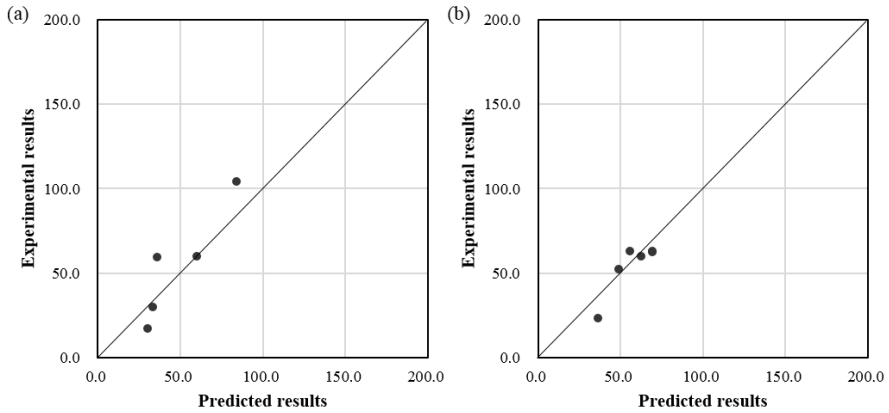

Fig 4-24 Comparison of experimental results with theoretical predictions about cracking moment

Table 4-11 Comparison of experimental results with theoretical predictions about cracking moment

	Name	I_{gt}	y_{top}	f_r	M_{cr_exp}	M_{cr_cal}	cal/exp
For Positive moment	T	1.89E+09	218.2	3.5	17.4	30.2	**1.74**
	T-U2	2.96E+09	209.7	4.3	60.2	60.1	1.00
	T-U4	4.13E+09	209.7	4.3	104.7	83.8	0.80
	T-T2	2.2E+09	231.4	3.5	30.1	33.1	1.10
	T-T4	2.53E+09	244.3	3.5	59.4	36.1	**0.61**
	T-F2	1.89E+09	218.2				
	T-T2F2	2.2E+09	231.4				
	T-T4F2	2.53E+09	244.3				
For Negative moment	T	1.89E+09	181.8	3.5	23.5	36.2	**1.54**
	T-U2	2.96E+09	210.3	3.5	52.4	49.0	0.93
	T-U4	4.13E+09	230.3	3.5	60.2	62.4	1.04
	T-T2	2.2E+09	168.6	4.3	62.9	55.6	0.88
	T-T4	2.53E+09	155.7	4.3	62.8	69.3	1.10
	T-T4F2	2.53E+09	155.7	4.3	63.0	69.3	1.10

About flexural strength for positive moment, only U-shaped jacketed beams are positioned. Likewise U-shaped jacketed beam which had rectangular section in **Chapter 3**, the predictions are overestimated than test results about 20%. On the other hand, for negative moment, they are mostly underestimated About the shear strength, due to interfacial failure, UHPC overlay beams showed that the predictions are less than test results.

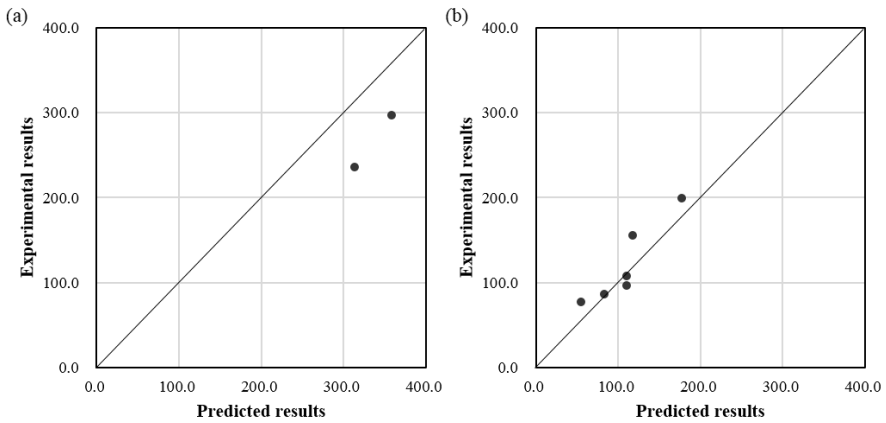

Fig 4-25 Comparison of experimental results with theoretical predictions about flexural strength: a) for positive moment b) for negative moment

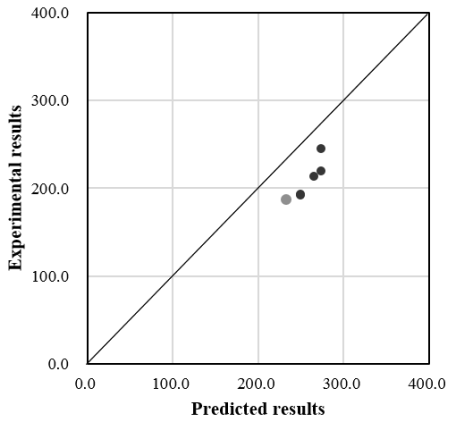

Fig 4-26 Comparison of experimental results with theoretical predictions about shear strength

Table 4-12 Comparison of experimental results with theoretical predictions

	Name	Failure	Cal		Exp	Exp/Cal
			M_n/a	V_n	V_{test}	
For Positive Moment	CON	S	281.9	232.7	187.7	0.81
	U2	SF	314.0	330.7	235.9	0.75
	U4	F	358.7	421.2	297.1	0.83
	T2	S-interface		249.7	192.6	0.77
	T4	S-interface		249.7	193.3	0.77
	F2	S-interface		265.6	213.4	0.80
	T2F2	S-interface		273.2	220.1	0.81
	T4F2	S-interface		273.2	244.8	0.90
For Negative Moment	CON	F	54.6	242.2	77.5	1.42
	U2	F	117.3	409.4	155.5	1.33
	U4	F	177.8	583.4	199.7	1.12
	T2	F	83.1	330.3	86.9	1.05
	T4	F	110.7	411.0	96.3	0.87
	T4F2	F	110.7	433.7	108.3	0.98

4.4.4 Shear stress

Shear stress in the beam is distinguished interfacial shear stress with shear stress in the section. Interfacial shear stress generated in the horizontal direction at the interface between concrete and UHPC due to the difference of material properties. Shear stress in the vertical direction at the section calculated in the elastic states.

1) Interfacial shear stress about UHPC U-shaped jacketing

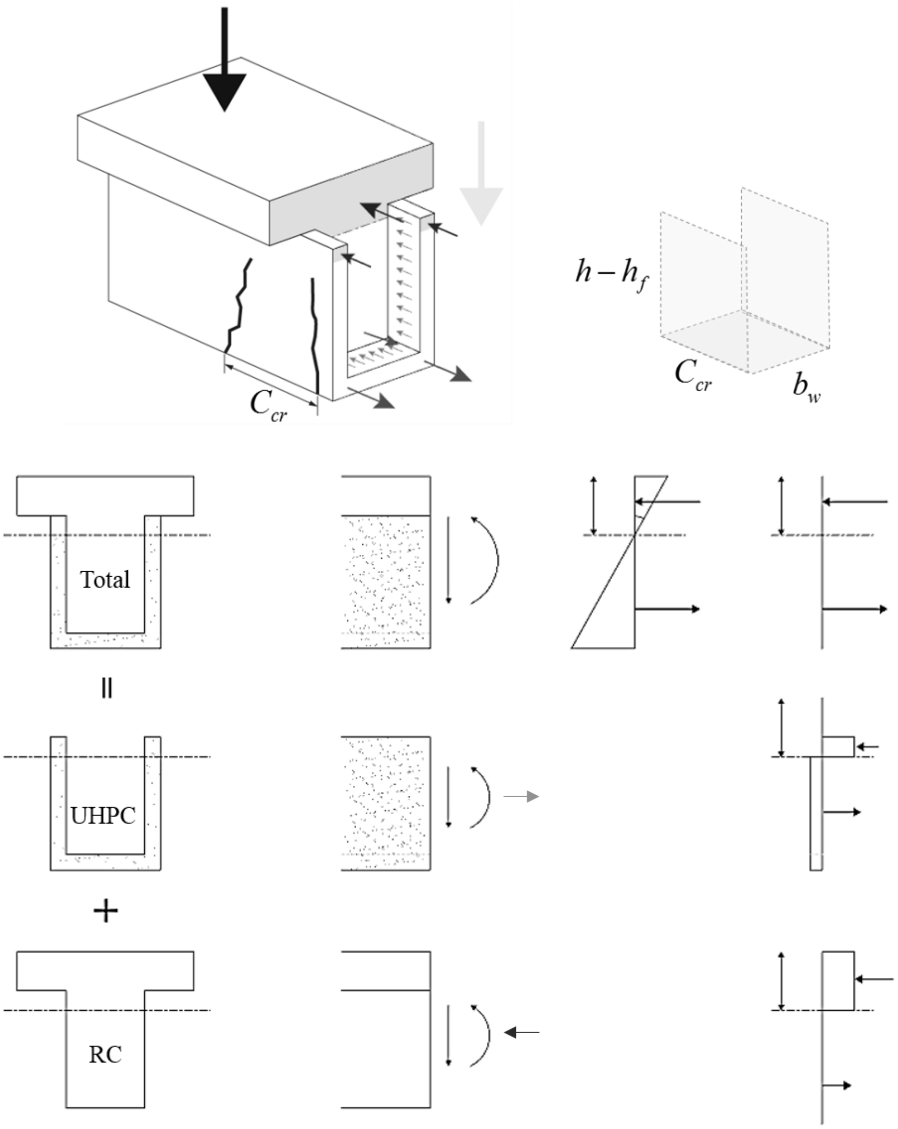

Fig 4-27 Average interfacial shear stress

In case of U-shaped jacketing which is failed in flexure, for any curvature, the free body diagram of total beam consists of shear and moment. But, when the beam considered separately, keeping the same depth of compression zone, both elements produce an axial force which is canceled in total beam. This axial force means average of the interfacial shear force which is transferred from the internal core to the outer shell through the interface in the form of shear stress flow. It can be determined from one element's different force between tension and compression. (Chalioris, Thermou, and Pantazopoulou 2014) So the shear stress demand was estimated:

$$\tau_b = \frac{C - T}{C_{cr}(b + 2(h - h_f))} \tag{34}$$

where

τ_b = Interfacial shear stress

C_{cr} = crack spacing

Instead of C_{cr}, span length, a, was used due to the UHPC showed localized macro crack after close of micro crack. Its results for both positive and negative moment are shown in **Fig 4-28, 29** and **Table 4-13, 14.**

2) Interfacial shear stress about UHPC Overlay

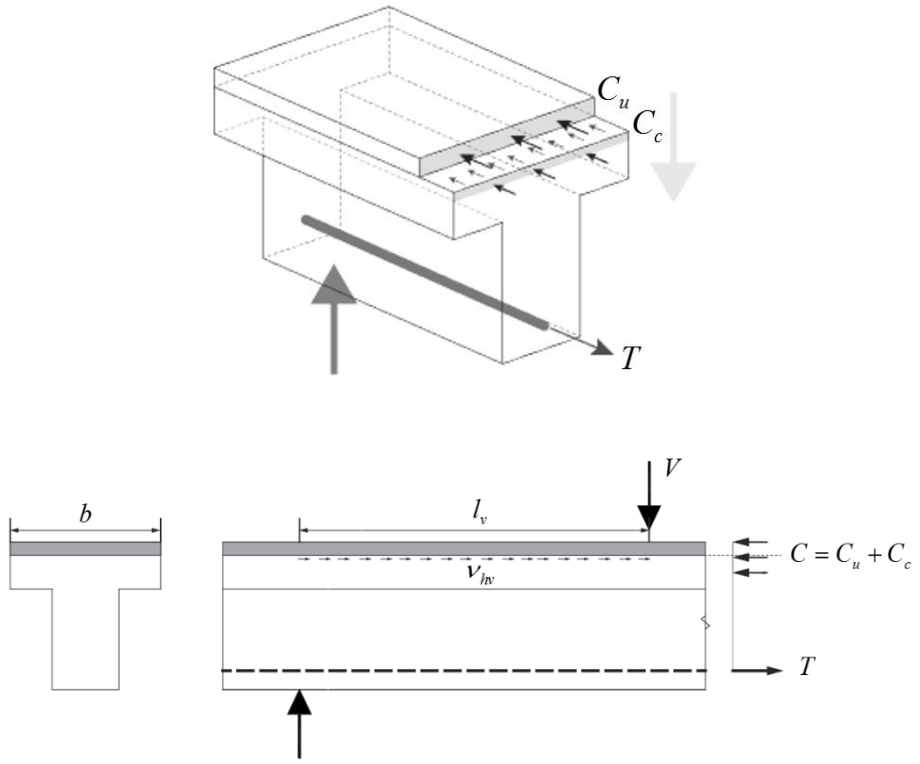

Fig 4-28 Average interfacial shear stress

For UHPC overlaid beam which is failed in debonding, the interfacial shear stress between UHPC plate and T-beam is calculated from vertical shear stress(**Equation 35, 36**) or actual variation of compressive force or tensile force(**Equation 37**) based on AASHTO LRFD 2012. Especially strengthened UHPC layer is so thin that the interfacial shear stress should be equaled with the compressive stress resisted in UHPC layer.

$$V_{hv} = \frac{V \cdot l_v}{jd} \tag{35}$$

$$v_{hv} = \frac{V_{hv}}{b_v \cdot l_v} \tag{36}$$

$$v_{hv} = \frac{C_u}{b_v \cdot l_v} \tag{37}$$

where

V_{hv} = Interfacial shear force

l_v = length from inflection point to maximum moment point

v_{hv} = horizontal shear stress

C_u = Compressive stress resisted in UHPC layer

C_c = Compressive stress resisted in flange of T-beam

3) Comparison interfacial shear stress with current code

According to the codes, interfacial shear stress is composed of the sum of adhesive bond/interlocking, shear friction and dowel action. For this experiment performed without dowel action, only interlocking and shear friction affect to interfacial shear stress. Interlocking portion was calculated based on the lower compressive strength concrete. So, Enlarging the contact area could be a way to reduce horizontal shear stress if shear connector wasn't considered.

In **Table 4-13**, according to ACI 318-11(ACI committee 318 2011) and KCI 2012 (KCI 2012), shear friction is 4.94 MPa. But with considering interlocking effect, horizontal shear stress is 0.55 MPa for ACI 318-11 and 0.56 MPa for KCI 2012. In the viewpoint of Model Code 2010(Walraven, 2012), the design limit value for the interface shear stress is 0.42 MPa for rough surface and 0.2 MPa for smooth surface. About AASHTO LRFD 2012(AASHTO 2012), shear stress is 1.65 MPa for 6mm intentionally roughened surface and 0.51 MPa for smooth surface.

From the slant shear test between normal strength concrete(30.5 MPa) and UHPC(147.6 MPa), the shear stress was calculated as 8.3 MPa for sandblast and 0.4 MPa for smooth surface. Though each concrete compressive strength didn't match exactly with this study, the value deserved to be referred. However, due to effect of axial force in slant-shear test, shear stress in sandblasted surface is too high not to compare with calculated values.

In **Fig 4-27, 28** and **Table 4-14, 15** showed the comparison between calculated values in **4.4.4.1, 4.4.4.2**. To avoid debonding failure,

For positive moment, UHPC Overlay specimen T4 recorded the highest shear stress, and next T2 did.

Table 4-13 Design codes of horizontal shear strength

Code	Interfacial shear
ACI 318-11	**Shear friction** For normalweight concrete either placed monolithically or placed against hardened concrete with surface intentionally roughened to a full amplitude of approximately 6 mm. $V_n \le \min(0.2 f_c' A_c, (3.3 + 0.08 f_c') A_c, 11 A_c)$ where A_c = area of concrete section resisting shear transfer f_c' = the lower-strength concrete **Horizontal shear strength** Where contact surfaces are clean, free of laitance, and intentionally roughened or where minimum ties are provided and contact surfaces are clean and free of laitance, but not intentionally roughened, $V_{nh} \le 0.55 b_v d$ Where ties are provided and contact surfaces are clean, free of laitance, and intentionally roughened to a full amplitude of approximately 6 mm, $V_{nh} = (1.8 + 0.6 \rho_v f_y) \lambda b_v d \le 3.5 b_v d$
KCI 2012	Except the coefficients of the horizontal shear strength in case without ties as 0.56, there is no difference with ACI 318-11 $V_{nh} \le 0.56 b_v d$
Model Code 2010	**The ultimate shear stress at the interface** The ultimate resistance of an interface subject to shear forces can be approached by superposition of the single mechanisms of adhesion and mechanical interlocking, shear-friction and dowel action. $\tau_u = \tau_a + \mu \cdot (\rho \cdot \kappa_1 \cdot f_y + \sigma_n) + \kappa_1 \cdot \rho \cdot \sqrt{f_y \cdot f_{cd}} \le \beta_c \cdot \nu \cdot f_{cd}$ where ρ = ratio of reinforcement crossing the interface (ρ = A_s/A_c) β_c = a coefficient for the strength of the compression strut ν = the effectiveness factor for the concrete **Interface without reinforcement (rigid bond-slip behavior)** $\tau_{Rdi} = c_a \cdot f_{ctd} + \mu \cdot \sigma_n \le 0.5 \cdot \nu \cdot f_{cd}$ where c_a = the coefficient for the adhesive bond; 0.4(strongly roughened surface) μ = the friction coefficient acc. Table 7.3-2; 0.7 for rough surface σ_n = the (lowest expected) compressive stress resulting from an eventual normal force acting on the interface.

AASHTO LRFD 2012

Nominal shear resistance

The nominal shear resistance of the interface plane shall be taken as:

$$V_n = cA_{cv} + \mu(A_{vf} f_y + P_c)$$

The nominal shear resistance, V_{ni}, used in the design shall not be greater than the lesser of:

$$V_{ni} \le K_1 f'_c A_{cv} \text{ or } V_{ni} \le K_2 A_{cv} \quad \text{in which : } A_{cv} = b_v \cdot l_v$$

where

A_{cv} = area of concrete considered to be engaged in interface shear transfer

A_{vf} = area of interface shear reinforcement, crossing the shear plane within the area A_{cv}

c = cohesion factor specified in Article 5.8.4.3 of AASHTO LRFD

μ = friction factor specified in Article 5.8.4.3

P_c = permanent net compressive force normal to the shear plane; if force is tensile, $P_c = 0$

K_1 = fraction of concrete strength available to resist interface shear, as specified in Article 5.8.4.3

K_2 = limiting interface shear resistance specified in Article 5.8.4.3

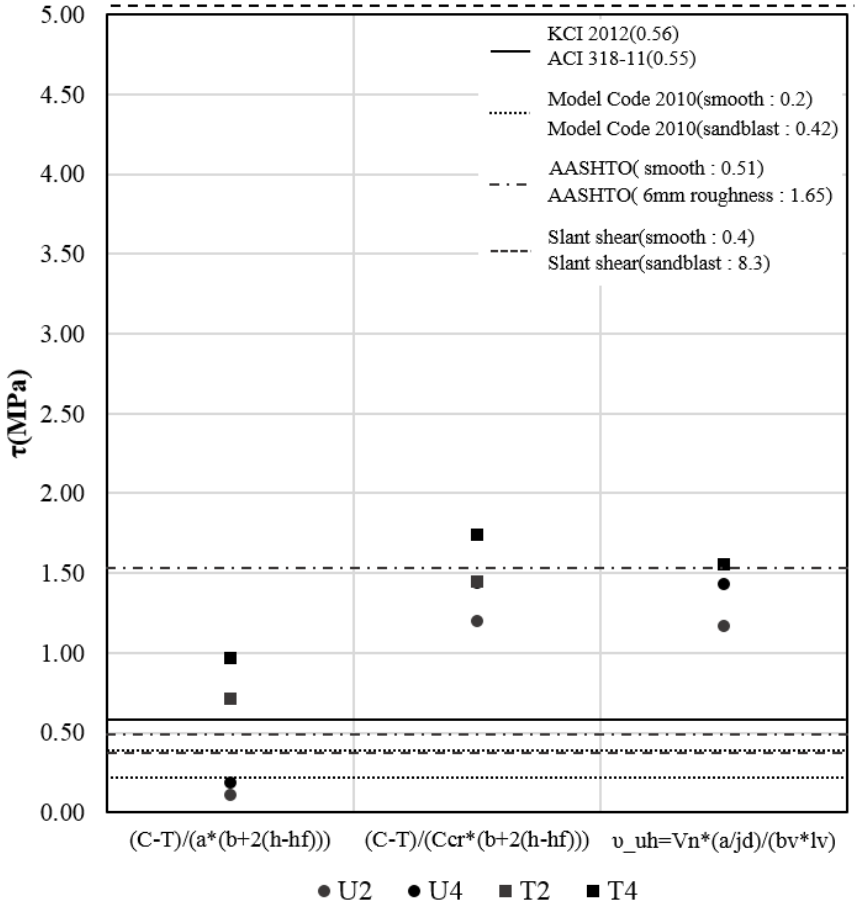

Fig 4-29 Comparison shear stress with Code for positive moment

Table 4-14 Comparison shear stress with Code for positive moment

		τ_d[MPa]		
		$\tau_b = \frac{(C-T)}{a*(b+2(h-h_f))}$	$\tau_b = \frac{(C-T)}{C_{cr}*(b+2(h-h_f))}$	$\upsilon_{uh} = \frac{V_n*(a/jd)}{(b_v*l_v)}$
For Positive Moment	U2	0.11	0.61	1.17
	U4	0.19	1.44	1.43
	T2	0.72	1.45	1.55
	T4	0.97	1.74	1.56

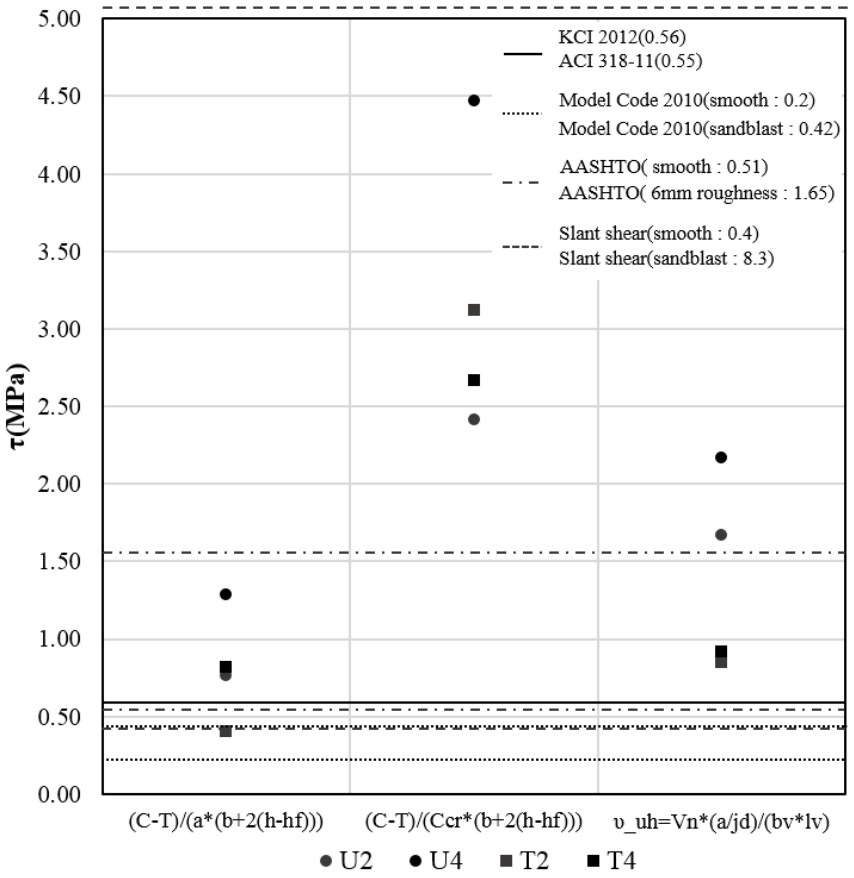

Fig 4-30 Comparison shear stress with Code for negative moment

Table 4-15 Comparison shear stress with Code for negative moment

		τ_d[MPa]		
		$\tau_b = \frac{(C-T)}{a*(b+2(h-h_f))}$	$\tau_b = \frac{(C-T)}{C_{cr}*(b+2(h-h_f))}$	$\upsilon_{uh} = \frac{V_n*(a/jd)}{(b_v*l_v)}$
For Negative Moment	U2	0.76	2.42	1.68
	U4	1.29	4.47	2.17
	T2	0.41	3.12	0.85
	T4	0.82	2.67	0.92

4) Vertical shear stress

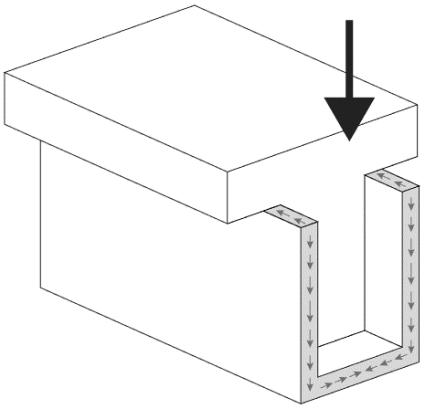

Fig 4-31 shear stress

The shear stresses at the interface are difficult to determine, since the composite UHPC-RC beam has a complicated geometry and as the material laws are non-linear. The shear stresses may be calculated in the elastic state with **equation 34**. (Habel 2004) The calculated values are listed in **Table 4-14**. UHPC overlay beam could be omitted for the lack of effect on shear resistance.

$$\tau = \frac{V \cdot Q}{It} \tag{34}$$

where

τ = vertical shear stress

V = shear force

Q = equivalent section modulus

I = equivalent moment of inertia

t = UHPC jacketing thickness

Table 4-16 Vertical shear stress in UHPC

	Name	P_{cr_exp}	I_{gt}	Q(of UHPC)	t	$\tau = \frac{VQ}{It}$
For positive moment	U2	60.2	2.96E+09	1.4.E+06	20	1.47
	U4	104.7	4.13E+09	3.3.E+06	40	2.11
	T2	30.1	2.20E+09	2.0.E+06	450	0.06
	T4	59.4	2.53E+09	4.0.E+06	450	0.21
For negative moment	U2	52.4	2.96E+09	4.8.E+05	20	0.42
	U4	60.2	4.13E+09	1.4.E+06	40	0.51
	T2	62.9	2.20E+09	2.2.E+06	450	0.14
	T4	62.8	2.53E+09	4.8.E+06	450	0.26

4.5 Discussion

T-shaped RC beams strengthened by UHPC overlay and jacketing with other methods are investigated for their efficiency in this study.

1. Only the UHPC jacketing demonstrated the increases in strength (1.58 / 2.58 times), stiffness (1.33 / 1.77 times), ductility (1.19 / 1.13times) improvement compared with the reference beam (increased ratio in positive / in negative moment).

2. In conclusion the overlay method in this study showed small increase in strength and ductility. However, the overlay method also showed the improvement in flexural stiffness of beams in positive moment. Under negative moment, due to the thin layer in tensile zone, it showed also the increase in strength and stiffness.

3. The retrofit using AFRP increased flexural strength by high material strength. However, the flexural stiffness and ductility were not increased without the combination of hybrid method.

4. Based on observation of the strengthening methods in this study, it is shown that the increase in structural performance of retrofitted members are in proportion to the thickness of UHPC.

5. Based on sectional level analysis, theoretical values showed 21% tolerance with experimental values.

Chapter 5. Conclusions

This study investigates the structural performance of reinforced concrete beams retrofitted by ultra-high performance concrete (UHPC) to compare the effectiveness of strengthened beams with different regions, thickness of layers and additional reinforcement. In **Chapter 3**, rectangular cross sectional RC beam without stirrup was strengthened with UHPC. In **Chapter 4**, T-shaped RC beams was strengthened by UHPC jacketing and overlay with other methods.

1. Strengthened beams with UHPC showed higher ultimate resistance and stiffness than RC element alone. The experiments show that the additional UHPC reinforcement can increase the ultimate resistance to up to 2.42 times that of the RC beam in case of rectangular beam. For T-shaped beam, resistance increased up to 1.58 times that of the reference beam.

2. U-shaped jacketing demonstrated the increases in strength (1.58 / 2.58 times), stiffness (1.33 / 1.77 times), ductility (1.19 / 1.13times) improvement compared with the reference beam not only in positive moment but also in negative moment.

3. About additional reinforcement, rebars showed the best combination with UHPC(2.42 times, which is the most highly increased case). AFRP with UHPC and additional steel fiber in UHPC showed a little increase in strength. Wire mesh didn't help to increase performance.

4. Strengthening effects are proportion to the strengthened thickness without shear failure. However considering the workability, 40 mm should be recommended.

5. For UHPC overlay, it need to improve adhesion performance by embedding additional dowel bars or to extend interconnected surface by giving groove to the surface.

6. Theoretical analysis determined by a cross-sectional analytical model

based on plane section showed 21% error range. Also interfacial shear stress obtained from the moment equilibrium condition at overlaid UHPC panel is great than design value given by current codes in positive moment. For negative moment, even though average interfacial shear stress on U-shaped shell is higher than any cases, delamination of UHPC panel didn't happen.

References

Aaleti, S., Bradley, P., and Sri, S. 2013. "Design Guide for Precast UHPC Waffle Deck Panel System, Including Connections." FHWA-HIF-1(June): 127.

AASHTO LFRD. 2012. AASHTO LRFD 2012 Bridge Design Specifications, Washington, DC: American Association of State Highway and Transportation Officials.

ACI committee 318. 2011. American Concrete Institute, Farmington Hills, MI *Building Code Requirements for Structural Concrete and Commentary*.

ACI committee 440. 2004. ACI committee 440 *Guide for the Design and Construction of Externally Bonded FRP Systems for Strengthening Existing Structures*.

Bissonnette, B., Alexander, M. V., and Kurt, F. F. 2012. "Best Practices for Preparing Concrete Surfaces Prior to Repairs and Overlays." (May): 92.

Chalioris, C. E., Georgia, E. T., and Stavroula, J. P. 2014. "Behaviour of Rehabilitated RC Beams with Self-Compacting Concrete Jacketing - Analytical Model and Test Results." *Construction and Building Materials* 55: 257–73.

CHO, H.-W. 2011. "Flexural Experiments on Reinforced Concrete Beams Strengthened with ECC and High Strength Rebar." KCI, 23(4): 503–509.

Hong, S.-G., and Kang, S.-H. 2013. "Formwork development using UHPFRC" UHPFRC 2013. RILEM-Fib-AFGC International Symposium on. Marseille, France: 197-206.

Ekkehard, F., Michael, S., Torsten, L., Joost, W., and Susanne, F. 2014. *Ultra-High Performance Concrete UHPC*: Wiley 210.

Habel, K. 2004. "Structural behavior of elements combining Ultra-High Performance Fibre Reinforced Concrete." EPFL PhD Thesis 3036.

Habel, K., Emmanuel, D., and Eugen, B. 2006. "Structural Response of Elements Combining and Reinforced Concrete." *Journal of structural engineering* (November): 1793–1800.

Harris, D. K., Jayeeta, S., and Theresa, M. A. 2011. "Characterization of Interface Bond of Ultra-High-Performance Concrete Bridge Deck Overlays." *Transportation Research Record: Journal of the Transportation Research Board* 2240(-1): 40–49.

Ioannis, P. Z., Maria, K. K., and Prodromos, D. Z. 2006. "Shear Strength of Reinforced Concrete T-Beams." *ACI Structural Journal* 103(S71): 693–700.

Kamal, A., Minoru, K., Naoshi, U., and Hikaru, N. 2008. "Assessment of Strengthening Effect on RC Beams with UHP-SHCC." *JCI Structural Journal*, 30(3): 1483-1488.

Karihaloo, B., L. and Alaee, F.J. 2003. “Retrofitting of RC Beams with CARDIFRC.” (August): 174–86.

KCI. 2012. “Korean Structural Design Code.” *Korean Concrete Institute*.

Giovanni, M., Meda, A., Plizzari, G.A., and Rinaldi, Z. 2010. “Strengthening and Repair of RC Beams with Fiber Reinforced Concrete.” *Cement and Concrete Composites* 32(9): 731–39.

Meda, A., Serena M., and Paolo R. 2014. “Shear Strengthening of Reinforced Concrete Beam with High-Performance Fiber-Reinforced Cementitious Composite Jacketing.” *ACI Structural Journal* (111): 1059-1068.

Noshiravani, T. 2012. “Structural Response of R-UHPFRC – RC Composite Members Subjected to Combined Bending and Shear.” EPFL PhD 5246.

Noshiravani, T., and Eugen B. 2010. “Behaviour of UHPFRC-RC Composite Beams Subjected to Combined Bending and Shear.” 8th fib PhD Symposium in Kgs. Lyngby, Denmark

Oesterlee, C. 2010. “Structural Response of Reinforced UHPFRC and RC Composite Members.” EPFL PhD 4848.

Ö nal, M., Mustafa, B. Z., Ali K., and Bilge, D. 2014. “An Experimental Investigation on Flexural Behavior of RC Beams Strengthened with Different Techniques.” *KSCE Journal of Civil Engineering* 18(7): 2162–69.

Richard, P., and Marcel, C. 1995. “Composition of Reactive Powder Concretes.” *Cement and Concrete Research* 25(7): 1501–11.

Namboorimadathil, S.M., Tumialan, J.G., and Nanni, A. “Behavior of Rc T-Beams Strengthened in the Negative Moment Region With Cfrp Laminates.” 440(Aci 440).

Skazlić, M. 2009. “Utilization of High Performance Fiber-Reinforced Micro-Concrete as a Repair Material.” *Civil Engineering*: 859–62.

Miguel A. C., Devin K. H., Sarah V. S., and Theresa, M. A. 2012. "Bond strength between UHPC and Normal Strength Concrete (NSC) in accordance with split prism and freeze-thaw cycling tests." *Heft 19 Schriftenreihe Baustoffe Und Massivbau Ultra-High Performance Concrete and Nanotechnology in construction*. 3rd Hipermat International Symposium. Kassel, German. 377-384

Tayeh, B. A., Abu Bakar, B. H., and Megat Johari, M. A. 2012. “Characterization of the Interfacial Bond between Old Concrete Substrate and Ultra High Performance Fiber Concrete Repair Composite.” *Materials and Structures*: 743–53.

Walraven, J. (fib bulletin 66). 2012. *Model Code 2010-2*.

Yang, I.-H., and Joh, C.-B. 2010. “Prediction of Flexural Capacity of Steel Fiber-Reinforced Ultra High Strength Concrete Beams.” (2009): 317–28.

Yehia, A. H. 2013. “Flexural Behavior of Strengthened and Repaired R.C. Beams by Using Steel Fiber Concrete Jacket under Repeated Load.” 3(3): 564–78.

초 록

초고성능 콘크리트를 이용한 보 보강 실험

최 정 택

서울대학교 건축학과 대학원

본 연구는 초고성능 콘크리트인 UHPC를 이용하여 보 보강 성능을 평가하고 이를 통해 보강방법을 제시하는 실험논문이다. UHPC는 압축강도뿐 아니라 인장강도 또한 높은 콘크리트로서, 기존의 시멘트계열의 보수보강재료보다 얇은 두께로 보강할 수 있으며, 특히나 인장과 압축 모두에 힘을 받을 수 있는 장점을 지닌다. UHPC의 부착을 위하여는 샌드블라스트를 이용하여 계면처리한 후, 별도의 스터드없이 보강을 실시하였다.

실험은 총 2타입으로 진행되었고, 3장에서 다룬 직사각형 단면의 전단철근이 없는 13개의 보에 대하여 보강실험이 진행되었고, 변수로는 보강범위, 두께, 추가 보강제의 사용으로 나뉘었다. 4장에서는 14개의 T형보에 대한 보강을 실시하였고, 이 실험에서는 UHPC의 성능을 고려하여 정/부모멘트 구간을 나눠 보강범위, 두께, 아라미드섬유의 사용에 따라 보강성능을 보고자 하였다.

실험결과는 강도와 처짐에 있어 확실한 보강효과가 있음이 검증이 되었고, 특히나 U형 자켓팅 공법이 정/부모멘트 전구간에 걸쳐 강도, 강성, 연성 증가가 있음을 보였다. 반면 오버레이공법은 계면파괴가 발생하여 추가적인 부착성능향상이 필요하리라 판단되었

다. 보강성능은 두께에 비례하여 증가하는 양상을 보였고, 철근을 추가한 실험체의 보강 성능이 전체 실험체 중 가장 우수하였다. 아라미드 섬유시트와 추가 강섬유를 넣은 실험체는 미비하게 강도증가의 효과가 나타났고, 와이어메쉬를 넣은 실험체의 경우 보강에 도움이 되지 않았다.

베르누이 가정하에 단면 해석을 하여 실험값을 이론값과 비교해보았으며, 직사각형 보의 경우 15%의 오차를 T형보의 경우 21%의 오차를 가졌다. 계면파괴가 일어난 오버레이로 보강된 실험체의 경우 계면에서의 전단응력이 현행기준에서 제시한 값보다 크게 나타남을 볼 수 있었다.

핵심용어 : 초고성능콘크리트(UHPC), 보강, 합성보

학번 : 2014-20519